

**The early instrumental climate period (1760–1860) in Europe**  
**Evidences from the Alpine region and Southern Scandinavia**

**DIPLOMARBEIT**

zur Erlangung des  
Magistergrades der Naturwissenschaften  
an der  
Fakultät für Geowissenschaften, Geographie und Astronomie  
der  
Universität Wien

eingereicht von

**Johann HIEBL**

am

Institut für Geographie und Regionalforschung  
Studienzweig Theoretische und Angewandte Geographie

Wien, im Dezember 2006

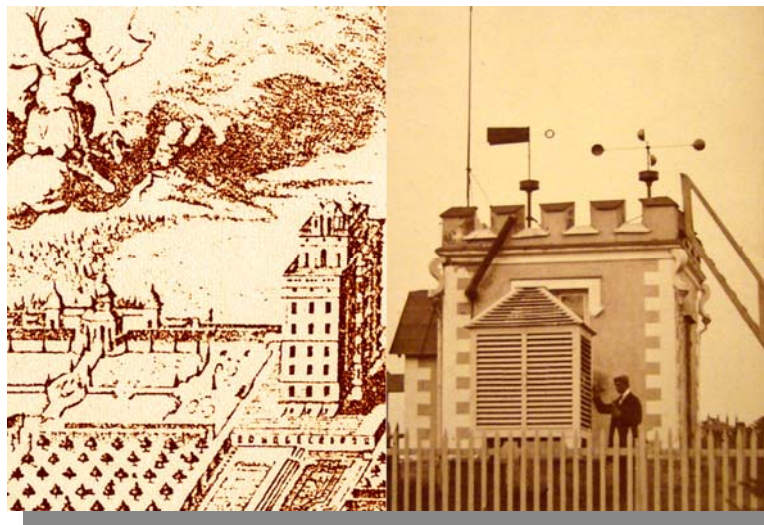


# The early instrumental climate period (1760-1860) in Europe

## Evidences from the Alpine region and Southern Scandinavia

### Diplomarbeit

zur Erlangung des Magistergrades der Naturwissenschaften  
an der Fakultät für Geowissenschaften, Geographie und Astronomie  
an der Universität Wien



eingereicht von

**Johann Hiebl**

am Institut für Geographie und Regionalforschung  
Studienzweig Theoretische und Angewandte Geographie

Betreuer

**Univ.Prof. Dr. Erich Mursch-Radlgruber**

in Zusammenarbeit mit

**Dr. Wolfgang Schöner**

Abteilung für Klimatologie, Zentralanstalt  
für Meteorologie und Geodynamik

**Prof. Anders Moberg**

Department of Physical Geography and  
Quaternary Geology, Stockholm University

Wien, im Dezember 2006

# Contents

|   |           |
|---|-----------|
| List of figures .....   | ii        |
| List of tables.....   | iv        |
| Abstract.....   | v         |
| Zusammenfassung .....   | vii       |
| Sammanfattning.....   | ix        |
| Acknowledgements.....   | xi        |
| <b>1 Introduction</b> .....   |           |
| 1.1 Temperature variability in the greater Alpine region and Scandinavia .....                | 1         |
| 1.2 Atmospheric circulation over Europe .....   | 7         |
| 1.3 Global climate modelling .....  | 12        |
| 1.4 The early instrumental period .....   |           |
| 1.4.1 History of instrumental measurements in the greater Alpine region and Scandinavia ..... | 14        |
| 1.4.2 The early instrumental paradox.....   | 18        |
| 1.5 Purpose of the thesis .....   | 23        |
| <b>2 Data</b> .....   | <b>26</b> |
| 2.1 The HISTALP dataset .....   | 26        |
| 2.2 The Uppsala and Stockholm records .....   | 30        |
| 2.3 Additional instrumental records.....  | 35        |
| 2.4 Proxy data.....   | 36        |
| 2.5 Temperature data from model simulations .....   | 40        |
| 2.6 Sea level pressure data.....  | 42        |
| <b>3 Methods</b> .....  |           |
| 3.1 General data handling .....   | 43        |
| 3.2 Statistical data treatment .....  | 44        |
| 3.3 Further homogenisation of the Uppsala and Stockholm records .....                         | 45        |
| 3.4 Creation of atmospheric circulation indices .....   | 50        |
| <b>4 Results</b> .....  |           |
| 4.1 Early instrumental temperature trends .....   | 52        |
| 4.2 Comparison with instrumental air pressure data .....                                      | 65        |
| 4.3 Comparison with proxy data .....  | 67        |
| 4.4 Comparison with model run .....   | 73        |
| 4.5 Linkage to atmospheric circulation.....   | 76        |
| <b>5 Discussion</b> .....   |           |
| 5.1 Natural temperature variability .....   | 84        |
| 5.2 Reliability of results.....   | 87        |
| 5.3 The early instrumental paradox reconsidered .....   | 90        |
| <b>6 Conclusions</b> .....  | <b>94</b> |
| Used abbreviations.....   | 96        |
| References.....   | 99        |

## List of figures

Front picture: *The “mathematical tower” of the monastery in Kremsmünster on a copperplate engraving from 1778 (left; Auer et al. 2001, appendix CD). The new observatory of Uppsala on an undated photograph (right; archive of the Sonnblickverein).*

|      |   |    |
|------|---|----|
| 1.1  | Temperature change at different geographical scales 1850–2005.....  | 2  |
| 1.2  | The NAO-related mode representing zonal flow over Europe reflected in the leading EOFs of gridded monthly mean SLP 1780–1995.....                                 | 8  |
| 1.3  | The EI paradox depicted by the graphical comparison between instrumental and proxy data 1722–2002.....  | 19 |
| 2.1  | Selected sites of EI data acquisition used in this thesis.....  | 27 |
| 2.2  | The locations of the 27 longest HISTALP temperatures series and available proxy records from the GAR.....   | 29 |
| 2.3  | The locations of UST, the actual reference series and available proxy records from Southern Scandinavia.....  | 34 |
| 3.1  | Monthly temperature corrections applied to the UST series before the mid-19 <sup>th</sup> century giving rise to four diverging versions.....                     | 46 |
| 3.2  | The Q- and T-series for monthly temperature series of May in UPPo and June in STO as example for SNHT results.....  | 49 |
| 4.1  | Mean annual temperature evolution and variability in the different subregions of the GAR 1760/81–2005 and UST 1722–2004 .....                                     | 53 |
| 4.2  | Comparison of mean winter, spring, summer and autumn temperature evolution and continentality index in the GAR 1760–2005 and in UST 1722–2004.....                | 54 |
| 4.3  | Comparison of the change of summer and annual temperature trends with different length for the GAR, UST and USTh.....   | 57 |
| 4.4  | Running correlations over a 21-year window of mean summer and annual temperature between the GAR and UST 1760–2004 .....  | 62 |
| 4.5  | Isopleth diagram showing seasonal differences and temporal evolution of the running correlations between the Alpine subregions CRS-NE-NW and US 1760–2004 .....   | 62 |
| 4.6  | Comparison of mean summer and annual temperature evolution in the Alpine subregions CRS-NE-NW 1760–2005, UST and USTh 1722–2004 at different temporal scales..... | 63 |
| 4.7  | Differences of mean summer and annual temperature between the Alpine subregions CRS-NE-NW and UST and USTh respectively 1760–2004 .....                           | 64 |
| 4.8  | Comparison between instrumental summer temperature and air pressure time series 1722–04 .....   | 66 |
| 4.9  | Comparison between instrumental and proxy data for the Alpine region 1720–2005.....   | 71 |
| 4.10 | Comparison between instrumental and proxy data for Southern Scandinavia 1722–2005 .....   | 71 |
| 4.11 | Mean summer temperature anomalies during six subperiods from 1722–1990 over Europe as simulated by Erik2 .....  | 74 |
| 4.12 | The same as in Figure 4.11 but for mean annual temperature.....   | 74 |

|      |   |    |
|------|---|----|
| 4.13 | Comparison of mean summer and annual temperature evolution 1720–1990 as simulated by Erik2 for three grid points corresponding with the location of the GAR and one grid point corresponding with the location of UST – Differences between simulated temperature by Erik2 and observed GAR and UST temperature respectively 1722–1990 for the summer season and the whole year ..... | 75 |
| 4.14 | The four leading EOFs out of the ADVICE air pressure dataset 1780–1995 for the average of the whole summer season and the individual summer months .....  | 77 |
| 4.15 | Temporal evolution of the L/H-like and NAO-like ECs and their 20-years Gaussian low-pass filtered trends in comparison to the 20-years Gaussian low-pass filtered trends of GAR, UST and USTh temperatures 1770–2005 for the average of the whole summer season and the individual summer months .....  | 80 |
| 4.16 | Temporal evolution of the NAO-like EC and its 20-years Gaussian low-pass filtered trend in comparison to the 20-years Gaussian low-pass filtered trends of GAR, UST and USTh temperatures 1770–2005 for the winter season .....   | 81 |
| 4.17 | Running correlations over a 21-year window between the L/H-like and NAO-like ECs and GAR and US temperatures respectively 1780–1995 for the average of the whole summer season and the individual summer months .....   | 83 |
| 5.1  | Running correlations over a 21-year window of mean summer temperatures between the GAR and UST against the temporal evolution of 10-year Gaussian filtered trends of the L/H-like and NAO-like ECs 1760/80–1995/2004 .....  | 86 |
| 5.2  | Difference series between homogenised and original temperature data 1760–1998 from 19 of the 27 EI temperature series out of the HISTALP dataset for the summer season and the whole year .....   | 89 |
| 5.3  | Overview over accomplished analyses in connection with the EI paradox.....  | 92 |

## List of tables

|      |  |    |
|------|--|----|
| 1.1  | Long-term change of mean annual temperature in the GAR and Scandinavia in different subperiods.....  | 4  |
| 2.1  | The EI subset of the 27 longest HISTALP temperature series.....  | 28 |
| 2.2  | The UST temperature series and potential reference series .....  | 33 |
| 3.1  | Monthly temperature corrections applied to the different versions of the UST series .....  | 46 |
| 3.2  | Reference series utilised in and primary breaks detected by SNHT procedures .....  | 48 |
| 4.1  | Long-term change of mean summer and annual temperature in the GAR in different subperiods and subregions and for UST in different subperiods and different versions.....   | 56 |
| 4.2  | List of the negative and positive monthly, seasonal and annual extreme values at single stations, subregions and the entire regions of the GAR and UST .....   | 59 |
| 4.3  | Correlation table of the mean summer and annual temperature series of the GAR and its subregions with different versions of the UST temperature series .....   | 61 |
| 4.4  | Differences of mean summer and annual temperature between the Alpine subregions CRS-NE-NW and UST and USTh respectively in different subperiods from 1760–2004.....  | 65 |
| 4.5  | Correlations between the mean temperature and air pressure series of the GAR and UST and USTh respectively in different periods.....   | 66 |
| 4.6  | Long-term change of observed and reconstructed proxy summer temperature in the GAR and Southern Scandinavia in different subperiods .....  | 68 |
| 4.7  | Correlations between instrumental and proxy data time series for the Alpine region and Southern Scandinavia .....  | 69 |
| 4.8  | Comparison between observed instrumental and simulated model mean summer and annual temperature anomalies for six subperiods .....   | 73 |
| 4.9  | Explained variance and cumulative explained variance of air pressure variability according to the ADVICE dataset 1780–1995 by the four leading EOFs shown in Figure 4.14 for the average of the whole summer season and the individual summer months ..... | 77 |
| 4.10 | Correlation table of the mean temperature series of the GAR subregions and UST versions with the L/H-like and NAO-like ECs for the whole summer season and the individual summer months.....   | 82 |

## Abstract

*The early instrumental climate period (1760–1860) in Europe – Evidences from the Alpine region and Southern Scandinavia*

To assess the anthropogenic contribution to the ongoing climate change in the light of natural long-term climate variability is one of the major tasks in climate research. Unfortunately, the start of most long-term series of instrumental meteorological observations around 1860 coincides temporally with the onset of full industrialisation. In this regard, the 27 carefully homogenised instrumental temperature records from the greater Alpine region starting between 1760 and 1830 and the two series from Uppsala and Stockholm in Southern Sweden starting in 1722 and 1756 respectively are of unique value. From both regions, an episode of outstandingly warm summers around 1800 is known. Interestingly, local proxy data clearly contradict this decadal-scale climate feature in both cases. The discrepancy between observational and proxy climate trends around 1800 is referred to as the “early instrumental paradox”.

The present thesis is the first comprehensive study that solely addresses this problem in an interregional approach employing a variety of data sources and analysis techniques. Firstly, existing doubts about the high summer temperature level before the 1850s in Uppsala and Stockholm motivated further relative homogeneity testing using five independent North European long-term series. These homogeneity tests lead to negative summer temperature adjustments before 1853 (for Uppsala) and 1859 (for Stockholm) of up to one degree. Still, direct comparative investigations of summer temperature evolution in the Alps and Sweden support the existence of the warm early period with different temporal accentuations. Generally, despite of individual peculiarities the overall agreement of decadal-scale trends in the two series can be described to be rather good, even if the climatic relationship is temporally instable and weakest in the warm season. Concurrent air pressure series reflect the high early summer temperature level in the Alpine region, a finding that can not be applied on Uppsala and Stockholm. The close investigation of available proxy reconstructions (Alps: tree-ring widths, ice-cores, glacier lengths; Southern Scandinavia: harvest dates and moraine stands), however, confirms the early instrumental paradox without exception. An examined run of simulated Alpine and Southern Scandinavian temperatures obtained with the general circulation model ECHO-g does not indicate any signal of warm summer conditions around 1800. The time series of leading atmospheric circulation patterns during summer as derived from EOF analysis on gridded air-pressure fields over Europe, based on barometer observations, are found to be too weakly correlated to temperature evolution to deduce any reliable assumptions.



Conclusively, the current summer warmth after around 1990 in the Alpine region and Southern Scandinavia is interpreted to have so far insignificantly exceeded beyond the limits of natural variability as indicated by 250 years of instrumental observations, specifically the warmth around 1800, which differs from the contemporary one by seasonal and regional restriction and temporal scattering. In spite of the obtained deeper insights in interregional summer temperature linkage and the deepened discussion of drawbacks of observational data and proxy methods, the early instrumental paradox itself could not be resolved.

## Zusammenfassung

### *Die frühe instrumentelle Klimaperiode (1760–1860) in Europa – Zeugnisse aus dem Alpenraum und Südsandinavien*

Eine der vorrangigen Aufgaben der Klimatologie ist es, den anthropogenen Anteil am aktuellen Klimawandel in Anbetracht der natürlichen, langfristigen Klimavariabilität einzuschätzen. Bedauerlicherweise fällt der Beginn der meisten meteorologischen Langzeitreihen um das Jahr 1860 zeitlich mit dem vollen Einsetzen der Industrialisierung zusammen. Vor diesem Hintergrund erscheinen die 27 sorgfältig homogenisierten, instrumentellen Temperaturreihen aus dem Alpenraum, die im Zeitraum zwischen 1760 und 1830 anlaufen, und die beiden Reihen aus Uppsala und Stockholm in Südschweden, welche in den Jahren 1722 bzw. 1756 beginnen, besonders wertvoll. Ein Abschnitt außergewöhnlich warmer Sommer um 1800 ist aus beiden Regionen überliefert, steht jedoch in beiden Fällen eindeutig im Widerspruch zu lokalen Proxydaten. Diese Widersprüchlichkeit zwischen beobachteten und indirekt rekonstruierten Klimareihen an der Wende zum 19. Jahrhundert wird als „frühe instrumentelle Paradoxon“ bezeichnet.

Die vorliegende Diplomarbeit widmet sich als erste eingehende Untersuchung ausschließlich dieser Problemstellung in einem interregionalen Ansatz und bedient sich dabei der unterschiedlichsten Datenquellen und Analysemethoden. Zunächst wurden bestehende Bedenken hinsichtlich des hohen Temperaturniveaus vor den 1850erjahren in Uppsala und Stockholm zum Anlass für weitere relative Homogenitätstests anhand fünf eigenständiger nordeuropäischer Langzeitreihen genommen, was zu negativen Anpassungen der Sommertemperaturen vor 1853 (in Uppsala) bzw. 1859 (in Stockholm) um bis zu ein Grad führte. Dessen ungeachtet wird das Vorhandensein der warmen frühen Periode in direkten Vergleichsstudien der Entwicklung von alpinen und schwedischen Sommertemperaturen mit unterschiedlichen zeitlichen Schwerpunkten bestätigt. Grundsätzlich kann die allgemeine Übereinstimmung dekadischer Trends in den beiden Regionen trotz individueller Besonderheiten als ziemlich gut beschrieben werden, wenngleich die klimatische Verbindung zeitlich unbeständig und während der warmen Jahreszeit am schwächsten ausgeprägt ist. Zeitgleiche Luftdruckreihen spiegeln das hohe Temperaturniveau der Sommer um 1800 im Alpenraum wider, eine Erkenntnis, die nicht auf Uppsala und Stockholm umgelegt werden kann. Die gründliche Analyse der zugänglichen Proxyrekonstruktionen (Alpen: Baumringbreiten, Eisbohrkerne, Gletscherlängen; Südsandinavien: Erntedaten und Endmoränenstände) bekräftigt hingegen durchgehend das frühe instrumentelle Paradoxon. Ein untersuchter Lauf von simulierten alpinen und südschwedischen Temperaturen aus dem allgemeinen Zirkulationsmodell ECHO-g beinhaltet keine Anzeichen für warme

Sommerverhältnisse um 1800. Die Verbindung von Zeitreihen der vorherrschenden atmosphärischen Zirkulationsmuster im Sommer, errechnet aus auf Barometermessungen beruhenden Gitterpunktfeldern des Luftdrucks über Europa mithilfe der EOF Analyse, zur Entwicklung der Temperatur wird als zu schwach angesehen, um daraus zuverlässige Schlüsse ableiten zu können.

Abschließend scheint die gegenwärtige sommerliche Wärmephase seit etwa 1990 im Alpenraum und Südkandinavien bisher in unerheblichem Ausmaß die Grenzen der aus instrumentellen Beobachtungen der letzten 250 Jahre bekannten, natürlichen Klimavariabilität, namentlich der Wärmephase um 1800, die sich von dem aktuellen Wandel sowohl durch ihre jahreszeitliche und regionale Beschränkung als auch durch die zeitliche Zergliederung unterscheidet, überschritten zu haben. Ungeachtet der gewonnenen tieferen Einsichten in die interregionale Verbindung der Sommertemperatur und der eingehenden Diskussion der Beeinträchtigungen von Beobachtungsdaten und Proxymethoden konnte das frühe instrumentelle Paradoxon an sich nicht aufgelöst werden.

## Sammanfattning

*Den tidiga instrumentella klimatperioden (1760–1860) i Europa – Indicier från den alpina regionen och södra Skandinavien*

En av klimatforskningens mest centrala uppgifter är att kvantifiera den antropogena delen av den pågående klimatförändringen, med hänsyn tagen till de naturliga, långsiktiga variationerna. Olyckligtvis sammanfaller början av de flesta långa meteorologiska observationsserierna runt 1860 med den industriella revolutionens fulla utblomning. Med detta som bakgrund förefaller de 27 grundligt homogeniserade instrumentella temperaturserierna från den alpina regionen, med start mellan 1760 och 1830, samt de två serierna från Uppsala och Stockholm i södra Sverige, med start 1722 respektive 1756, vara av unikt värde. En period med ovanligt varma somrar återfinns i båda regionerna omkring år 1800, vilket dock klart motsägs av lokala proxydata i bägge fall. Denna diskrepans mellan observerade och indirekt rekonstruerade tendenser i klimatet vid 1800-talsskiftet betecknas som den "tidiga instrumentella paradoxen".

Detta examensarbete är den första omfattande rapporten som uteslutande fokuserar på detta problem med en interregional ansats och med användande av en uppsättning olika datakällor och analysmetoder. Till att börja med lade befintliga tvivelaktigheter rörande den höga tidiga temperaturnivån i Uppsala och Stockholm grund för ytterligare relativa homogenitetstester baserade på fem oberoende nordeuropeiska långtidsserier. Dessa homogenitetstester ledde till en negativ justering av sommartemperaturerna före 1853 (i Uppsala) respektive 1859 (i Stockholm) med upp till en grad. Direkt jämförbara studier av utvecklingen mellan alpina och svenska sommartemperaturer stödjer ändå förekomsten av den varma tidiga perioden, om än med något olika tidsmässiga tyngdpunkter. Principiellt kan, trots individuella egenarter, den allmänna överensstämmelsen mellan dekadala trender i de två regionerna beskrivas som ganska god, även om klimatrelationen är temporärt instabil och som svagast under den varma årstiden. Samtidiga lufttrycksserier återspeglar de höga tidiga sommartemperaturerna i den alpina regionen. Ingen sådan iakttagelse kan dock appliceras på data från Uppsala och Stockholm. Den ingående analysen av tillgängliga proxyrekonstruktioner (Alperna: bredden hos träds årsringar, isborrskärnor, glaciärlängder; södra Skandinavien: datum för skörd och positionen av ändmoräner) styrker den tidiga instrumentella paradoxen utan undantag. Ett undersökt förlopp av den simulerade temperaturen i det alpina området och södra Skandinavien erhållet från den allmänna cirkulationsmodellen ECHO-g indikerar ingen signal med varma sommarförhållanden omkring 1800. Tidsserier över dominerande atmosfäriska cirkulationsmönster sommartid, beräknade med hjälp av EOF-analys utifrån rasterfält för lufttrycket över Europa baserat på

barometerobservationer, anses vara för svagt korrelerade till temperaturutvecklingen för att det ska kunna nyttjas till att dra pålitliga slutsatser.

Avslutningsvis verkar den nuvarande värmefasen efter omkring 1990 i det alpina området och södra Skandinavien hittills i försumbar utsträckning ha överskridit gränsen för naturlig variation indikerat av 250 års instrumentella observationer, speciellt värmefasen omkring 1800 vilken skiljer sig från den nutida avseende regional och årstidsmässig begräsning och tidsmässig spridning. Trots de fördjupade insikterna om den interregionala sommartemperaturkopplingen och den fördjupade diskussionen av problem hos observationsdata och proxymetoder kunde inte den tidiga instrumentella paradoxen redas ut.

## Acknowledgements

After ten months of concentrated work, the time has come to express my gratitude to a number of persons without whom I would not have made it. To begin with the professionals, I certainly have to thank *Dr. Wolfgang Schöner* and *Prof. Anders Moberg* who were a great help in defining the topic, suggested qualified research ideas, motivated improvements and corrected language mistakes. To be honest, the thesis would look quite different without their demanding but always constructive objections. I also want to mention the personal atmosphere that was typical for all meetings. For supervising the diploma thesis, I wish to thank *Univ.Prof. Dr. Erich Mursch-Radlgruber* and *Anders Moberg* again. Besides Wolfgang and Anders, *Ulf Büntgen*, *Dr. Dietmar Wagenbach*, *Prof. Dr. Hans Oerlemans*, *Dr. Øyvind Nordli*, *Dr. John Cappelen* and *Dr. Olga Bulygina* has to be thanked for data provision. *Dr. Reinhard Böhm*, *Linus Magnusson* and *Rezwana Mohammad* acted as helpful advisors. The *Research Services and International Relations Office* of the University of Vienna provided financial support. In organisational matters, I enlisted the assistance of *Karin Ebert* and *Pernilla Schuber*.

I am also grateful to my family and great-aunt for giving me the possibility of higher education, my friends for the amusing student days we had and the one.

This study was supported by the EU-project ALP-IMP (*Multi-centennial climate variability in the Alps based on instrumental data, model simulations and proxy data*; EVK2-CT-2002-00148).

# 1 Introduction

## 1.1 Temperature variability in the greater Alpine region and Scandinavia

Since area-wide climatologic recordings started about one and a half centuries ago, a prominent increase of global mean surface air temperature has been observed. Independently arranged studies (largely based on common data), primarily the *Climatic Research Unit* (CRU) global dataset (e.g. Jones and Moberg 2003), the *Global Historical Climatology Network* (GHCN) dataset (e.g. Smith and Reynolds 2005) and the *Goddard Institute for Space Studies* (GISS) analyses (e.g. Hansen *et al.* 2001), determine this global warming with a roughly similar size of 0.081, 0.06 and 0.065 K decade<sup>-1</sup> respectively for the 1901–2004 period. In general, the temperature rise has proceeded temporally and spatially irregularly (Fig. 1.1). It has mainly been confined to two phases that can approximately be defined by the periods from 1920–44 and from 1975 to date, and within these the boreal winter was the most affected season. Furthermore, a greater warming over Northern Hemisphere (NH) land areas and polar regions has been noted. The recent temperature rise beginning in the seventies has been an especially intense one (0.206 K decade<sup>-1</sup> for the 1977–2001 period; Jones and Moberg 2003, 218), and for the time being no end is in sight (IPCC 2001, 527–529). The 1990s were indisputably the warmest observed decade with 1998 and 2002–05 heading the list of the warmest years (Jones and Moberg 2003, 219; CRU 2006). Europe (Fig. 1.1c) is among those regions of the world where the temperature rose slightly more than the global average, namely by 0.076 K decade<sup>-1</sup> during the 20<sup>th</sup> century; notably, the ongoing warming (0.425 K decade<sup>-1</sup> for the 1977–2001 period) has been especially strong there (Jones and Moberg 2003, 215). Luterbacher *et al.* (2004, 1499–1500, 1503) suggest that this late 20<sup>th</sup> century warmth is unique in Europe for at least the past 500 years and subsume that most “early instrumental and documentary evidence ... support the conclusion that the warmth of the late 20<sup>th</sup> century is likely unprecedented in the Northern Hemisphere in the past 1,000 years and cannot be explained by natural forcings alone”.

The sole existence of long European instrumental temperature records in itself as they are present in Alpine and Scandinavian countries is a good reason to take a closer comparative look at temperature climate trends during the early instrumental period (1722/60–1860; see p. 18 for the definition). The rich and far back-reaching homogenised instrumental climate information available in the Alps offered by the HISTALP (*Historical Instrumental Climatological Surface Time*

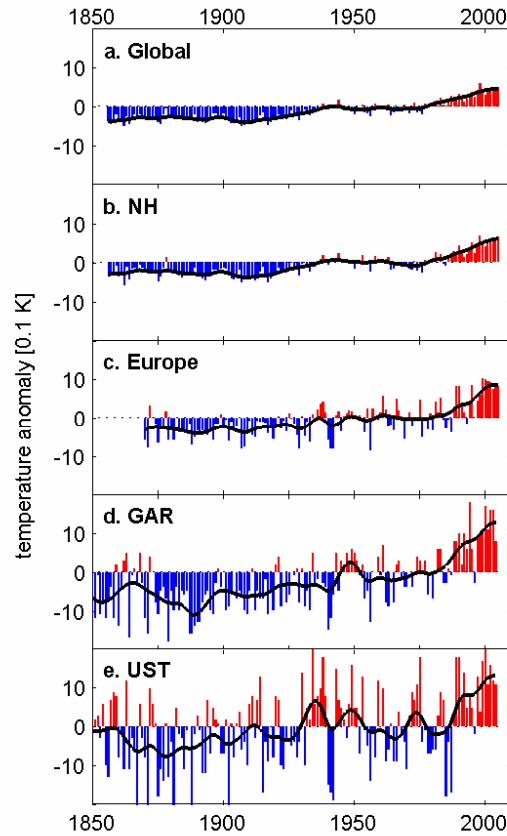


**Figure 1.1** Temperature change at different geographical scales. **a.** Global 1856–2005 (up to about 3,800 stations on land plus marine observations from HadCRUT2v, Jones and Moberg 2003) **b.** Northern Hemisphere 1856–2005 (up to about 3,200 stations, *ibid.*) **c.** Europe 1887–2005 (35°N15°W–60°N60°E, *ibid.*) **d.** Greater Alpine region 1850–2004 (27 longest stations from HISTALP, Auer et al. 2006) **e.** Uppsala and Stockholm mean 1850–2004 (2 stations, Bergström and Moberg 2002; Moberg et al. 2002). Shown are annual temperature anomalies from the 1961–90 average (bars) and their 20-years Gaussian low-pass filtered trends (lines).

Series of the Greater Alpine Region) database (Auer et al. 2006), which also underlies large parts of the present thesis (for data description see Chapter 2.1), allows an unusually extensive study of climate development on a regional scale. This instance is so much the more valuable as the greater Alpine region (GAR, 43°N4°E–49°N19°E) comprehends a variety of different climate regimes. With a length of 1,200 km and a width of up to 300 km the mountain chain combines three principal climates: Maritime influences from the North Atlantic, primarily dominating in Western and North-western parts of the GAR, and also from the Mediterranean Sea in the South interfere with continental influences from the Eurasian land mass farther to the East. The zonal extension of the Alps intensifies the division between moderate westerly climate north and Mediterranean climate south of the main chain. West-east discrepancies are therefore in general less marked than meridional ones. The mean annual temperature (1961–90) reaches typically values from 8 °C in the Northern Alpine foreland (e.g. Augsburg) to 16 °C off the Dalmatian coast (e.g. Hvar). Whereas the



difference between the coldest and the warmest monthly means are usually about 17 K in the west (e.g. Nancy), the annual temperature range in the east (e.g. Budapest) accounts for 22 K. Significantly, climate in the winter months is largely controlled by the North Atlantic Oscillation (NAO) with influence also from the Siberian high. During the summer months, more localised low-pressure systems dominate the weather pattern. Due to the structured relief, the Alps are characterised by small-scale climate modifications. Valley and basin positions (e.g. annual temperature range of 23 K in Klagenfurt) in contrast to saddle and summit positions introduce local topographic effects in climate, e.g. related to temperature inversions. Ranging from low-elevation plains to high-mountainous regions above the tree- and snowline, annual mean temperature drops by about 0.65 K 100 m<sup>-1</sup> with increasing altitude, leading to a total decrease of 24 K (16 to -8 °C) at the vertical 3.5 km for which station data exists. Additionally, with increasing altitude the coldest and warmest months of the average year move forwards from January to February and from July to August respectively, together with the annual temperature range becoming smaller (Matulla *et al.* 2005, 13–18; Böhm *et al.* 2001, 1779; Casty *et al.* 2005, 1856).

The Alps are a highly vulnerable region to climate change. According to the first comprehensive temperature trend analyses out of the HISTALP data pool (Auer *et al.* 2006; Matulla *et al.* 2005) the GAR has warmed by 0.119 K decade<sup>-1</sup> on average and the 27 longest series thereof by 0.128 K decade<sup>-1</sup> during the 20<sup>th</sup> century (Tab. 1.1), which is nearly twice as much as the global average trend, e.g. according to Jones and Moberg 2003 (Fig. 1.1d). National studies for Austria (Auer *et al.* 2001a), Switzerland (Begert *et al.* 2005) and North-western Italy (Brunetti *et al.* 2006) confirm this magnitude with values of 0.106–0.117 (period 1890–1999), 0.06–0.12 (period 1864–2000) and 0.1 K decade<sup>-1</sup> (period 1865–2003) in the respective areas. Similarly to global findings, Casty *et al.* (2005, 1859) place 1994, 2000 and 2002–03 at the top of the list over the warmest years in the Alpine region – in this case even for the last half-millennium (including climate proxy data). Instrumental data availability in the Alps facilitates analyses reaching into the 18<sup>th</sup> and 19<sup>th</sup> centuries: After an initial warming trend in the end of the 18<sup>th</sup> century (0.222 K decade<sup>-1</sup> for the 1768–1800 period), the 19<sup>th</sup> century showed a cooling trend by -0.062 K decade<sup>-1</sup>. The globally observed stepwise temperature rise during the 20<sup>th</sup> century is also reproduced in the GAR data and conveniently captured by the subperiods 1901–40 (first warming by 0.085 K decade<sup>-1</sup>), 1941–70 (intermediate cooling by -0.082 K decade<sup>-1</sup>) and 1971–2004 (intense warming by significant 0.483 K decade<sup>-1</sup>). The breakdown into half-years reveals that winters, which ever since 1500 had been colder than during the 20<sup>th</sup> century, underwent a strong transition phase from 1890–1915, leading to a milder climate. The colder climate conditions can be said to have lasted longer if only the summer temperature is considered; the transition in this season occurred first around 1910, after which the two warming steps have been more pronounced (Auer *et al.* 2006, 17; Casty *et al.* 2005, 1859). Furthermore, Matulla *et al.* (2005, 31–32, 40) found the dissimilarity among the months

**Table 1.1** Long-term change of mean annual temperature in the GAR and Scandinavia in different subperiods. For each series, the upper italic values indicate the respective trends [K decade<sup>-1</sup>] derived from linear regression and the lower roman numbers give the total temperature change [K] during the respective periods, as explained by the linear trends. Underscored trends are significant at the 95 % level, double underscored trends at the 99 % level. For series acronyms see Tables 2.1 (p. 28) and 2.2 (p. 33).

| time period     |                                    | a <sub>1</sub> –<br>2004 | a <sub>1</sub> –<br>1860 | 1861–<br>2004 | a <sub>1</sub> –<br>1800 | 1801/ a <sub>1</sub> –<br>1900 | 1901–<br>2000 | 1901–<br>40 | 1941–<br>70 | 1971–<br>2004 |
|-----------------|------------------------------------|--------------------------|--------------------------|---------------|--------------------------|--------------------------------|---------------|-------------|-------------|---------------|
| number of years |                                    | 176–283                  | 42–139                   | 144           | 34–79                    | 72–100                         | 100           | 40          | 30          | 34            |
| series          | starting<br>year (a <sub>1</sub> ) |                          |                          |               |                          |                                |               |             |             |               |
| GAR             | 1760                               | <u>0.03</u>              | -0.02                    | <u>0.10</u>   | <u>0.22</u>              | <u>-0.06</u>                   | <u>0.13</u>   | 0.09        | -0.08       | <u>0.48</u>   |
|                 |                                    | 0.69                     | -0.24                    | 1.42          | 0.91                     | -0.62                          | 1.28          | 0.34        | -0.25       | 1.64          |
| KRE             | 1768                               | <u>0.02</u>              | <u>-0.07</u>             | <u>0.09</u>   | 0.30                     | <u>-0.08</u>                   | <u>0.11</u>   | 0.03        | -0.08       | <u>0.43</u>   |
|                 |                                    | 0.46                     | -0.63                    | 1.28          | 0.98                     | -0.83                          | 1.08          | 0.13        | -0.24       | 1.46          |
| BAS             | 1760                               | <u>0.04</u>              | -0.02                    | <u>0.11</u>   | <u>0.20</u>              | -0.05                          | <u>0.14</u>   | 0.13        | -0.09       | <u>0.56</u>   |
|                 |                                    | 0.92                     | -0.17                    | 1.59          | 0.80                     | -0.52                          | 1.44          | 0.52        | -0.28       | 1.92          |
| PAD             | 1774                               | <u>0.01</u>              | -0.05                    | <u>0.08</u>   | -                        | <u>-0.06</u>                   | <u>0.09</u>   | 0.09        | -0.02       | <u>0.46</u>   |
|                 |                                    | 0.33                     | -0.44                    | 1.11          | -                        | -0.60                          | 0.94          | 0.34        | -0.05       | 1.57          |
| TOR             | 1760                               | <u>0.03</u>              | <u>-0.04</u>             | <u>0.10</u>   | <u>0.22</u>              | <u>-0.04</u>                   | <u>0.10</u>   | <u>0.13</u> | -0.07       | <u>0.55</u>   |
|                 |                                    | 0.79                     | -0.39                    | 1.40          | 0.89                     | -0.43                          | 1.04          | 0.53        | -0.21       | 1.89          |
| GSB             | 1818                               | <u>0.05</u>              | <u>-0.26</u>             | <u>0.09</u>   | -                        | -0.04                          | <u>0.13</u>   | 0.12        | -0.23       | <u>0.46</u>   |
|                 |                                    | 0.99                     | -1.11                    | 1.24          | -                        | -0.35                          | 1.34          | 0.46        | -0.68       | 1.58          |
| UPP             | 1722                               | 0.01                     | <u>-0.05</u>             | <u>0.09</u>   | -0.10                    | -0.03                          | <u>0.08</u>   | 0.26        | -0.19       | <u>0.43</u>   |
|                 |                                    | 0.20                     | -0.74                    | 1.33          | -0.78                    | -0.28                          | 0.82          | 1.04        | -0.58       | 1.47          |
| STO             | 1756                               | <u>0.02</u>              | -0.02                    | <u>0.09</u>   | 0.09                     | -0.02                          | <u>0.07</u>   | 0.22        | -0.18       | <u>0.32</u>   |
|                 |                                    | 0.56                     | -0.16                    | 1.28          | 0.40                     | -0.15                          | 0.69          | 0.89        | -0.54       | 1.08          |
| KOP             | 1789                               | <u>0.08</u>              | -0.13                    | <u>0.14</u>   | -                        | -0.02                          | <u>0.14</u>   | <u>0.23</u> | 0.04        | 0.16          |
|                 |                                    | 1.71                     | -0.81                    | 1.95          | -                        | -0.18                          | 1.36          | 0.92        | 0.12        | 0.55          |
| OSL             | 1816                               | <u>0.10</u>              | 0.06                     | <u>0.10</u>   | -                        | <u>0.10</u>                    | <u>0.07</u>   | 0.16        | -0.19       | 0.30          |
|                 |                                    | 1.89                     | 0.29                     | 1.42          | -                        | 0.88                           | 0.72          | 0.63        | -0.58       | 1.03          |
| HEL             | 1829                               | <u>0.07</u>              | 0.26                     | <u>0.08</u>   | -                        | 0.07                           | <u>0.07</u>   | 0.26        | -0.03       | 0.27          |
|                 |                                    | 1.28                     | 0.82                     | 1.17          | -                        | 0.51                           | 0.75          | 1.03        | -0.10       | 0.90          |

to be high, showing a striking warming in November to March but a weak one in April and September (period 1768–2003). Regarding this complete 234-year-long time span, features like zero or even insignificantly negative trends for May to August are revealed, implying that summers in the late 18<sup>th</sup> century were at least as warm as today's – a result that among other things (which are posed in Chapter 1.5) prompts the current thesis. The combined reconstruction-observation approach of Casty *et al.* (2005, 1859) identified the 1590s, 1960s, 1730s and 1890s to be the coldest decades of the past 500 years; 1740 was the very harshest year (1829/30 and 1816 were the coldest winter and coolest summer season respectively). On the other hand, the warmest periods occurred from 1780–1810, 1890–1945 and from 1970 onwards, with the above-mentioned warmest years

taking place very recently. Considering individual years, 1606/07 and 2003 stand out as the mildest winter and hottest summer respectively.

High spatial similarity in temperature trends has been spotted within the GAR between smaller and rather homogeneous subregions. Little difference in low-frequency temperature variability is also seen between high and low-elevation stations; since the high-Alpine summit observatories reveal the same long-term trend as the urban and rural stations in the valleys and forelands. Auer *et al.* (2006, 17) conclude that it is not the warming in the mountains that pushes the mean GAR-warming up. Rather, it is the GAR as a whole that has been affected by a twice as large temperature rise compared to global estimates. Direct comparison to the CRU-data shows that the Alps' warming is enhanced due to a lower temperature level of the GAR temperature during the last decades of the 19<sup>th</sup> century combined with a higher level in the 1980s and -90s.

A regular precipitation increase caused by a temperature forced enhanced water cycle has not been observed in the GAR data so far (Casty *et al.* 2005, 1868). By contrast, temperature impact is drastically visible in glacier response. Alpine glaciation plays a vital role in freshwater storage and water cycle regulation. Matulla *et al.* (2005, 55–58) remarked that significantly warm or cold periods in the HISTALP data strongly reflect Alpine glacier development. The cool 1810s summers, for instance, supported the strong glacial advance that lead to the Little Ice Age (LIA)-maximum around 1850, whereas the warm summers during 1856–73 initiated the contemporary retreat and the most recent warm temperatures lead to a very pronounced glacier melting from 1990 onwards. From 1850–1975 the Alpine glaciers lost about half of their volume; between 1975 and 2000 another 25 % of the remaining ice volume vanished and additional 10–15 % only since then (Haeberli *et al.* 2006). Rates of ice mass change seem to have exceeded beyond the limits of historically known extremes recently, as the mean loss rate of Alpine glaciers since 1980 has doubled compared to the whole 20<sup>th</sup> century's mean (Haeberli and Holzhauser 2003, 13).

Whereas the Alps and their surroundings are situated at the southern border of the cool temperate climate zone, the Scandinavian Peninsula lies on its northern periphery, reaching into the (cold temperate) boreal zone in the north. Considering the high latitudinal position that can be compared to Alaska's, the climate is rather mild due to the strong influence of the North Atlantic current, which moderates the annual radiation deficit by an intense eastward drift of warm sea water, which in turn warms the prevailing westerly winds towards Scandinavia. Additionally, the (Caledonian originated) Scandinavian mountain chain modifies the main pattern. Temperature conditions are characterised by a steep sea-land-gradient that alters strongly maritime climate along the Norwegian coast with a small annual temperature amplitude (no enduring winters) towards a more continental climate with colder winters and warmer summers, e.g. in sheltered South-eastern Norwegian valleys or in Finnmark. Typically, monthly mean temperatures for

January and July respectively range from 1 to 14 °C near the Atlantic coast (e.g. Bergen), from 0 to 17 °C in Skåne (e.g. Malmö) or from -14 to 13 °C in Finnish Lapland (e.g. Inari). In northern regions, climate is much harsher than further in the south; whereas the snow cover in the Lappish winter may last for more than 200 days, the snow cover in Southern Sweden lasts less than 50 days. Southern Sweden may also experience quite hot summer temperatures (Raab and Vedin 1995; Wallén 1970).

An investigation of 68 temperature series distributed across Scandinavia (Tuomenvirta *et al.* 2001, 8) revealed that almost all of these stations show a positive trend in the 20<sup>th</sup> century temperature; in half of the cases it was significant at the 95 %-level. Moberg *et al.* 2005a (114–117) quantify this warming at 0.64 K between the two periods 1891/1920 and 1971/2000), based on six selected station time series. The temporal development, as recognised from global and Alpine estimates, is similarly reproduced in Scandinavia too; a first warming from the 1850s to the 1930s was followed by a slight 30-year cooling, whereupon the so far enduring warming phase has joined. In matters of seasonal differentiation, springs have warmed most (0.94 K) while autumns have warmed least (0.44 K); the high temperatures of the 1990s arose primarily from warm winters in this decade. When Moberg and Alexandersson (1997, 47–49) gridded homogenised Swedish temperature data to derive six grid-box temperature series over the country, they found great spatial similarity. The relatively smallest temperature difference between 1861/90 and 1965/94 was received for the North-eastern part (0.51 K), the largest one for the South-western part (0.74 K) of Sweden. Within Scandinavia, Southern Sweden provides two series that allow for investigation of temperature variability back in time as far as 1722 and 1756 respectively, namely the long-time series of Uppsala and Stockholm (herein abbreviated as UST). The valuable data they contain has lately been homogenised and used in a number of studies (Moberg and Bergström 1997; Bergström and Moberg 2002; Moberg *et al.* 2002; Moberg *et al.* 2003; Moberg *et al.* 2005a; Moberg *et al.* 2007). One of these (Moberg and Bergström 1997, 678–681) examines temperature variability at different time scales. Concerning periods of ten years in the Uppsala series, 1862–71 show the largest downward (-0.84 K compared to the 1961–90 average) and the 1730–39 show the largest upward anomaly (+1.05 K). 1867 was the coldest (-2.7 K) and 1723 the warmest single year (+2.5 K) on record. Whereas the harshest winter (-5.9 K in 1942) and coolest summer seasons (-2.7 K in 1902) happened to occur in the last century, the mildest winter (+5.5 K in 1724) and the hottest summers (+3.4 K in 1752 and 1761) took place near the series' beginning. To critically place these interesting outcomes of far back reaching instrumental data – all positive extremes of the series were achieved in the 18<sup>th</sup> century – in the context of recent climate warming (warm years were to follow) is one of the main objectives of this study (cf. Chapter 1.5). In terms of decades, the Uppsala temperatures of the 1730s, 1770s, 1790s and 1820s lay even above the 1961–90 average and the summers of the 1760s, 1770s and 1850s are comparable to those of the warm 1990s too (*ibid.*, 682). The summers in

the 1830s and from 1880 to 1920, on the other hand, were relatively cool. In contrast to the GAR, no special change in the annual number of hot days in Uppsala can be seen yet (Moberg *et al.* 2005a, 117). Furthermore, the winters of the 1720s and 1730 in Uppsala, which were caused to be unusually mild by extremely maritime climate, and the abrupt drop in both UST summer temperatures around 1860 are remarkable. On the contrary, nothing exceptional was found for the 30 years of warming until 1995 that did not significantly differ from the climate two centuries earlier (Moberg and Bergström 1997, 681–683). Concerning precipitation variability in Scandinavia, Tuomenvirta *et al.* (2001, 12) detected a positive trend in annual precipitation sums that is at least significant for the western parts of Scandinavia. Although the behaviour of individual glaciers depends on a number of factors like summer temperature, exposition or slope, it is this precipitation intensification that accounts for the general equilibrium state or even advance that has been typical for maritime Western Scandinavian glaciers during the 1980s and -90s. Anyhow, even there a trend reversal has taken place during the last years (Haeberli *et al.* 2005, 89). On a somewhat longer time scale, maximum glacial extension was reached centuries ago even in Scandinavia (LIA maximum in the mid-18<sup>th</sup> century; Nesje and Dahl 2000, 147–151).

## 1.2 Atmospheric circulation over Europe

Regarding atmospheric circulation over Europe, two main circulation phenomena, the NAO and the Eurasian Pattern, directly affect regional air pressure, temperature and precipitation climate. There are thus several reasons that make it worth studying temperature variability in relation to atmospheric circulation: (1) Large-scale modes like the NAO have an evident impact on monthly to decadal temperature variability across Europe. (2) The interest in intern climate system dynamics has recently grown due to their central role in climate change. (3) Because of the NAO being one of the most important drivers of European weather, there are some efforts going on in forecasting the evolution of its behaviour a few months in advance. (Hurrell *et al.* 2003, 1–2, 17–18; Wanner *et al.* 2000, 27–29).

The NAO has been recognised and described for centuries (Stephenson *et al.* 2003). It is the most marked and robust pattern of natural atmospheric circulation variability over the North Atlantic Ocean and the neighbouring continents. As a quasi-cyclic large-scale alternation of atmospheric pressure fields, it refers to the redistribution of atmospheric mass between the Arctic and the subtropical Atlantic. The oscillation is represented by the pressure gradient between the two centres of action, the subpolar Icelandic Low and the subtropical Azores High. It swings on monthly to decadal time scales from one phase to another, strongly influencing changes in wind

speed and direction, heat and moisture transfers, intensity and number of storms and temperature and precipitation patterns from the east of the United States to Siberia. Especially during winters, variations in the NAO exert their effects on natural environment and society (Hurrell *et al.* 2003, 1; Jacobeit *et al.* 2001, 219; Beniston and Jungo 2002, 29–30). Fluctuations in the oscillation are, among other things, caused

- within the atmosphere by heating patterns (temperature contrasts between polar and tropical latitudes) and stratospheric greenhouse gas and ozone concentrations (affecting the radiative balance),
- within the ocean by interannual to decadal differences in convective water exchange between the lower and the higher layers of the Atlantic,
- in between atmosphere, ocean, sea-ice and land systems by heat exchanges and various chaotic non-linear processes.

Successively, these mechanisms affect the thermohaline circulation and sea surface temperatures in the North Atlantic Ocean. By simultaneous climatic variations over distant regions of the globe, so-called teleconnections, the NAO is linked to other circulations modes like the Pacific-North American pattern, which in turn is coupled to the El Niño-Southern Oscillation phenomenon in the South Pacific (Hurrell *et al.* 2003, 4–7). The NAO's mode, that is characterised by a North-South dipole, gets best visible in the spatial pattern of the leading empirically determined orthogonal function (EOF; for method description see Chapter 3.4) of 500 hPa geopotential height fields (*ibid.*, 7–10, 29); but even EOFs of sea-level pressure (SLP) fields clearly reproduce the NAO-like dipole-structure (Fig. 1.2).

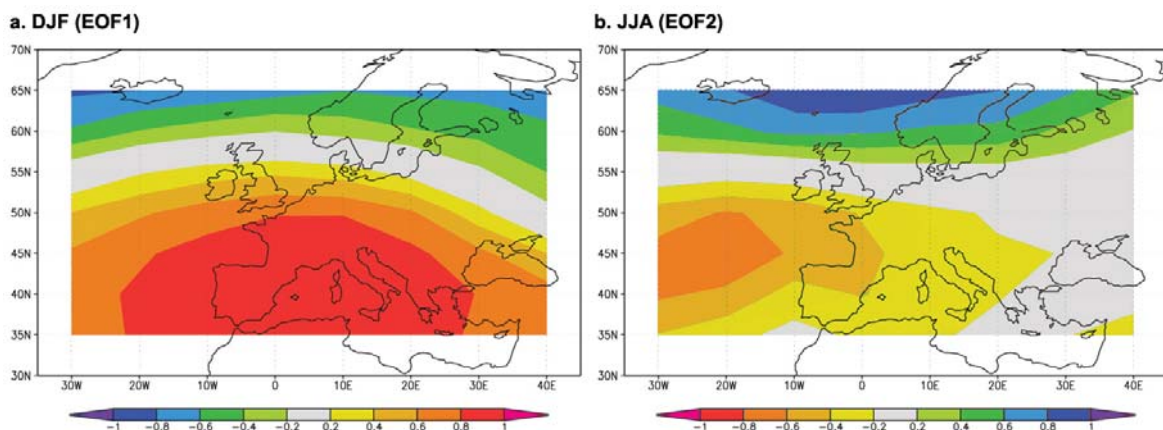


**Figure 1.2** The NAO-related mode representing zonal flow over Europe reflected in the leading EOFs of gridded monthly mean SLP 1780–1995 (Jones *et al.* 1999). **a.** During winters the centres of action roughly match the Icelandic cyclone and the Azores anticyclone. **b.** During summers the situation is more diffuse, as the centres shift towards the west (negative NAO-situation here).

The balance between atmospheric pressure gradients, the Coriolis force, and frictional forces largely determine air streams around the pressure systems (counterclockwise around cyclones, clockwise around anticyclones in the NH). Together, these factors produce the predominating atmospheric flow of westerly winds over Europe. Depending on the intensities of the pressure centres, positive and negative NAO phases are defined. During a positive phase, when the Icelandic Low and Azores High are strengthened, e.g. due to anomalously cold (warm) sea surface temperatures in the Northern (Southern) North Atlantic, an enhanced westerly flow, whose jet stream proceeds across Europe in a north-eastern direction, is the result. As a consequence, European winter weather conditions are windy, mild and wet. During a negative phase, when the pressure centres are not fully developed, eventually because of more even-tempered sea surface temperatures, the polar jet is weak. Hence, the calm, cold and dry winter Siberian high can extend its influence towards Europe. During summers, when the subtropical high gets stronger but the air pressure dipole's amplitude as a whole fades and shifts westwards, generally weak pressure gradients over Europe allow for more regional effects to determine weather conditions (Casty *et al.* 2005, 1869).

The sign and strength of a specific NAO-phase can be measured by an index, which hence is an indicator for the intensity of the westerlies across the North Atlantic into Europe (Beniston and Jungo 2002, 29). Among the variety of indices in use, three types can be distinguished: (1) Station-based indices (traditionally the air pressure difference of an Icelandic versus a Portuguese or Azorean station) are the oldest kind. They have a long temporal extent (back to around 1800), but are spatially fixed and influenced by small-scale weather effects. (2) Indices that account for the full spatial pattern of the atmospheric pressure field have advantages in this respect. This index type extracts time series, so-called principal component (PC) series, out of an EOF-pattern. However, extensive data to calculate PC series is mostly confined to the 20<sup>th</sup> century (Hurrell *et al.* 2003, 13). (3) In a third way, a mobile NAO index can be derived from correlation maps. Moving locations of maximum correlation between subpolar and subtropical SLP over the North Atlantic are used to calculate the pressure difference between the two centres of action (Portis *et al.* 2001, 2069-2070). For this thesis, a PC approach will be chosen later on (see Chapters 3.4 and 4.5).

An index allows to describe the temporal and – if mobile – spatial evolution of the NAO mode. Although no preferred time scale of NAO variability have been revealed, there are periods of persisting NAO phases, which cause interdecadal trends. Negative winter index values (until the 1850s) but positive summer values (until the 1870s), followed by a transition to a mostly negative mode in the 1870s and 1880s have been detected. From around 1900 to 1930 a generally positive winter phase arose from a southward displacement of the oscillation, later interrupted by a negative interval in the 1960s. Since the 1980s, partly strongly positive winter indices have become

common, whereas negative values are registered for summers (Hurrell *et al.* 2003, 14; Jacobeit *et al.* 2001, 224). The large upward NAO trend during winters in the recent decades seems to be exceptional in course of the last at least 500 years (Luterbacher *et al.* 2002, 554). This stepwise evolution, which shows similarities to the 20<sup>th</sup> century's temperature rise over the NH (see p. 1), suggests that the global-scale warming to some extent roots in a phenomenon with its centre in the North Atlantic region (Moberg *et al.* 2005a, 114).

In terms of spatial variability, the issue of seasonality is important because the focus of this study lies on summer conditions. Though the NAO is the NH's only large-scale circulation pattern that is evident all the year round, the dipole mode is not stationary (Hurrell *et al.* 2003, 8–9). The Azores High performs a general south-east to north-west movement over some 3,000 km from winter to summer, being preferably centred over the Eastern Atlantic or across the Iberian Peninsula in January and over the Gulf Stream in June and July (Portis *et al.* 2001, 2071). A migration of the action centres towards the east is a common feature of positive index months and has happened more frequently during the last decades. In addition, the variability of the pressure centres' amplitude, reaching its maximum values during winter, induces seasonal effects. The reason why the structure is more pronounced during the winter lies in larger temperature and, hence, pressure differences between subpolar and subtropical latitudes. As a result, the impact on climate variables and ecosystems is also most distinct in winter. Since more than one third of all SLP variance over the North Atlantic in winter can be explained by the oscillation's impact, the attention of NAO related studies has often been concentrated on winter months (Hurrell *et al.* 2003, 8–12).

Although the Alps are situated at the border of generally low temperature correlations with the NAO, the latter is one of the major climate driving factors in the GAR. The mountains act as a pivot, north of which the oscillation's influence on temperature variability is rather strong, whereas it diminishes noticeably with distance south of the Alps. In the main, high elevation sites that are more extensively exposed to the free atmosphere show a closer connection to NAO behaviour (Beniston and Jungo 2002, 38, 41; Casty *et al.* 2005, 1865; Auer *et al.* 2001b, 139–145). Actually, there is a positive correlation between the NAO and winter temperatures in the GAR, but it is neither stable nor always significant. The relationship is strongest during intervals with persistently mild winters due to strongly positive phases. Since the 17<sup>th</sup> century, two of so far four such significantly positive correlation phases (ca. 1750–1770 and 1800–1850) have occurred within the early instrumental period (Casty *et al.* 2005, 1865–1866). In modern times, good agreement between NAO variations and winter air pressure and temperature has been shown for the Swiss Alps (83 and 72 % explained variance respectively for 1961–1990). The notably warm winters since 1985 can largely be explained by the positive NAO behaviour. A considerable fraction of recent above global



average climate warming in the Alps may have arisen from high NAO episodes (Beniston and Jungo 2002, 34–40).

Circulation variability in Scandinavia is more closely connected to the NAO than in the GAR. Monthly temperatures relate well to NAO over the whole of Sweden (annual mean  $r = 0.46$  for 1865–1994; Chen and Hellström 1999, 509–510). Still, there are temporal and regional differences. Correlations vary largely from high values in winter to low or even negative ones in summer, as strong westerlies imply cooler summer temperature conditions in Scandinavia. However, a NAO-related index seems not to catch westerly flow over Scandinavia during the warm season. March is the month when the correlations are strongest. In the winter half-year, temperature in Southern Sweden agrees best with the oscillation, whereas during summer the relatively strongest (positive) correlation is seen in the North (*ibid.*, 510–513; Jacobeit *et al.* 2001, 238). From a historical view, the correlation between NAO and Stockholm winter temperatures was relatively low during the first half of the 19<sup>th</sup> and the beginning of the 20<sup>th</sup> centuries (*ibid.*, 233). An upward trend of the winter index towards the end of the 20<sup>th</sup> century caused increasing precipitation and, as a consequence, affected Western Scandinavian glaciers to stay at least stationary. NAO-driven wet or dry winters have provably even triggered the price of hydroelectric energy in Norway (Hurrell *et al.* 2003, 19, 23–24).

Apart from Atlantic influences, the continental impact plays an essential role for Europe's climate. Therefore, the Eurasian Pattern, which – in contrast to the NAO – describes meridional pressure gradient fluctuations between the British Isles in the west and the Northern Caspian Sea in the east, has to be taken into consideration. It implies a reasonable indicator for meridionally arranged, continental flow effects. This pattern shows a strong seasonal signal as well as a clear decadal-scale oscillation. The continental impact expresses itself in terms of a pronounced and extended near-ground high-pressure area, which arises from descending cold air masses, during winters and in terms of more locally effective low-pressure areas due to rising overheated air masses during summers. Both continental types, winter anticyclones and summer heat cyclones, are in permanent conflict with the NAO and, hence, exert their varying effect on European climate (Wanner *et al.* 2000, 30, 38–40).

To sum up the general discussion of atmospheric circulation, two things should be kept in mind: (1) By far not all atmospheric variations – especially not during summers – can possibly be explained by a single NAO index. (2) Much of the recent decades' warming over the NH and Europe, which has been strongest during winters, can largely be traced back to the prevalence of positive NAO episodes at the same time. It is not satisfactorily understood what has caused this rising trend. Among the forces that may trigger the NAO variability, slowly changing ocean

effects, human influence or just random behaviour is principally thinkable (Hurrell *et al.* 2003, 14, 17–18). Climate models can help to find the answer to, among other things, this question.

### 1.3 Global climate modelling

When some twenty years ago the dispute, whether the observed climate change should be interpreted as a natural variability feature or an atmospheric reaction to anthropogenic activities, broke out within geoscience, the opinions differed widely. Today the application of more and more reliable climate models has made it possible to give an answer. General circulation models (also called global climate models, GCMs) are the most powerful scientific tool to simulate the behaviour of the climate system. They can be regarded as a synthesis of the present state of knowledge, as basic conclusions on geoscientific processes, their interplay and their magnitude, are brought together, systematised and formalised or parameterised. Two main objectives can be distinguished; on the one hand, simulating past, present and furthermore future climate states, whereupon the simulated results are compared to observations in order to understand the roles of the various processes and their importance for climate changes, and, on the other hand, studying the climate system's sensitivity to the effects of boundary conditions or parameterisations, in order to calibrate the size of model processes (von Storch and Zwiers 1999, 12). Such calibrations or an advancement in input data availability lead to the obsolescence of previous climate models and the introduction of new and improved ones. A characteristic of climate modelling is the classical problem of distinguishing between signal and noise. Concretely, the supposed anthropogenic warming's magnitude shall be filtered out in opposition to natural variability (Schnur and Hegerl 2003, 63). Although all models are essentially built upon the same physical laws of nature, every model characterises insecure elements in its own specific way.

A fully comprehensive 3-dimensional GCM divides the atmosphere, the ocean and the ground in layers and columns and, in doing so, develops a 4-dimensional (three spatial plus one temporal dimension) grid. To start with, every gridpoint is assigned an input value for each of the variables that are considered by the model. At every calculation step the model simulates horizontal and vertical exchanges between the gridpoints and computes new values. Today, typical grid distances in climate simulations are 300 km horizontally and 20–40 layers vertically (with relatively finer resolutions in the surface-near layers of the atmosphere model) at half-hourly temporal intervals. Only halving the spatial distances results in a sixteen times longer computing time. Numerical climate models act as experimental laboratories where trial runs proceed under fixed controlled conditions. In practice, the initial conditions can be slightly varied, eventually artificially but often

to reflect existing insecurities in the input data. In this way, several experimental situations, so-called ensemble simulations, can be produced, which subsequently may diverge more or less from each other. By calculating the mean of individual simulations, runs with great consistence can be distinguished from outliers and a better division between signal and noise becomes possible. The finished sub-daily data are often subsumed to monthly, seasonal or other appropriate means for analyses (Roeckner 2004, 99–100).

Atmosphere and ocean models are the basis of any GCM. With increasing number of other system components, the capability of the model as a whole to simulate climate in a realistic way will increase. Essential components in fully comprehensive climate models are:

- Atmosphere general circulation models, which originally base on weather forecast models, are the core of every GCM. Air pressure, wind (velocity), air temperature, content of water vapour and cloudiness are the most important variables. But also the radiative properties of gases in the atmosphere and microscopically small pollutions like aerosols have to be considered due to their eminent impact on radiation balance.
- Ocean general circulation models play a primary role in climate modelling too because of the medium- and long-term variations they induce to the atmosphere. Among other things, flow (velocity), water temperature and salinity are computed. Lack of observational data makes it more difficult to verify ocean models compared to atmospheric models.
- Land surface models simulate the changes in ground temperature, content of ground water and snow cover.
- Sea ice models incorporate, for instance, the positive feedback effect between high albedo of ice surfaces and low air temperature.
- Other component models, like inland ice, biosphere, carbon and sulphur cycles are linked to GCMs in order to enhance simulation skills and include human activities.

By coupling atmosphere and ocean models, AOGCMs are derived. Even if the individual components are satisfactory when they run separately, this does not necessarily lead to a correct overall result when they are coupled (Schnur and Hegerl 2003, 65). There are two ways to deal with processes that run in between model components: Usually, the connection should be imitated by approximate physical-mathematical equations. But if the process lies beyond scientific comprehension, the definition of a constant value (parameterisation) is reasonable (Roeckner 2003, 8). To avoid climate drift in long simulations, some additional corrections are applied. As regards simulations of past climates, since there are no available initial conditions for the very beginning of a simulation, a so-called spin-down phase is designed to take the model to the conditions of the first historical forcing year.

The question, whether models provide reliable results at all, can be determined by simulations of past and present climate states. In fact, the 20<sup>th</sup> century's climate evolution is reproduced by AOGCMs with very good temporal and spatial agreement (Stott *et al.* 2000). Something that is important in respect to the climate change debate is the fact that the anthropogenic changes in atmospheric greenhouse gas concentrations can not explain the temperature evolution during the first half of the 20<sup>th</sup> century; however, without including this climate forcing the observed strong global warming since 1975 is irreproducible. Climate models can simulate the observed climate trend and also the projected changes resulting from supposed future emissions of greenhouse gases and atmospheric aerosols into the 21<sup>st</sup> century. An undamped and strong temperature rise with regionally differentiated precipitation changes, extensive ice mass loss and sea level rise is probable (IPCC 2001, 527–529). Spatial pattern, temporal behaviour and teleconnections of typical circulation modes like the Asian summer monsoon, the El Niño-Southern Oscillation phenomenon or the NAO are well visible in simulations (Roeckner 2003, 13–14; Min *et al.* 2005b). Atmosphere GCMs show that the recent upward NAO trend is statistically significant and – if not all of the according model simulations are unreliable – at least in parts due to external forcings. Increased greenhouse gas concentration and reduction of stratospheric ozone, which by radiative cooling of polar regions during winters may enhance meridional temperature differences and enforce positive NAO phases, are supposable (Hurrell *et al.* 2003, 25–26).

Important findings such as these demonstrate the potential of climate modelling within the simulation of past and future climate states. Yet, the model's growing reliability must not belie existing deficits in approximate equations, input data quality and grid resolution. An interpretation of model results can only be meaningful, if awareness of the actual model capability is guaranteed.

## **1.4 The early instrumental period**

### **1.4.1 History of instrumental measurements in the greater Alpine region and Scandinavia**

As mentioned at the outset, area-wide climatologic recordings started in the mid-19<sup>th</sup> century. Actually, the “prehistory” of climatologic measurement was induced already some 250 years earlier with the inventory of appropriate instruments in Italian Florence. It was Galileo Galilei's construction of a liquid density thermometer in 1592 and Evangelista Torricelli's creation of the barometer in 1643 that mark the beginning of setting numbers on the atmosphere's state. During the following four centuries, four stages of climate measuring development can be distinguished:

the phase of earliest experimental observations (1592–1700), the stage of first regular observations (1700s–1850s), the stage of national and international early networks (1780s–1850s) and finally the stage of the modern national station networks (1850s–today).

- When the very earliest climatologic observations were initiated in the second half of the 17<sup>th</sup> century, the Alpine region was already involved. It was in Florence where these “modern” scientific ideas flourished. There, Galileo’s students, under the auspices of the Tuscan grand duke Ferdinand II de’ Medici, founded a first experimental network, the Accademia del Cimento (Academy of Experiment), which lasted from 1654–67 (Brunetti *et al.* 2006, 346). It confined mainly to locations within Italy and included some of the GAR stations, namely Bologna, Milan and Innsbruck, but unfortunately for Innsbruck’s part, the data got lost (Auer *et al.* 2001a, 3). Even if it is situated far beyond the study regions, the well-known Central England Temperature series shall be mentioned here. Extending back to 1659 on a monthly basis, it is the world’s longest and most analysed “instrumental” series (actually, documentary evidence had to be integrated to obtain its full length; Manley 1974).
- The following 150 years from around 1700 to 1850 may be regarded as the epoch of farsighted engaged individual scientists that kept alive observations over many decades. In all European countries, they could mostly be found in monasteries, at universities and in astronomical observatories or they simply were personally interested private men who took the initiative. In this manner, the Swiss scholar Johann Jakob Scheuchzer stood up for climate research and noted the weather in Zürich from 1708 onwards. Johann Jakob d’Annone in Basel followed suit and began in 1755 what would later become the longest Swiss series. Continuous measurements are also maintained from Geneva since 1760. Turin in Italian Piedmont provides the longest reliable temperature series from south of the Alps starting in 1753 (Burga 2006). These three sites, Basel, Geneva and Turin, provide the oldest temperature series in the HISTALP dataset from 1760 onwards. Milan Padua. In the Austrian Empire, the Jesuit Order in Vienna collected meteorological measurements during 1734–73, which regrettably are not preserved. More fruitful were Benedictine monk Plazidus Fixlmillner’s recordings at the astronomical observatory of the monastery in Upper Austrian Kremsmünster to be; he started to chronicle the weather in 1762 and since 1767 his recordings are regarded to be systematic enough to constitute the longest Austrian temperature series (Fig. 2.1a, p 27). In 1775, the director of the old university astronomical observatory in the historic centre, Maximilian Hell, started the Viennese series there (Fig. 2.1b, p. 27) and two years later the University of Innsbruck established its record (Auer *et al.* 2001a, 3). In 1817, the Augustinian monks on the Great St. Bernard Pass (2,472 m a.s.l.) in Southernmost Switzerland commenced, equipped by the observatory in Geneva, the first high-Alpine climate record (Burga 2006).

In Scandinavia, Erik Burman, professor at the University of Uppsala, started systematic climatologic measurements as early as in 1722 and, in doing so, laid the foundation-stone to one of the longest and most investigated instrumental climate sources at all. After Burman's death in 1728, his student Anders Celsius carried on the observations. In the early 18<sup>th</sup> century's Sweden, many individuals showed more or less scientific interest in climate, which is reflected by a number of preserved journals. In the majority of cases however, these contain only singular years of measurements. In 1740, the temperature series at the astronomical observatory in Lund started, which unfortunately can not be applied to early instrumental climate research due to a plurality of inhomogeneities. An attempt of the *Kungliga Vetenskapsakademien* (Royal Swedish Academy of Sciences) in the early 1750s to collect the annual weather journals from eight stations over the country turned out to be unsuccessful. Another early initiative of the Academy was considerably more successful, when its secretary, Pehr Wargetin, started climatologic recordings at the astronomical observatory in Stockholm in 1754, which are available on a daily basis ever since then and usable since 1756 (Moberg 1998, 100–104). In Denmark, the Copenhagen series represents the longest temperature record; it starts in 1751 but is usable from 1767, when the thermometer was moved outdoors (Cappelen *et al.* 2005, 10). In Finland, temperature measurements were carried out at eleven different locations in the 18<sup>th</sup> century; however, these mostly lasted over too short periods with unknown practices. The Physics professor Gustaf Gabriel Hällström started the unbroken Helsinki series in the autumn of 1828 (Heino 1994, 13–14).

- These regular observations of the second phase share a common feature; they were essentially local initiatives, made more or less independent from each other. This situation changed in 1780, when the idea of building widespread meteorological observation networks was for the first time effectively realised. From then on, the third stage continues contemporaneously with the second one until the 1850s. The starting shot for the hitherto most successful international network was given in 1780 in German Mannheim, where the *Societas Meteorologica Palatina* (Palatine Meteorological Society), managed by its secretary Johann Jakob Hemmer and subsidised by Prince-Elector Karl Theodor, was located. It brought together the data from 39 stations ranging from New England to the Ural, amongst others, already bringing together data from Geneva, Kremsmünster, Hohenpeißenberg, Uppsala and Stockholm. The real innovation was, however, that the Society demanded standardised measuring methods, fixed observation routines and identical instrumental equipment. Although this network's end came suddenly in 1792 with the French revolution, triggering decades of conflict over Europe, its idea endured in regional networks (Auer *et al.* 2001a, 3–4; Moberg 1998, 104). In such a way, meteorological observation networks for agricultural planning were installed in Carinthia in

1813, where an amount of 15 stations was reached by 1848, and in Bohemia four years later (Auer *et al.* 2001a, 4).

In Sweden, a national observation programme was initiated by the Royal Academy already in 1785 on decree from King Gustav III. Forms and instructions were sent out to the gymnasiums' mathematics teachers to obtain uniform information on the climate over the country. Even if the project was quite successful in the beginning, the interest faded in the early 19<sup>th</sup> century. Only the already long series at the astronomical observatories in Uppsala, Lund and Stockholm survived (Moberg 1998, 104–107). Some reliable records are also derived from the experimental network that was established by the Finnish Society of Sciences and Letters, which started in 1845 (Heino 1994, 14).

- In the 1850s and 1860s, the next step in the history of instrumental observations was undertaken, namely the institutionalisation of weather observations. The foundation of national meteorological services in the European countries led to a sudden increase of data coverage until around 1900, a level that has mainly been maintained since then. In 1851, the Austrian Emperor Franz Joseph approved the request from the Academy of Sciences and its member Karl Kreil, the director of the astronomical observatory in Prague, to found the *Centralanstalt für Meteorologie und Erdmagnetismus* (since 1904 *Zentralanstalt für Meteorologie und Geodynamik*, ZAMG; Central Institute of Meteorology and Geodynamics) in Vienna; Kreil became the first director. Thus, the ZAMG is the world's oldest independent meteorological service. In 1873, the *International Meteorological Organisation* (predecessor of the *World Meteorological Organization*, WMO) was founded on the first international meteorological congress in Vienna. By 1890, the Central Institute successfully handled the collected data from more than 400 stations over the entire Austrian Empire (around 200 thereof in today's Austria), which makes it also the parent organisation of the meteorological services in the monarchy's successor states. Therefore, the history of meteorological observations in Austria overlaps with the corresponding history in other countries within the GAR, which is reflected in the ZAMG's data pool. Just once more the extent of early instrumental data was to be affected, when original historical records and metadata was destroyed in the bombing of Berlin in 1944, where they had been transported after the occupation of Austria (Auer *et al.* 2001a, 3–5). In Switzerland, the first national network of 88 stations was established in 1863 (Maurer *et al.* 1909, 6).

For Sweden's part, the initiation for a national station net was again taken by the Academy of Sciences, which built up a network of 25 initial stations in 1859–60. Growing continuously, it fell under the responsibility of *Statens Meteorologiska Centralanstalt* (predecessor of the *Swedish Meteorological and Hydrological Institute*, SMHI), which was founded in 1873 (Moberg 1998, 107). The national meteorological services of Denmark, Norway and Finland were brought into being

in 1866, 1870 and 1881 respectively; in Finland, the magnetic observatory of the University of Helsinki had previously, since 1838, been in charge of meteorological observations.

Given the historical background, it is relevant to ask how the “early instrumental (EI) period” should be specified for the purpose of this study. Being forced to set dates on it for consequent analyses, the answer is 1722/60–1860. The starting date has to be set at the beginning of regular observations, which is 1722 for Scandinavia and 1760 for the GAR. The first described stage has to be completely dismissed, due to systematic deficits and lack of data tradition. The end is defined by the onset of stage four, i.e. the organisation of climatic observation in national agencies, which is more difficult to mark, because of temporally different developments among the countries. However, confining to the foundation dates of Austria’s (1851) and Sweden’s (1859–60) meteorological networks, the year of 1860 seems to be the best fitting estimate for the definite ending of the EI period. Accordingly, the stages of the first regular observations and of early networks are objectives to the thesis. This definition is henceforth going to be followed in course of the next chapters. Within the EI period one major challenging uncertainty is prominent. It is referred to as the “early instrumental paradox”.

### **1.4.2 The early instrumental paradox**

The term “EI paradox” that has recently been introduced by Böhm (2005) denotes a prominent feature of temperature evolution within the instrumental period. It is a phase of comparatively high temperature level in the observations from around 1760/90–1810, especially marked in spring and summer months, that has been detected both in the GAR and in UST. It was followed by a sudden temperature drop in the 1810s. Lauscher (1980) named it “Josephinische Wärmeinsel” (“Josephine Heat Island” according to Emperor Joseph II’s reign) and interpreted the phenomenon to be confined to the Danube region rather than to the whole of Europe (Matulla *et al.* 2005, 54). Auer *et al.* (2001a, 119–120) as well as Böhm *et al.* (2001, 1789–1790, 1794) and Auer *et al.* (2006, 18) identified the warm summer interval in Alpine series, but did not excessively go into detail; in Matulla *et al.* 2005 (54, 58–61) it appeared as an outstanding period of warm summer temperatures from 1792–1807. For Sweden’s part, Moberg and Bergström (1997, 682) described the summers from the mid-1740s to around 1860 in the UST data to be (in case of 1751–1810 even significantly) warmer than the reference period 1961–90, a finding that attracted closer attention by Moberg *et al.* 2003. The contradiction that is represented by the EI paradox consists in the disagreement of the high summer temperatures around 1800 with proxy evidence from that time like tree-ring widths, harvest recordings and glacial evidence (Fig. 1.3). The exact beginning and ending of the paradox are uncertain and depend on which proxy record the instrumental data is related to. The proposed phase of comparatively high temperature level in the observations, however, lasts from around



1790 to 1810 in the GAR and is more marked and temporally extended in UST where it lasts from the beginning of measurements until about 1860 (see p. 53). At present, the paradox is a matter of discussion between instrumental and proxy climatologists. The following composition of arguments pro and con the observed early warm summers puts together the pieces brought up by literature so far (Böhm 2005):

- To begin with the GAR, the first issue that puts EI summer warmth into perspective are doubts concerning the EI data's quality. The insecure period is essentially the time before around 1820 when the number of station series is fairly low. Homogeneity tests, where the station series have been compared to each other, resulted in average positive corrections for the observed temperatures in the summer half-year, which lead to an artificial increase of homogenised summer temperatures compared to the raw data (Böhm *et al.* 2001, 1783; Büntgen *et al.* 2005, 149). On the other hand, the early temperature data could be positively biased, due to presumably poor or missing sheltering of the thermometers. If there is a warm bias in the EI temperature data, one may also ask when this postulated inhomogeneity started to occur. Perhaps a warm bias affects all EI summer temperature recordings back to the beginning of each record. Alternatively, it started sometime in the second half of the 18<sup>th</sup> century after a change from earlier cooler conditions. The metadata aspects of HISTALP will be regarded more closely in Chapter 2.1.
- The foremost and also most confusing argument contradicting the early observations is the disagreement with results from Alpine tree-ring proxy data, whose extensively analysed

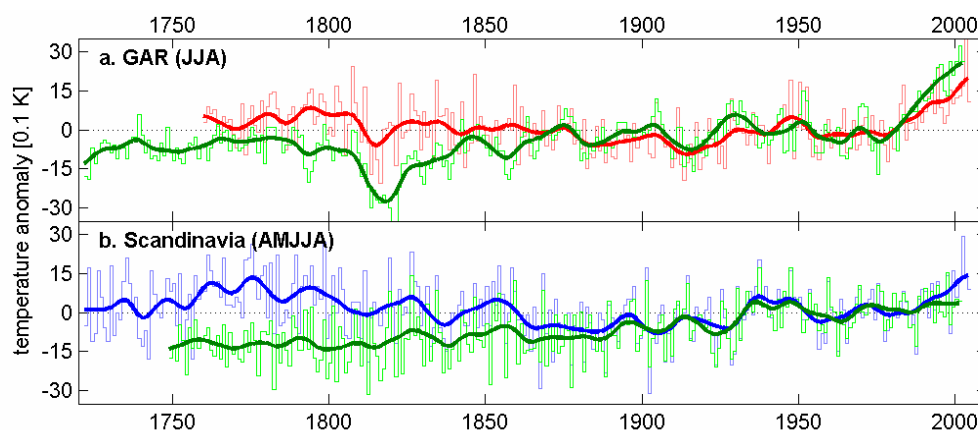


**Figure 1.3** The EI paradox depicted by the graphical comparison between instrumental and proxy data 1722–2004. **a.** Summer (JJA) temperature anomalies of GAR observational data (red; 27 longest stations from HISTALP, Auer *et al.* 2006) versus tree-ring width data (green; Büntgen *et al.* 2005) **b.** Late spring and summer (April–August) temperature anomalies of UST observational data (blue; Bergström and Moberg 2002; Moberg *et al.* 2002) versus grain harvest data from Austlandet (green; Nordli 2001b). Shown are anomalies from the 1961–90 average (stairs) and their 20-years Gaussian low-pass filtered trends (lines).

summer temperature reconstructions show an opposing trend around 1800. Whereas the correlation between reconstructed (from ring-width in the Central Alps) and instrumental summer temperatures is rather strong for 1934–2002 ( $r = 0.60$ ), it is much weaker during the EI period ( $r = 0.35$  for 1760–1863), when instead a lasting cool period is seen in the tree-ring data (Büntgen *et al.* 2005, 147). Consistently, another study (from ring-width and maximum latewood density in the Western and Central Alps) shows a substantially lower level of reconstructed summer temperatures compared to observed high-elevation summer temperatures in the late 18<sup>th</sup> and early 19<sup>th</sup> centuries in spite of the good general agreement between tree-ring and instrumental data (Frank and Esper 2005, 1448).

- Moreover, glacial evidences oppose the indication of warm summers during the first half of the 19<sup>th</sup> century. Instrumental evidences do not support the 1850-maximum (Schöner and Böhm 2007). Most Alpine glaciers advanced uninterruptedly to their LIA-maximum of 1850, regardless of some instrumentally observed, relatively warm summers around 1800 and during the 1820s (Matulla *et al.* 2005, 58).
- On the other hand, a number of arguments supports the existence of warm Alpine summers in the EI period. To derive the present state of the HISTALP dataset, broad quality enhancement by further data addition, homogeneity reanalysing and outlier correction has been accomplished (Auer *et al.* 2006, 15, 17). This induces more confidence to the EI data, in which – still – the high level of early summer temperatures remains. Furthermore, at some very long temperature series, which do show warm early summer temperatures (e.g. Kremsmünster, Hohenpeißenberg), the station history proves that no change of shelter has occurred in the relevant period.
- Another point that attests to warm summers around 1800 is the strong consistency of air temperature to another climate variable, namely air pressure. The HISTALP's EI temperature data shows a remarkable similarity to air pressure, which has been homogenised separately. The instance, that air pressure reached high mean values during the EI period too, gives more confidence to early temperature measurements (Auer *et al.* 2006, 17–18).
- Just as instrumental data quality is re-evaluated, the precision of proxy reconstructions is discussed too. In the case of tree-rings, the question concerning to what extent each month's mean temperature is critical for ring growth does not respect influences of different season's precipitation or longer-term effects. Is the temperature signal strictly confined to the current year? How do cold winters, that may cause a long lasting snow cover, affect annual ring growth? The possibly better relation of ring growth to annual rather than to summer temperature variability has been proposed (Büntgen *et al.* 2005, 149; Frank and Esper 2005,

1448–1450). The fact that these questions are subject to controversial discussions among dendrochronologists shows that the question of climate response seasonality of high elevation trees has not been given a satisfying answer yet.

- Similar matters bother glaciologists. Can higher precipitation be the answer to the advance of glaciers in the 1810s in spite of previous high summer temperatures? Because of the strong regional alteration of precipitation, its influence on glacier behaviour is more difficult to determine. Actually, the first half of the 19<sup>th</sup> century was according to observations especially wet in summers and autumns, which may lead to a better understanding of glacier advance then (Matulla *et al.* 2005, 61).
- High-Alpine ice-core isotope proxy temperature records from the Monte Rosa massif in the Western Alps confirm summer temperatures during the last decade of the 18<sup>th</sup> century being at the rather high level of the late 20<sup>th</sup> century (see p. 38; Wagenbach *et al.* 2001, 103–104).

Not at last, pro early summer warmth argues, that similar trends have been observed not only over all low-elevation regions within the GAR, but warm EI summers are also known from elsewhere, e.g. Scandinavia. Therefore, a closer look to the status quo in EI paradox research there shall be taken now:

- Similarly to the GAR's data quality, the station histories of UST contain some clues that question the homogeneity of the Swedish EI data. In Uppsala, the thermometer was moved twice, radiation sheltering was varied three times and observation hours were changed twice in the years from 1853–1874. Also the Stockholm series is altered by a routine change in 1859 and a radiation screen exchange in 1878, which both may have lead to an artificial cooling of measured temperatures (Moberg *et al.* 2003, 1497–1499; for details see Chapter 2.2).
- The detailed investigation of other climate variables within the UST data archive does not support the high early temperature level. Moberg *et al.* (2003) used a subset chosen among nine predictor variables (precipitation, air pressure, cloud amount and six air circulation indices) to estimate UST summer temperatures from a multiple regression model (see also p. 33–34). They demonstrated a clear similarity between the estimated and the observed temperature during the calibration period 1873–2000, but also a notable correlation drop further back into the EI period. The authors concluded that the summer temperatures during 1780–1860 is “very likely” positively biased and assumed this difference to amount to about 0.5–0.8 K. Any data before 1780 has not been investigated.
- Even in Scandinavia, proxy data conflicts with instrumental observations concerning the level of summer temperatures. Nordli (2001a) interpreted the start dates of grain harvest at Central Norwegian farms to reconstruct May to August temperatures from 1813 onwards. A

comparison with the instrumental series from Trondheim reveals that the observational data contains much warmer values. An overheating of the thermometer is proposed as an explanation and partly huge adjustments from 0.3–2.6 K are suggested before 1854. In a similar study, Nordli (2001b) bases the reconstruction of April to August temperatures back to 1749 on grain harvest data from farms in South-eastern Norway, the Austlandet region near the border to Sweden (“Austlandet series”). The fact that the agreement with the 400 km far apart UST series is strong in the fully developed instrumental period ( $r = 0.89$  for 1873–2000) but considerably weaker before 1860 ( $r = 0.62$ ; Moberg *et al.* 2003, 1499) confirms doubts concerning the instrumental data quality.

- Glacial evidence was used in relation to summer temperature when Nordli *et al.* (2003) reconstructed April to August temperatures from 1734–1923 for Western Norway from terminal moraines and harvest data (“Vestlandet series”). The scheme of the correlation to Uppsala is the same – even though with an earlier date this time: From 1815 onwards Vestlandet proxy data accords with Uppsala instrumental data very well, before this date, however, Uppsala lies constantly 1 K higher.
- Several arguments pro the correctness of early temperature data have also been discussed. Among these, the high level of homogenisation procedures applied to the UST temperature data is mentionable. Even though – obviously – uncertainties remain, many other early series miss a similar degree of homogeneity, which is one of the reasons why just UST is chosen for climate investigations that often.
- Also a sketchy comparison of UST with a previous version of the GAR data suggested that they partly approve each other’s high summer temperature levels, even though the early warmth seems to have been less marked in the Alps (Moberg *et al.* 2003, 1512).
- Counter-arguments against the relatively cold early summers suggested by proxy data may be found in the accuracy of the reconstruction methods. Which major inhomogeneities are to be found within the proxy data? Do the harvest proxies meet their goal and reflect real climate conditions or are they systematically (negatively) biased in some periods? To what extent are glacier proxy data of annual resolution superimposed by non-climatic and long-term effects? In how far do historic glacier stands reflect past temperature conditions (e.g. recent glacier advance in Western Norway parallel to strong warming; *ibid.*, 1514; Nordli *et al.* 2003, 1837–1838)?

Apparently, the EI paradox will still be up to discussion in the near future and remains unresolved so far. The numerous questions raised above underline the need for more pertinent research.

## 1.5 Purpose of the thesis

In the course of the introductory subchapters, principal themes within the increasingly important subject of historical climatology have been presented and their problems have been discussed. These topics shall be brought together now, as the motives that prompt the thesis are pointed out. Chapter 1.1 showed that the 20<sup>th</sup> century's climate change in its regional and temporal characteristics is quite satisfactorily understood and that the observed temperature increase is regarded as a fact. For the attribution of anthropogenic climate change, it is vital to gain as much information on past climate variations as possible (IPCC 2001, 700–701). Climate modelling is one credible path to follow (Chapter 1.3). Model studies, however, need to be accompanied by investigations of long records of observed climate data (Chapter 1.4) and proxy evidences.

To be able to separate the roles of anthropogenic and natural forcing of global temperatures, the reconstruction of climate states before the onset of anthropogenic manipulation is crucial (Moberg *et al.* 2003, 1495). Unfortunately, the start of widespread instrumental climate observations around 1850 essentially coincides with the onset of industrialisation and emission of greenhouse gases. Due to this instance, most instrumental temperature series are potentially affected by some human bias already from the very beginning. The amplitude of natural temperature variations within pre-industrial, pre-greenhouse-climate conditions is not well understood so far (Büntgen *et al.* 2005, 151). But this understanding is required as background knowledge for the improvement of climate models and future climate change predictions (Moberg *et al.* 2005b, 614).

Global datasets are, because of a lack of data coverage, confined to industrial times. Extension into pre-industrial times is the great potential of EI data and this advantage has not been fully utilised yet. Europe is the only world region that provides widespread EI observational climate information. However, it has to be assumed that much of these data remain unemployed and unhomogenised in archives and libraries to date. Two positive exceptions are the Alpine region and Scandinavia where extensive efforts have been undertaken to derive highly homogenised and trustable temperature series, represented in form of the HISTALP database and the UST records (Chapters 2.1 and 2.2). These long-time series, which have been developed totally independently from each other, are capable to assess regional temperature changes, (in the GAR case) to build larger-scale networks and to study the anthropogenic impact on temperature. The relatively new HISTALP dataset has been analysed basically so far (Auer *et al.* 2006; Matulla *et al.* 2005) and is ready for further analyses. Similarly, the UST records constitute the probably most homogeneous long-term observational information from Northern Europe (Moberg *et al.* 2003, 1515).

The most confusing and recently most discussed EI uncertainty, that evidences from both the Alpine region and Scandinavia have in common, is the divergence between (warm) instrumentally observed and (cold) proxy data-derived summer temperatures around 1800, which is referred to as the EI paradox (Chapter 1.4.2). The aim of the thesis is to estimate the plausibility of the early temperature climate in the study regions. No detailed comparison on this subject has been accomplished yet. For this reason, both instrumental and proxy climatologists from Central and Northern Europe plead in general for continuative and closer studies of the rich early climate information and emphasise in particular the need for attempts to examine the EI paradox (Moberg *et al.* 2003, 1515; Nordli *et al.* 2003, 1838; Böhm 2003). This would contribute to an improvement of temperature change reliability since the 18<sup>th</sup> century, even for other parts of Europe. The following main research questions will be addressed:

- Does the EI period show a consistent picture of air temperature variability in the Alpine region and Scandinavia? How is Alpine and Scandinavian temperature climate linked together and how is it linked at different temporal scales? The individual results from the GAR and from UST cannot be exploited beyond these regions. But if similar trends would be found, uncertainties could be reduced as well as conclusions for a larger region could be drawn (Chapter 4.1).
- How do the observed temperature trends in the GAR and UST harmonise with the respective instrumental air pressure data (Chapter 4.2)?
- To what extent are the results from observational data supported by independent proxy evidence? Can climate proxy data series from the Alps and Scandinavia proof or reject the instrumental series results and are adjustments feasible? This integrative kind of approach, in which both measured and proxy data are used equally, instead of playing one off against the other, becomes increasingly common within historical climate research (Chapter 4.3).
- How do the overall observed regional temperature trends and especially early summer temperatures agree with the simulations of a climate model run (Chapter 4.4)?
- How are instrumental temperature trends linked to atmospheric circulation (especially to the NAO) at different time scales over the GAR and Scandinavia? Are the high early summer temperatures reflected in the strength of the NAO over Europe? Is a NAO-related index a suitable indicator for temperature during summer months at all (Chapter 4.5)?
- What can the EI period tell us about the anthropogenic influence on climate change and natural climate variability? How is the recent warming trend to be placed within the longer-term context of 250 years (Chapter 5.1)?

As these problems are going to be faced in the course of the thesis, it is – in spite of all quality enhancements made by previous investigators – indispensable to keep early data quality and limitation issues in view. Conclusions in this regard are discussed in Chapter 5.2. Since it is, to the author's knowledge, the first time that a larger-scale perspective is applied to the issue, deeper insight into the EI paradox is expected. It is, however, certainly not the ambition of the thesis to definitely resolve the paradox (Chapter 5.3).

## 2 Data

To meet the demands formulated in the research questions, data of high quality reaching back into the 18th century are necessary. As mentioned above, the Alpine region and Southern Sweden are, due to great efforts that are described below, outstanding in terms of instrumental data from that time (Chapters 2.1 and 2.2). Proxy data series that meet the target of early summer temperatures are difficult to construct and hard to obtain for the Southern Swedish region, as Chapter 2.4 will show. Descriptions of other North European instrumental series that are going to serve as reference series for statistical homogeneity tests of UST later on (Chapter 2.3), climate modelling data that are going to be set in relation to observed temperatures (Chapter 2.5), and gridded SLP data that are going to be interpreted in terms of atmospheric indices (Chapter 2.6) complete the sets of various data types that are applied in the thesis.

### 2.1 The HISTALP dataset

To take advantage of the unusually rich long-term climate information in the Alpine region and to acquire and improve existing data resources extensively, turned out to be a promising idea during the 1990s when it became realised on national basis in several Central European countries. Emanating from the ZAMG's attempts, the Austrian long-term dataset of digitised meteorological observations have grown continuously during the last few years, first by a few nearby stations (ALOCLIM; Auer *et al.* 2001a), later through efforts coordinated by international projects and now encompasses the whole GAR in the form of the HISTALP (*Historical Instrumental Climatological Surface Time Series of the Greater Alpine Region*) database (Matulla *et al.* 2005, 21).

Auer *et al.* (2006) introduce the dataset to the scientific community and outline the main climatic features. It contains homogenised instrumental climate data for temperature, pressure and precipitation and largely also sunshine and cloudiness, at monthly resolution. Temperature and pressure are the very longest incoming elements, as the first series start in 1760. To make the balancing act between best spatial and temporal coverage, the longest possible extension back in time and an optimal data quality improvement for all multi-elemental data was the overall aim. In this sense, HISTALP is superior to most other climate data collections. After exhaustingly carrying together data from more than 30 administrative authorities from eleven nations, the final





**Figure 2.1** Selected sites of EI data acquisition used in this thesis. **a.** The “mathematical tower” of the monastery in Kremsmünster with the thermometer site in front of the central window on the second floor (1767–1886) **b.** The old astronomical observatory of the old university in the inner city of Vienna where the thermometer was situated on the building’s terrace at roof level (1775–1878) **c.** The old observatory (Celsius House) in the old town of Uppsala (1722–1853) **d.** The old observatory on a hill in the city of Stockholm where measurements have been executed in front of the left-most window on the first floor (1756–1875), in front of the left-most window on the ground floor (1875–1960) and at the modern weather station in the background of the photo (since 1961).

compilation comprehends altogether 516 series (whereof 131 temperature series) from 242 stations. The achieved network density, which allows for reasonable quality checks, declines appreciably back in time towards and within the EI period, but the major climate variability is – due to the given high spatial coherence of mean temperature fields – well captured by the available data even then (*ibid.*, 2–3, 5).

The main problem of data preparation within HISTALP was to reach and hold a high standard of quality and homogeneity. The procedure of data improvement – only for temperature – involved the adjustment of more than 700 inhomogeneities, the elimination of more than 4,000 outliers and the closing of more than 12,000 temporal data gaps. The rigorous homogenising

process was performed with the aid of relative homogeneity testing of series within regional subgroups of about ten neighbouring stations (with the HOCLIS software; Auer *et al.* 1999) as well as by crosschecking against metadata, a tool that becomes increasingly important in the EI period when reference stations are few. The differences between original and homogenised temperature data amount up to as much as 2 K (*ibid.*, 8–13). Systematic biases of temperature are in their magnitude comparable to the long-term climatic trends. For the time after 1850, biases result from a combination of specific national matters, like change of observation times or introduction of new radiation screens, and common evolutions, like the general station relocations from city centres to airfields that became usual in the middle of the 20<sup>th</sup> century. The latter lead, interestingly, to a

**Table 2.1** The EI subset of the 27 longest HISTALP temperature series. (The subset's mean is denoted as GAR.)

| acr. | station name            | nation | WMO-index | lon E<br>[°] | lat N<br>[°] | height<br>[m a.s.l.] | starting<br>year | last<br>year* | data coverage [%] |           | CRS  |
|------|-------------------------|--------|-----------|--------------|--------------|----------------------|------------------|---------------|-------------------|-----------|------|
|      |                         |        |           |              |              |                      |                  |               | 1760–1860         | 1861–2005 |      |
| BAS  | Basel/Binningen         | CH     | 06601     | 7.60         | 47.60        | 316                  | 1760             | 2005          | 100               | 100       | NW   |
| GNV  | Genève/Cointrin         | CH     | 06700     | 6.15         | 46.19        | 380                  | 1760             | 2005          | 100               | 100       | NW   |
| TOR  | Torino                  | IT     | 16059     | 7.67         | 45.07        | 275                  | 1760             | 2005          | 100               | 100       | SW   |
| MIL  | Milano/Brera            | IT     | 16080     | 9.19         | 45.47        | 103                  | 1763             | 2005          | 97                | 100       | SW   |
| KRE  | Kremsmünster            | AT     | 11012     | 14.13        | 48.05        | 389                  | 1767             | 2005          | 93                | 100       | NE   |
| RBG  | Regensburg              | DE     | 10776     | 12.10        | 49.03        | 366                  | 1773             | 2005          | 87                | 100       | NE   |
| PAD  | Padova                  | IT     | 16095     | 11.88        | 45.40        | 14                   | 1774             | 2005          | 86                | 100       | SE   |
| WIE  | Wien/Hohe Warte         | AT     | 11035     | 16.35        | 48.22        | 209                  | 1775             | 2005          | 85                | 100       | NE   |
| INN  | Innsbruck/Universität   | AT     | 11320     | 11.38        | 47.27        | 609                  | 1777             | 2005          | 83                | 100       | NW   |
| BER  | Bern/Liebefeld          | CH     | 06631     | 7.42         | 46.93        | 565                  | 1777             | 2005          | 83                | 100       | NW   |
| KAR  | Karlsruhe               | DE     | 10727     | 8.35         | 49.03        | 112                  | 1779             | 2005          | 81                | 100       | NW   |
| BUL  | Budapest/Lörinc         | HU     | 12843     | 19.22        | 47.45        | 130                  | 1780             | 2005          | 80                | 100       | NE   |
| HOP  | Hohenpeißenberg         | DE     | 10962     | 11.02        | 47.80        | 986                  | 1781             | 2005          | 79                | 100       | high |
| MUN  | München/Stadt           | DE     | 10865     | 11.55        | 48.18        | 525                  | 1781             | 2005          | 79                | 100       | NE   |
| VER  | Verona/Villafranca      | IT     | 16090     | 10.87        | 45.38        | 67                   | 1788             | 2005          | 72                | 100       | SW   |
| STU  | Stuttgart/Schnarrenberg | DE     | 10739     | 9.20         | 48.83        | 311                  | 1792             | 2005          | 68                | 100       | NW   |
| STR  | Strasbourg/Entzheim     | FR     | 07190     | 7.64         | 48.55        | 150                  | 1801             | 2005          | 59                | 100       | NW   |
| UDI  | Udine                   | IT     | 16045     | 13.24        | 46.06        | 51                   | 1803             | 2005          | 57                | 100       | SE   |
| NIC  | Nice/Aéroport           | FR     | 07690     | 7.20         | 43.65        | 4                    | 1806             | 2005          | 54                | 100       | SW   |
| KLA  | Klagenfurt/Flughafen    | AT     | 11231     | 14.33        | 46.65        | 459                  | 1813             | 2005          | 48                | 100       | SE   |
| AUG  | Augsburg                | DE     | 10852     | 10.93        | 48.42        | 463                  | 1813             | 2005          | 48                | 100       | NE   |
| BOL  | Bologna/SI              | IT     | 16140     | 11.34        | 44.50        | 60                   | 1814             | 2004          | 47                | 99        | SW   |
| LIN  | Linz/Stadt              | AT     | 11060     | 14.28        | 48.30        | 263                  | 1816             | 2005          | 45                | 100       | NE   |
| TRT  | Trento                  | IT     | 16020     | 11.12        | 46.07        | 199                  | 1816             | 2005          | 45                | 100       | SW   |
| GSB  | Gr. St. Bernhard        | CH     | 07390     | 7.18         | 45.87        | 2,472                | 1818             | 2005          | 43                | 100       | high |
| MAN  | Mantova                 | IT     | –         | 10.79        | 45.15        | 20                   | 1828             | 2005          | 34                | 100       | SW   |
| ZUR  | Zürich/Meteo Schweiz    | CH     | 06660     | 8.57         | 47.38        | 556                  | 1830             | 2005          | 31                | 100       | NW   |

\* as available to the author

negative average trend in the urban bias of temperature – in contradiction to the often postulated urbanisation warming trend effect. Homogenisation of data in the EI period is more individual due to the specific conditions at the different sites, but leads on average to a positive trend (Böhm *et al.* 2001, 1783–1785).

For the purpose of the thesis, exclusively the homogenised, outlier-corrected and gap-filled station data mode of the HISTALP temperature database is used. A subset containing the 27 longest series, starting before 1830, is chosen. General metadata are found in Table 2.1. The size of the network allows for subregional trends to be analysed already during EI times. To this end, the temperature regionalisation of Matulla *et al.* (2005, 25–28), which is based on all 131 series for the period 1930–2000, is followed. They classified the low-elevation GAR series into four subregions based on PC Analysis. The four leading EOFs were taken as coarse resolution subregions (CRS) and an additional subgroup was defined using high-elevation summit sites (CRS-high). The division corresponds roughly to the ordinal directions (CRS-NE, CRS-NW, CRS-SE, CRS-SW) and reflects continental scale climate features. As expected, the border between the northern and the southern subregions runs along the Alpine main chain. The separation between the western and eastern subgroups (no distinct topographic, seasonal migration of the border) and between low- and high- elevation sites was less obvious. The classification of the North Alpine hilltop station Hohenpeißenberg (986 m a.s.l.) was discerned as a borderline case; Matulla *et al.*

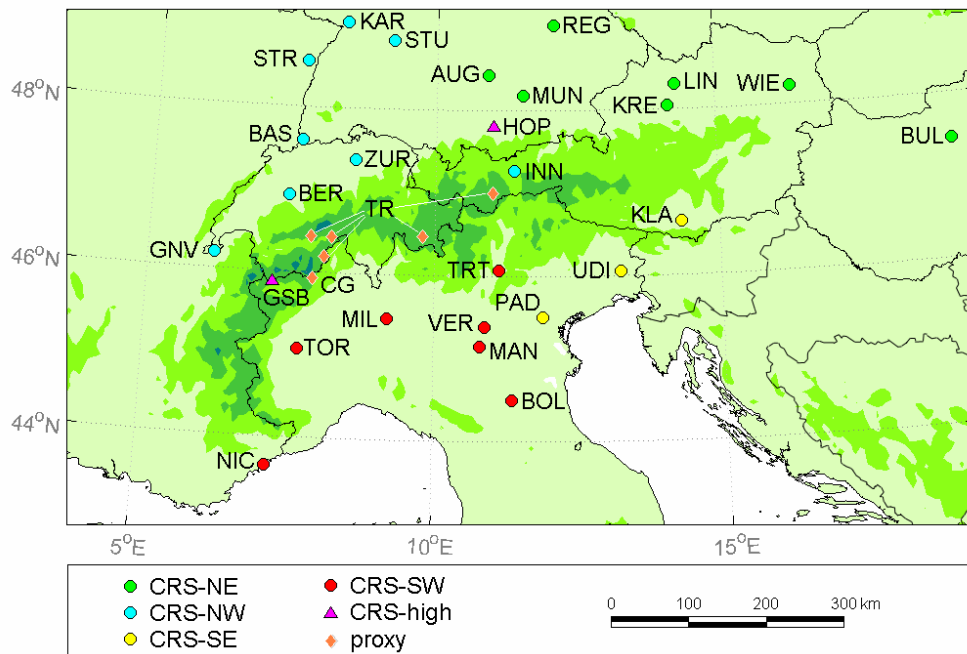


**Figure 2.2** The locations of the 27 longest HISTALP temperature series and available proxy records from the GAR.

(2005) finally assigned the series to the high-elevation group (which else typically contain stations above 1,500 m a.s.l.).

Although this regionalisation is based on all series in the 20<sup>th</sup> century, it is going to be applied here unmodified to the subset of the 27 stations, since spatial temperature patterns are supposed to stay, in the main, stable over time. Furthermore, the regionalisation has been characterised to be robust and ready for further analyses (*ibid.*, 23). The most important features of temperature development over the GAR subregions are shown in Figure 4.1a (p. 53).

The early air pressure data out of HISTALP will also be used here. From several of the 27 EI temperature stations also pressure time series have survived, the first one starting in 1760 (Basel). Until 1830 the number of pressure records grew to 14. They represent climate information of similarly high quality as the temperature data. For several pressure series, however, barometer temperature was not measured from the very beginning and could, therefore, not be used for pressure correction.

## 2.2 The Uppsala and Stockholm records

Early temperature data are also available for Southern Sweden. In this case, however, not a whole network exists, but rather long series from two nearby stations, Uppsala and Stockholm (UST). What unites GAR and UST data are the extensive efforts made by previous investigators to make homogeneity tests, quality control and data homogenisation. As it was the case with the HISTALP database, comprehensive data improvement techniques have been applied to the raw UST data during the late 1990s to achieve the today's level of comparatively high homogeneity. Relocations and varying instruments, positions and practices have biased the original data seriously. The most important metadata aspects and homogenising efforts of UST are depicted below.

The meteorological observations at the old astronomical observatory in the centre of the then small town of Uppsala, initiated in 1722 by the university professor Erik Burman and the *Society of Science in Uppsala*, are the earliest of their type in Scandinavia (Fig. 2.1c, p. 27). Data is available since January 1722. Already from the beginning, temperature, air pressure, wind direction and strength and soon also precipitation supplemented with short notes were noted every day. At first, no measuring standards were followed, although recommendations of the *Royal Society in London* were considered partly. This was a mixed blessing, as the regulation to place the thermometer inside a ventilated, north-facing, unheated room was followed in the 1720s and early 1730s. As a result, the diurnal temperature cycle turned out to be suppressed and delayed, causing temperature information in this period to be less accurate. From the year 1739, the thermometer

was placed outdoors at a location that is reported to have lain in the shadow in a shelter. There is a long data gap from June 1732 to December 1738 and also some shorter gaps later in the 18<sup>th</sup> century. Until 1750, a variety of different thermometer types and scales has been used, but, fortunately, periods of overlapping measurements allow for retroactive calibration. Anders Celsius' description of a temperature scale with the water's boiling point at 0° and the freezing point at 100° in 1742 was a major step towards a lasting standardisation. From 1747 onwards, the inverted present-day scale has been used. In 1832, fixed observation hours three times a day were introduced. Before that year, measurements were carried out two to four times daily at varying hours. The Uppsala series' most substantial change occurred in September 1853, when the station moved around 1 km to a newly built observatory, lying outside the town surrounded by open fields. At the same time, a radiation shelter of Lawson type was installed. Since then, the population has increased considerably (8,000 inhabitants in 1860, more than 135,000 today), which has given rise to a measurable urbanisation warming effect (Moberg 1998, 110–111; Moberg and Bergström 1997, 668–669; Bergström and Moberg 2002, 214–222).

Bergström and Moberg (2002) reconstructed the daily averages of homogenised temperatures by adjusting the detected inhomogeneities. In doing so, they created the Uppsala series in the form that can be regarded as its “official” state today (UPP). More precisely, they tried to eliminate the effect of varying numbers and hours of observations, and of the initial indoor placement, on the daily temperature averages by taking into account observational hours and cloud cover records in a formula of the diurnal temperature cycle. Inconsistencies induced by different thermometer types were numerically calibrated for the time before 1747. Periods of missing data were filled by extrapolation from other contemporary observations. The 1732–38 gap, for instance, could be filled with linearly transformed data from the about 170 km distant site of Risinge (*ibid.*, 218–232). Furthermore, a relative homogeneity test (SNHT, Standard Normal Homogeneity Test; see p. 47) against the nearby Stockholm temperature series (62 km) revealed significant negative shifts in annual and seasonal data before the early 1850s, except for summer data. These shifts were interpreted to be caused by the 1853 relocation and have been corrected. A relative all-year warming trend by about +0.47 K since the 1860s relative to an average of eight reference series (1861–1994) within a radius of 200 km, which was attributed to the urban influence, has been corrected (Moberg and Bergström 1997, 670–684). The adjustment before 1854, based on comparison with the independently reconstructed data from Stockholm is considered to have induced even more reliability to Uppsala data. This adjustment causes the two anyway very similar series (correlation coefficient of 0.98 before 1850 and 0.99 afterwards for annual mean temperatures) to agree very well as regards the overall level and long-term trends. The fact that they their temporal variations are nearly identical during modern instrumental times argues for

this kind of homogenising. However, not all doubtful aspects could be quantified and erased (Bergström and Moberg 2002, 250–251).

With 250 years of uninterrupted daily meteorological observations at one and the same location – an anniversary that is celebrated this year – the long-time series at the astronomical observatory in Stockholm is one of the oldest and most valuable ones. On January 1<sup>st</sup>, 1754, the *Royal Swedish Academy* in person of Pehr Wilhelm Wargetin initiated the measurements once per day. The start of the useable part of the series, however, is appointed to 1756, when two daily observation times (around sunrise and 1 p.m.) were introduced. Since 1761, an additional third observation has been carried out, but precise points of time were still not documented until May 1784, when fixed hours were introduced in line with the Mannheim standardisation. Besides temperature, air pressure, wind direction and strength, various descriptive notes were reported from the very beginning. The first thermometer position, in the free air on the northern side of the building outside a window on the first floor (5.8 m above ground), is in described to have been well protected against the morning sun in original notes, but no further details have been annotated. The Celsius thermometer scale with 0° at the freezing and 100° at the boiling of water, has been used ever since the first observation in 1754. In January 1859, new measurement procedures superseded the former ones, as the modern Swedish station net was initiated. Thereby, the morning observation was shifted from 6 a.m. to 8 a.m., with the result that direct sunlight, that had hit the north-facing wall during the months of high sun altitude so far, did not affect the morning observation any longer. In September 1875, the thermometer was relocated to the front side of a window on the ground floor (1.5–1.9 m above ground) and, in 1878, a white painted metal radiation screen was installed too. In January 1961, the weather station was moved to a position 10 m away from the building and a Stevenson screen sheltered the thermometer until the summer of 2005. Since then, the temperatures are recorded automatically with a platinum resistance thermometer, placed in modern radiation screen located about two metres from the Stevenson screen (Fig. 2.1d, p. 27). During the whole period of observations, Stockholm underwent strong urban development. Whereas the observatory hill lied about 1 km outside the town in rather rural environment when the series started, it is a small park in the city centre of Stockholm today (Moberg 1998, 101, 110; Moberg and Bergström 1997, 669–670; Moberg *et al.* 2002, 172–173, 177–178).

The “official” Stockholm series (STO) has been published by Moberg *et al.* (2002). Correspondingly to the creation procedure of UPP, they reconstructed the complete series of daily means from the existing observational data and corrected it by the aid of metadata, statistical tests and comparison to Uppsala. The latter one revealed, for instance, an inhomogeneous period from August 1819 to January 1825 caused by an incorrectly calibrated thermometer that entailed a correction of -0.7 K to all original Stockholm temperature data (*ibid.*, 171, 177). Moreover, SNHT

**Table 2.2** *The UST temperature series and potential reference series.*

| acr. | station name      | nation | WMO-index | lon E<br>[°] | lat N<br>[°] | height<br>[m a.s.l.] | starting<br>year | last<br>year* | data coverage [%] |           |
|------|-------------------|--------|-----------|--------------|--------------|----------------------|------------------|---------------|-------------------|-----------|
|      |                   |        |           |              |              |                      |                  |               | 1760–1860         | 1861–2004 |
| UPP  | Uppsala           | SE     | 02458     | 17.64        | 59.85        | 25                   | 1722             | 2004          | 100               | 100       |
| STO  | Stockholm         | SE     | 02485     | 18.07        | 59.35        | 44                   | 1756             | 2004          | 100               | 100       |
| VIL  | Vilnius           | LT     | 26730     | 25.25        | 54.68        | 126                  | 1777             | 1990          | 82                | 88        |
| KOP  | København         | DK     | 06186     | 12.55        | 55.68        | 9                    | 1768             | 2004          | 78                | 100       |
| OSL  | Oslo/Blindern     | NO     | 01492     | 10.72        | 59.95        | 94                   | 1816             | 2005          | 45                | 100       |
| TAL  | Tallinn           | EE     | 26038     | 24.43        | 59.75        | 3                    | 1806             | 2001          | 39                | 82        |
| HEL  | Helsinki          | FI     | 02978     | 24.95        | 60.17        | 4                    | 1829             | 2005          | 32                | 100       |
| SPE  | St. Petersburg    | RU     | 26063     | 30.30        | 59.97        | 6                    | 1743             | 2001          | 96                | 98        |
| RIG  | Riga              | LV     | 26422     | 24.10        | 56.95        | 9                    | 1795             | 1989          | 46                | 90        |
| BRG  | Bergen/Florida    | NO     | 01317     | 5.33         | 60.38        | 12                   | 1816             | 1999          | 45                | 97        |
| SOV  | Sovetsk (Tilsit)  | RU     | 26615     | 21.80        | 55.10        | 18                   | 1820             | 1930          | 41                | 48        |
| GDA  | Gdańsk/Rebiechowo | PL     | 12150     | 18.47        | 54.38        | 135                  | 1807             | 1987          | 40                | 28        |

\* as available to the author

(against eight nearby reference series, 1861–1994) identified urban warming from the mid-19<sup>th</sup> century until around 1970. The annual correction due to urbanisation effect amounts up to +0.71 K with respect to the reference stations (Moberg and Bergström 1997, 675). The relocation of the thermometer and installation of a shelter in August 1875 may have exerted an artificial cooling effect on measured temperature. The main uncertainty in the Stockholm series, however, consists in the morning observation time change on January 1<sup>st</sup>, 1859. In combination with changed radiation conditions (i.e. no morning sunlight on the wall where the thermometer was placed), this may imply a potential positive bias of observed summer temperatures prior to 1859. In an attempt to judge how serious this problem is, a comparison between separate temperature series calculated for days with different cloud amounts has been performed, assuming that this would reveal a sunlight-related bias. However, no such effect could be confirmed from these calculations (Moberg *et al.* 2002, 179–183).

As doubts about the EI summer temperatures in both UST series – primarily due to the 1853 relocation in Uppsala and the 1859 observation hour change in Stockholm – remained, Moberg *et al.* (2003) had a closer look at a potential positive bias. They applied a stepwise multiple regression technique for estimating summer temperatures from various predictor variables, chosen among six air circulation indices (obtained from gridded monthly SLP data) together with local precipitation, air pressure and cloud amount data from the UST records. The chosen model, containing three predictor variables, explains 65 % of summer temperature variance in the calibration period 1873–2000. When applied to the period 1780–1872, it still is responsible for 52 % explained variance. Yet, the model predicts cooler summer temperatures than those measured, providing an indication of a



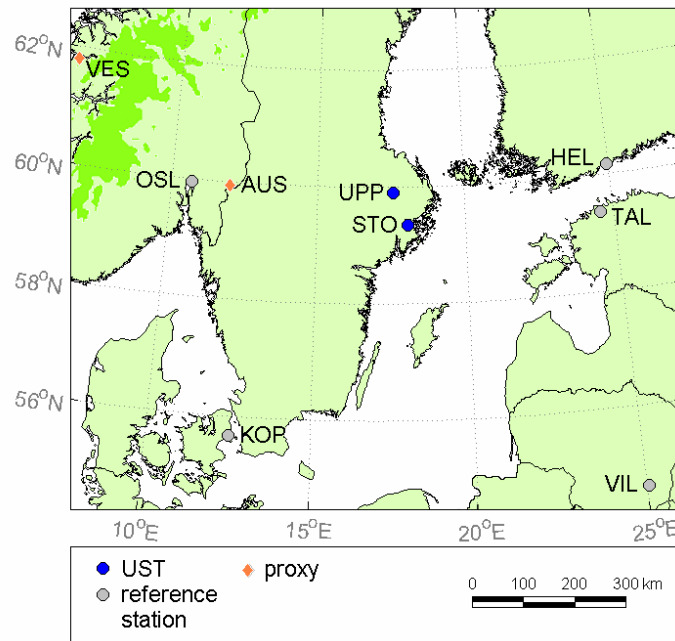


**Figure 2.3** The locations of UST, the actual reference series and available proxy records from Southern Scandinavia. (Note the difference in scale compared to Figure 2.1!)

positive bias of an estimated size of about 0.5 K. Inspired by these findings of Moberg *et al.* (2003), Moberg *et al.* (2005a, 118) consult, for the first time, a summer-corrected version of the Uppsala series. To allow for more insecurities like this in the UST series, other different versions of the two individual series and their average will be used in the course of this thesis. Further comments on the handling of these different versions are given in the methods chapter (see p. 45–46). Table 2.2 provides short metadata facts from UST and several reference stations that are going to be described soon.

Apart from temperature data, also the air pressure time series from UST are published in the state-of-the-art papers (Bergström and Moberg 2002; Moberg *et al.* 2002). These series start in the same years as the temperature records and underwent comparable homogenisation procedures.

Altogether, the availability of parallel EI data from two nearby stations, that are situated only 62 km apart, is extremely valuable. However, in spite of homogenisation efforts, the highlighted quality problems lower the data's reliability prior to the mid-19<sup>th</sup> century, when uncertainties remain (Moberg *et al.* 2002, 205–206). Moreover, the UST series constitute only evidences of regional climate variations which can hardly be extended far beyond Southern Sweden (Moberg and Bergström 1997, 687).



## 2.3 Additional instrumental data

To be able to apply further relative homogenisation procedures to the UST data reaching back into the problematic period before the 1850s, other long-term series are needed. Such data have been obtained from different sources, which shall be mentioned now.

The *Climatic Research Unit* (CRU) at the University of East Anglia holds an extensive database of more than 5,000 temperature records from stations worldwide, which has been revised and described by Jones and Moberg (2003), who improved the data's quantity and also included data of higher homogeneity standard, whenever it was possible. However, the bulk of the records is confined to the most recent decades. For the present study, a European subset of the CRU temperature series beginning before 1820 was available. Thereof, nine long-term series of different data quality have been selected as possible reference station for the UST series: St. Petersburg, Copenhagen, Vilnius, Riga, Tallinn, Gdańsk, Oslo, Bergen and Sovetsk (former Tilsit in the Kaliningrad Oblast).

Direct contact to pertinent researchers from different countries has been established to obtain more information and to possibly improve the records by merging them with additional data. In the cases of St. Petersburg, Vilnius, Riga and Tallinn, only single gaps could be closed, but it is not definitely known, if these had been removed due to data insecurities in the first place. The series of Riga is regarded to be seriously inhomogeneous because of two relocations from the suburbs to a boulevard inside the town in 1839 and further to the university in 1924. For St. Petersburg, Vilnius and Tallinn, data interruptions are typical. For the Tallinn record, three thermometer changes in the 19<sup>th</sup> century are reported (Olga N. Bulygina, RIHMI, personal communication). As regards the Copenhagen series, relocations from the tower of the astronomical observatory to the botanic garden in 1820 and therefrom to the present site in a park in 1860 are known. 14 years of early data in the 18<sup>th</sup> century are totally missing. Moreover, the station is regarded to have been subject to urbanisation (Cappelen *et al.* 2005, 10, 24). The Oslo series has not been thoroughly tested for possible inhomogeneities yet. The series is affected by a relocation in 1937, when the station was moved from the city centre to the meteorological institute outside the city at higher altitude. The temperature values before this event have been adjusted in the CRU dataset. Besides the displacement, the series is probably quite homogeneous, even though an urban trend may be present in the data. As for Bergen, the older part of the series before 1868 is problematic because of inadequate homogenisation (Øyvind Nordli, DNMI, personal communication).

A completely independent record could be received from Finland. The continuous Helsinki series starting in 1828 has been relocated once in its early years when it was moved to the

meteorological institute and later when it was relocated to its current site in a nearby park in 1844. The present version is well homogenised and regarded as a climatologic record of high standard (Heino 1994, 14).

Despite attempts to contact individual scientists, no more data or homogenised versions for the interesting stations could be obtained. This concerns especially Sovetsk and Gdańsk, for which no details are available at all. The presented data seems to be the state-of-the-art of Northern European EI temperature data. For basic metadata and the locations of most records discussed in this section see Table 2.2 and Figure 2.3 respectively!

## 2.4 Proxy data

To describe and analyse the EI paradox, proxies for summer temperature have to be used. Five sources of proxy data that will be explored, three from the GAR and two from Scandinavia, are presented below. As diverse natural archives as tree-rings, ice-cores, glaciers and harvest dates will be interpreted.

The largest dataset of Alpine tree-ring records (herein TR) so far is provided by Büntgen *et al.* (2005). They utilised four larch chronologies from Switzerland and one pine chronology from Austria (Fig. 2.2) to reproduce long-term summer temperature variability for the region. The specific climate reconstruction target is the mean JJA temperature for every year. By using a total of more than 1,500 samples from living trees as well as from dry-dead and sub-fossil wood, the Central Alpine record could be extended back to the year 951. Exclusively wood material from elevations above 1,500 m a.s.l. was used because JJA temperature is regarded to be the main climate factor determining annual tree-ring growth there. The composite detrending technique of regional curve standardisation was executed to preserve long-term trends. All samples were aligned by cambial age and the variance has been stabilised to reduce the effect of changing sample sizes. Thereafter, the chronology was calibrated to its target on the basis of eleven high-elevation meteorological stations, three of which go back to 1864 (Böhm *et al.* 2001). A correlation between proxy and observation series by 0.65–0.86 demonstrates a strong response. This proxy database of more than 1,000 years of Alpine summer temperatures is highly qualified for regional climate history research. Typical inter-decadal to centennial temperature variability features like the medieval warmth period, the LIA, cold summers around 1815–20 and the following rising trend are captured well (see Fig. 1.3a, p. 19). Yet, the discrepancy with instrumental data in the EI period stands out (Büntgen *et al.* 2005, 141–144, 148–150).

Another temperature proxy, stable-oxygen-isotope ice-core records, is available from the Western Alps. This proxy is based on the theoretical approach that the oxygen isotopes  $^{16}\text{O}$  and  $^{18}\text{O}$  are naturally fractionated during phase changes. In case of evaporation, the lighter  $^{16}\text{O}$  fades sooner to vapour. In case of condensation, e.g. cloud formation and precipitation, rather the heavier  $^{18}\text{O}$  passes more easily over to the fluid phase. Because less  $^{16}\text{O}$  evaporates and deposits during colder climate epochs, annual ice layers in glacial areas from such times are expected to contain a relatively high fraction of  $^{18}\text{O}$  with respect to  $^{16}\text{O}$ . Thus, with the aid of the  $^{16}\text{O}/^{18}\text{O}$ -relation ( $\delta^{18}\text{O}$  values) in ice-cores the mean temperature of past local condensation temperatures can be approximated. Consequently, this proxy captures temperatures on precipitation days only. Cold Alpine glaciers above 4,000 m a.s.l. are suitable for ice-core studies. The special potential of Alpine ice-cores (compared to e.g. Greenland) lies in the dense instrumental temperature information surrounding them (Böhm *et al.* 2001, 1780). The Colle Gnifetti (4,450 m a.s.l.), a small firn saddle in the Monte Rosa massif (Fig. 2.2) is a unique site for long-term ice-core records. The extremely exposed geographical situation allows only for low annual accumulation of snow (0.1–0.5 m water equivalent year<sup>-1</sup>). There, the *Institute of Environmental Physics* (IUP, University of Heidelberg, Germany) supervises three cores reaching down to bedrock (60–100 m), one dating back to around 1630 and two to 940. Recently, additional ice-cores covering the entire Holocene have been investigated (Boliuss *et al.* 2006). A combined series of all three cores underlies coming analyses (herein, CG according to Colle Gnifetti). Several effects, however, reduce the ice-core record's reliability: Strong wind erosion conserves only a small fraction of annual precipitation. Therefore, the measured  $\delta^{18}\text{O}$  values reflect a seasonally weighted atmospheric signal; specifically the precipitation of the summer months is conserved. Besides, wind erosion causes annual accumulation to vary strongly, which constrains dating precision; back to the mid-18<sup>th</sup> century, the uncertainty grows from around three to 15 years. Due to a complex ice flow pattern, systematic upstream effects lay spatial variations over the temporal ice-core trends. The consequential non-linear age-depth relation has been estimated and corrected employing additional shallow cores. Still, this upstream correction is not definite. Comparisons with instrumental temperature data have shown that the coherence of the low-accumulation cores is best when related to weighted monthly temperatures from March to September. This so-called growing season temperature of a certain year consists of the portioned monthly temperatures of March (1 %), April (11.5 %), May (24 %), June (26.5 %), July (17 %), August (14.5 %) and September (5.5 %; Wagenbach *et al.* 2001, 97–98). Very similar long-term trends of high and low-elevation temperatures allow even lowland sites to be properly compared to the ice-core records. A linear regression between  $\delta^{18}\text{O}$  variations and instrumental temperature variations during the 20<sup>th</sup> century leads to a sensitivity of 1.7 ‰ K<sup>-1</sup>. Hence,  $\delta^{18}\text{O}$  variations can directly be recalculated into growing season temperature variations. Results show large divergences caused by dating uncertainty and depositional noise for single

years. Decadal trends, however, agree remarkably well with observed temperatures; decreasing temperatures during the 19<sup>th</sup> century, warm summers in the 1940s and the 20<sup>th</sup> century warming are recognised features of Alpine temperature variability. Also warm summers at the end of the 18<sup>th</sup> century appear. Nevertheless, partly large differences to tree-ring records get obvious going further back in time (*ibid.*; Schöner *et al.* 2002).

A proxy that is fully independent from instrumental data is offered by Oerlemans (2005). His reconstruction is based upon the simple hypothesis that changes in glacier length (GL) correspond to changes in air temperature. In his study, information on maximum glacier stands from sketches, paintings and photographs as well as from still existing moraine systems was compiled from differing sources. From the resulting number of 169 glacier records from all parts of the world, a subset of 93 records from all over the Alps was available. This dataset starts with two records in 1600, grows slowly to four records in 1760, 17 records in 1860 and increases rapidly towards the end of the 19<sup>th</sup> century. Before around 1900, the records typically consist of not more than 10 data points, but afterwards annual resolution becomes standard. Gaps were filled by interpolation. To estimate the climatic signal out of glacier length records, differences in climate sensitivity and response time of the individual glaciers have been taken into consideration by means of a linear inverse model integrating both mass balance and ice flow. Potential sources of errors are the influence of other factors (e.g. solar radiation, precipitation), uncertainties in climate sensitivity and response times of the glaciers and the number of records. Climate sensitivity has been roughly assessed by the slope of the glacier surface and annual precipitation amount, response time results from slope and balance gradient (rate of mass gain with elevation). However, it is assumed that decadal to centennial glacier fluctuations are predominantly driven by temperature. The outcomes of Oerlemans' survey hint at a mean glacier length maximum around 1800 suggesting that the LIA reached its maximum already then. Because of the small sample size before 1800, the reconstructed temperature signal must be interpreted carefully. The overall temperature evolution since 1600 as seen by this glacier reconstruction is generally in line with other proxy and instrumental evidence.

To find proxies targeting at summer temperatures in the surroundings of UST, is difficult. Swedish tree-ring based temperature reconstructions are either concentrated remote away northern parts of the country (Grudd *et al.* 2002) or cover different historical episodes (Grudd *et al.* 2000). Ice break-up dates are available for the nearby Lake Mälaren, but this proxy naturally aims at the cold season's temperature (Eklund 1999). On the contrary, an interesting warm season temperature proxy is available from the Norwegian-Swedish border some 330 km to the west of UST. There, for the south-eastern Norwegian region of Austlandet and the adjacent Swedish county of Värmland, Nordli (2001b) reconstructed late spring and summer temperatures from the start dates of grain harvest as noted in farmers' diaries back to 1749 (AUS). The reconstruction

period as well as climate target seem appropriate for the purpose of the thesis. As regards the rather long distance to UST, the more critical factor, namely that both the instrumental and the proxy region are located within the same climate region, is reasonably granted, as Austlandet is situated to the east of the Norwegian mountain ridge. Nordli selected ten farm diaries containing the first dates of rye, barley or oats harvest for periods of 13 to 66 years. For the first 25 years from 1749–1773, data from only one farm is documented. The comparison of overlapping data periods from different farms permits a check that all series are homogeneous; the only detected break was caused by the instance that a farmer changed the cultivation area. Afterwards, the technique of linear regression analysis between start dates of grain harvest and observed mean summer temperature was chosen to transfer information from dates to temperature. To this end, instrumental series from five temporary local stations had been nested together and homogeneity tested, resulting in an observational control record for 1871–2000. The establishing of a regression equation was complicated due to the fact that only one diary actually overlapped sufficiently long with the instrumental record (1871–1918). However, the regression worked best with April–August mean temperature as dependent variable and revealed rather high correlations with the instrumental control record ( $r = 0.82$ ). The final, variance inflated reconstruction shows good agreement with the independent Oslo instrumental series (1837–1870).

In addition, a somewhat similar spring-summer temperature reconstruction from the region of Western Norway (Vestlandet) may broaden the view on the EI paradox (Nordli *et al.* 2003). The Vestlandet proxy record (VES) is based on a combination of grain-harvest dates combined with terminal moraine stands from two South Norwegian glaciers. Because Vestlandet is located on the western side of the Norwegian mountains and more directly influenced by Atlantic climate, the relation to UST conditions is expected to be not as close. However, this multi-proxy approach is interesting because it takes glacial evidence into account in addition to the harvest dates. Again, mean April–August temperature was reconstructed by a linear regression against meteorological observations from Bergen. Then, the glacier equilibrium line altitude was estimated in a stepwise multiple regression by means of generated circulation indices and the spring-summer temperature. In addition, the equilibrium line altitude was modelled from moraine sequences. To derive the continuous Vestlandet April–August temperature series, for the period 1734–1842 both long-term variations based on dated moraines in front of the glaciers and the annual variations based on the first dates of grain harvest were interpreted, whereas for the period 1843–67 solely harvest dates were used. From 1868 onwards, VES is based on homogenised instrumental series from Bergen. During the reconstruction period, the composite series shows good general agreement with the instrumental observations from Bergen. Anyway, an unresolved late 18<sup>th</sup> century and early 19<sup>th</sup> century offset between the Vestlandet proxy and the Uppsala instrumental temperature becomes obvious (*ibid.*, 1835–1838).

## 2.5 Temperature data from model simulations

Observational EI temperature data will also be set in relation to climate model simulations. The model ECHO-g will be consulted for this purpose and will contribute to the matter of early observed and proxy-reconstructed temperatures. ECHO-g denominates the coupled version of an AOGCM that consists of the atmospheric model ECHAM4 (Roeckner *et al.* 1996) containing a land surface scheme and the ocean model HOPE-g (Wolff *et al.* 1997) including an embedded sea-ice model with snow cover. Both ECHAM4 (fourth generation of the *European Centre Hamburg Model*) and HOPE-g (global version of the *Hamburg Ocean Primitive Equation Model*) were developed at the *Max Planck Institute for Meteorology* (MPI-M, Germany). Originally, ECHAM had emerged from the weather forecasting model of the *European Centre for Medium-Range Weather Forecasts* (ECMWF, United Kingdom) and been modified for long-term climate simulation uses (Min *et al.* 2005a, 606–607; Matulla *et al.* 2005, 44). ECHO-g has been extensively used and validated in numerous surveys (e.g. Zorita *et al.* 2004; Min *et al.* 2005ab; González-Rouco *et al.* 2006; Gouirand *et al.* 2006).

The atmospheric component ECHAM4 is based on primitive equations. Vorticity, divergence, surface pressure, temperature, specific humidity and total cloud water are among the computed variables. The atmosphere GCM also treats greenhouse gases through a radiation scheme (Matulla *et al.* 2005, 45). The atmosphere is vertically defined by 19 pressure levels. They are irregularly ordered, as resolution increases towards the boundary layer; the highest level is placed at 10 hPa (height of about 30 km) and only five levels lie above 200 hPa, whereas the bottom level is at height of about 30 m above the surface. The horizontal resolution in ECHAM4 is approximately  $3.75 \times 3.75^\circ$  (Min *et al.* 2005a, 607). The ocean GCM HOPE-g is also based on primitive equations and includes a thermodynamic sea-ice model with snow cover. Again, the vertical layers are irregularly ordered; the top eight of overall 20 horizontal levels lie within 200 m from the ocean surface. The horizontal resolution is given by a Gaussian grid of about  $2.8 \times 2.8^\circ$ . In the tropical oceans (between  $10^\circ\text{N}$  and  $10^\circ\text{S}$ ), however, the meridional grid is progressively refined, reaching a value of  $0.5^\circ$  at the equator. This allows for a more realistic simulation of El Niño-Southern Oscillation variability. The model time-steps are 30 min (radiation 2 h) for ECHAM4 and 12 h for HOPE-g (Min *et al.* 2005a, 607; Zorita *et al.* 2004, 273). The coupling of ECHAM4 and HOPE-g is governed by the OASIS software (Valcke *et al.* 2000). Every 24 h, they exchange mean atmospheric fluxes (zonal and meridional flux over water and over ice, freshwater fluxes, heat fluxes) and four surface conditions (sea surface temperatures, sea ice concentration and thickness, snow depth; Min *et al.* 2005a, 607). To prevent climate drift due to the interactive coupling between atmosphere and ocean in long simulations, additional heat and freshwater fluxes are applied to the ocean. These temporally

constant adjustments drive the sea surface temperatures and salinity to their observed values when using constant present-day forcing (González-Rouco *et al.* 2006, 1; Zorita *et al.* 2004, 273).

Three external forcing factors drive the transient 1,000 year long climate simulation with ECHO-g used here: solar variability, atmospheric concentrations of greenhouse gases (CO<sub>2</sub>, CH<sub>4</sub>) and volcanic activity (radiative effects of stratospheric volcanic aerosols). Changes in vegetation cover or land use have been neglected. The external forcings are determined in accordance with available estimations from proxy data; the rating of the effect of solar variability and volcanic aerosols is the most doubtful factor and introduces large uncertainties to the model simulation (*ibid.*, 273–274; Gouirand *et al.* 2006, 3–4). To what extent a model responds to a particular change in the external forcings, that is to say its sensitivity, is a critical point within climate experiments. The ECHO-g model's sensitivity (1.7 K temperature increase for a doubling of the present atmospheric CO<sub>2</sub> concentrations) lies somewhat in the middle of the range of the IPCC simulations and is, therefore, in line with that of many other models. Yet, ECHO-g resolves the stratosphere coarsely and represents photochemistry there not realistically enough, which might involve somewhat too low sensitivity, at least at decadal time scales. The model is, however, reasonable when compared to the temperature increase of the 20<sup>th</sup> century (Matulla *et al.* 2005, 45–46; Zorita *et al.* 2004, 273, 286).

Many studies based on ECHO-g show the model's skills in realistic simulation of climate conditions. Min *et al.* (2005a), for instance, attested ECHO-g good capacities in simulating the seasonal mean climatology and interannual variability of three main surface variables (temperature, precipitation and SLP) by examining a control run. When Zorita *et al.* (2004) applied ECHO-g to simulate the climate evolution during the last five centuries they found that the broad patterns of temperature deviations were well captured by the model. Generally, the simulated earlier climate was colder than the 20<sup>th</sup> century's average. But the simulated cooling was stronger than in most reconstructions that depend on proxy and observational data. Remarkably, the temperatures resulting from the model agreed more closely with a particular proxy reconstruction based on extratropical tree-ring chronologies (*ibid.*, 271). Among other things, this makes it interesting to interpret ECHO-g model data in the context of EI paradox discussion.

In this thesis, simulated temperature data from a model experiment called Erik2 will be used (González-Rouco *et al.* 2006). This historical simulation starts in the year 1000 and runs until 1990. Prior to this target period, a fictitious spin down has been added to level off to realistic conditions. From 1000 onwards, the experiment is driven by the estimated forcing values deriving from values used in the energy-balance climate simulation by Crowley (2000) with a re-scaling of the solar forcing amplitude (Gouirand *et al.* 2006, 15–17).

## 2.6 Sea level pressure data

One aim of the European-wide research project ADVICE (*Annual-to-Decadal Variability in Climate over Europe*), carried out in the 1990s, was to reconstruct gridded mean SLP data for each month since 1780, so even back into EI times. Jones *et al.* (1999) presented the finished gridded data for the years 1780–1990.

The raw data, originating from observed station time series, were taken from two sources. For a sector covering the North Atlantic and Europe (35°N30°W–70°N40°E), an earlier existing version of a grid point pressure dataset for the NH extending back to 1873 on a 5° latitude by 5° longitude grid was chosen. In addition, pressure series from 51 long-term stations across Europe, starting between 1755 and 1871, were employed. Each station's data were homogeneity tested in two stages; firstly, the individual values' reliability was estimated by the four surrounding grid point values; secondly, the neighbouring stations were compared over their whole record length by visual control of difference series and with the aid of relative homogenisation techniques. Adjustments were applied whenever reasonable. To reconstruct the required monthly SLP charts, the grid point as well as the station network data were separately transformed into PCs. Each of the grid point PCs was regressed against all station network PCs. Then, the linear equations for each month, which relate the pressure at each grid point to all station data, were calibrated against independent data during a period from 1936–95, verifying the performance of the equations over 1881–1935. The quality of the reconstructions derived from this PC regression technique is regarded to be generally high, but is reduced during the earliest years towards the edges of the grid. Comparisons with other pressure reconstructions show larger systematic differences before 1820. Due to weaker atmospheric circulation during summer months, the quality is lowered compared to the other seasons. However, the ADVICE data seem convenient as a basis for calculating circulation related indices. How this problem has been dealt with and other techniques within the thesis are presented in the methods section.



## 3 Methods

### 3.1 General data handling

All instrumental temperature data from different sources (HISTALP, CRU, individual supplies) were available as monthly means and have, for practical reasons, been transformed into a standardised shape. Thereby, seasonal and annual means have been calculated. Seasonal averages have been obtained by averaging the three appropriate monthly values (DJF, MAM, JJA and SON) weighted by the number of days per months. Winter means consist of the December temperature of the preceding year and the January and February temperatures of the current year. For the most part, summer means (JJA) are considered in comparison to the annual average (J-D). To provide appropriate means corresponding to the seasonal target period of a certain proxy record, special seasonal averages (e.g. April to August) have been calculated and, whenever appropriate, weighted monthly. Nearly all temperature series are expressed in terms of anomalies from the average of the standard climate period 1961–90; only model results have been calculated with respect to 1901–29 to allow for direct comparison to the study of Moberg *et al.* (2007) where this period was chosen for practical reasons.

To this point, the notations GAR and UST mostly indicated a collection of stations within a certain geographic area. Hereafter, these abbreviations rather intend to represent the mean values of specific series. In this manner, GAR denotes the mean of the HISTALP series. More precisely, this mean derives from a subset of the longest series starting before 1830. Thereby, a sufficiently long period of 30 years of climate observations within the EI period is guaranteed for each individual series in the GAR average. This constraint applies to 27 stations. To keep the conditions of data supply constant through time after 1830, no additional series are considered this year. In the following, all references to a GAR mean refer to this subset. Furthermore, the EOF-based regionalisation of the Alpine temperature series into four low-elevation and one high-elevation subregion is adopted directly for the EI subset, leading to subregion sizes of only two to eight stations (see Table 2.1, p. 28, and Fig. 2.2, p. 29). The representativity of the small subregional samples for the whole area, especially in case of the high-elevation subregion CRS-high, has to be met with scepticism. The regionalisation itself, originating from all temperature stations during the period 1930–2000, is assumed to be valid for the GAR subset during EI times too. In fact, the subregional mean series agree quite strongly among each other (Fig. 4.1a, p. 53). It should be noted

that before 1830, all regional and subregional series are averaged over an inconstant number of individual series. The ingoing station number for the GAR mean, for instance, grows from only three in 1760 to finally 27 from 1830 onwards. Due to their high degree of homogeneity, only the Uppsala and Stockholm series are a proper Scandinavian counterpart to be investigated in connection with the GAR. Their mean (UST) represents long-term temperature variability for Southern Sweden; of course no further subregional separation was possible. Nevertheless, different versions of UST have been considered and are introduced in Chapter 3.3.

The entire instrumental period is often divided into subperiods for analysis. The central pivot in this connection is 1860. This year involves several advantages: (1) It has been defined as the end of the EI and the beginning of the modern observation period, (2) only one identical UST version exists from then on (see Chapter 3.3) and (3) it falls roughly in the middle of the total regarded time span (1722–2005). In many cases, a further temporal subdivision around 1860 into shorter subperiods has been undertaken.

## 3.2 Statistical data treatment

The calculation of the most frequently used statistical measures is briefly outlined now. Temperature trends in the time series have been estimated by simple linear regression. The corresponding absolute temperature change has been obtained by simply multiplying the relative trend by the period length. The significances of the detected decreasing or increasing trends have been estimated by the non-parametric Mann-Kendall test.

Correlations between series have generally been computed with the Pearson correlation coefficient. A high correlation in general, for the kind of data series analysed here, hints at a strong similarity of high-frequency (annual) variability in two series. In addition, a high value can also indicate a good low-frequency (multi-decadal) relationship (Schöner *et al.* 2002, 159). This non-dimensional index is limited on two sides (-1 to 1), which makes it difficult to carry out calculations of significance. Fisher's *z*-transformation converts the correlation coefficient over its entire range of values into an approximate normal distribution. This makes it possible to apply testing techniques. After standardising the transformed correlations (*z*-values) by their standard deviation, the significance levels of the normally distributed variables can be estimated. Running correlations have been generated with the aid of a 21-years running window. Correlation significance tests were operated taking the natural autocorrelation within a climatological time series into account. To counteract underestimation of significance levels, the actual sample size *N* was replaced by the so-called effective sample size *N<sub>eff</sub>*. This effective size is the smaller, the larger the lag-1

autocorrelation of the considered series is (von Storch and Zwiers 1999, 114–115, 148–149; Slonosky *et al.* 2001, 67–68).

Specialised statistical procedures like relative homogeneity testing (Chapter 3.3) and the EOF-based computation of geographical correlations (Chapter 3.4) are presented in separate subchapters.

### 3.3 Further homogenisation of the Uppsala and Stockholm records

As exhaustively discussed in Chapter 2.2, despite of careful homogenisation efforts some doubts about EI temperatures in the UST records maintain. They affect essentially summer temperatures and are connected to the relocation of the Uppsala site in September 1853 and the observation hour change in Stockholm in January 1859 (see p. 31–33). To investigate these uncertainties, four different versions of the UST series with an increasing degree of homogenisation before 1853 and 1859 respectively were created here. Table 3.1 and Figure 3.1 may help to clarify the at first confusing picture of different monthly temperature corrections leading to different UST versions.

- Starting with the standard versions, UPP and STO stand for the homogenised (“official”) series exactly as published by Bergström and Moberg (2002) and Moberg *et al.* (2002) respectively. Because Stockholm had never experienced major relocations, this record was believed to be more reliable by these authors. Therefore, they applied no corrections before 1859 to the original Stockholm temperature series (apart from 1819–1825; see p. 32). In contrast, the Uppsala version of Bergström and Moberg (2002) is actually adjusted according to Stockholm, such that there is no jump in the difference between the two series in September 1853. UST averages the official versions UPP and STO.
- In the course of the analyses here, it will appear useful for certain purposes to utilise the Uppsala series in a version that, indeed, has been gap-filled and otherwise homogenised as made by Bergström and Moberg (2002), but not homogenised for the 1853-break. When doing so, this “original” series will be marked as UPPo. Accordingly, USTo consists of the versions UPPo and STO.
- The regression techniques that had been employed by Moberg *et al.* (2003) to assess the level of potentially too high early summer temperature in the UST data have been retraced in Chapter 2.2 (p. 33–34). Moberg *et al.* (2005a, 118) first refer to summer-corrected versions of UPP and STO, hereafter called UPPm and STOm. Monthly temperatures from May to August were

negatively corrected before 1853/59. Thus, UPPm contains supplementary modifications building upon UPP. USTm denotes the mean of UPPm and STOm.

- In this thesis, yet another approach is chosen to derive possible temperature corrections. UPPh and STOh are generated by applying results from relative homogeneity testing with respect to other North European long-term series in the wider surroundings of Southern Sweden. The applied technique is described below. The notation USTh emerges from the average of UPPh and STOh.

**Table 3.1** Monthly temperature corrections [K] applied to the different versions of the UST series. The versions UPPo and STO have zero corrections before September 1853 and January 1859 respectively. The other versions have various corrections before these time points.

|   | UPPo           | UPP   | UPPm  | UPPh  | STO            | STOm  | STOh  |
|---|----------------|-------|-------|-------|----------------|-------|-------|
|   | before 1853-09 |       |       |       | before 1859-01 |       |       |
| J | 0.00           | -0.11 | -0.11 | -0.60 | 0.00           | 0.00  | -0.50 |
| F | 0.00           | -0.47 | -0.47 | -0.70 | 0.00           | 0.00  | -0.30 |
| M | 0.00           | -0.66 | -0.66 | -0.90 | 0.00           | 0.00  | -0.30 |
| A | 0.00           | -0.55 | -0.55 | -0.90 | 0.00           | 0.00  | -0.30 |
| M | 0.00           | -0.27 | -0.57 | -0.90 | 0.00           | -0.30 | -0.70 |
| J | 0.00           | -0.15 | -0.85 | -0.90 | 0.00           | -0.70 | -1.10 |
| J | 0.00           | -0.11 | -0.81 | -0.80 | 0.00           | -0.70 | -0.90 |
| A | 0.00           | -0.03 | -0.33 | -0.60 | 0.00           | -0.30 | -0.50 |
| S | 0.00           | -0.08 | -0.08 | -0.20 | 0.00           | 0.00  | -0.10 |
| O | 0.00           | -0.19 | -0.19 | -0.20 | 0.00           | 0.00  | 0.00  |
| N | 0.00           | -0.24 | -0.24 | -0.10 | 0.00           | 0.00  | 0.00  |
| D | 0.00           | -0.22 | -0.22 | -0.50 | 0.00           | 0.00  | -0.20 |

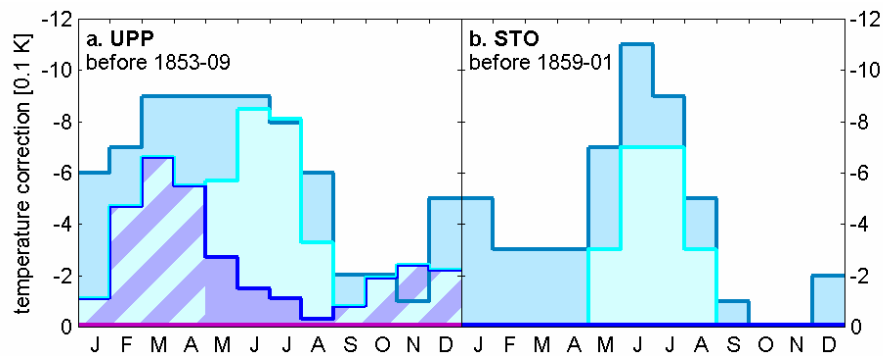


**Figure 3.1** Monthly temperature corrections applied to the UST series before the mid-19<sup>th</sup> century giving rise to four diverging versions: the “original” USTo (violet), the “official” UST (dark blue), the Moberg et al. (2003) prompted USTm (turquoise) and the specifically for this thesis created USTh (light blue).

The SNHT, one of the most sensitive statistical methods of data homogeneity testing, is mainly based on the idea of comparison of a candidate series with a reference series defined as a weighted average of series from surrounding stations. The technique is presented by Alexandersson (1986) and Alexandersson and Moberg (1997). Here, it shall be outlined only regarding its basics. To begin with, an appropriate reference series has to be created. This reference series consists optimally of a set of nearby, homogeneous individual series which are averaged and weighted by their squared correlation coefficients with the candidate station series. In a next step, the time series of differences between the candidate and the reference values are computed. These differences are denoted as  $Q$ -values and altogether form the  $Q$ -series. When the  $Q$ -series is standardised by its standard deviation the  $Z$ -series emerges. Now, the null ( $H_0$ ) and alternative hypothesis ( $H_A$ ) are formulated.  $H_0$  implies that the record is homogenous;  $H_A$ , however, involves that the series experienced an abrupt change of the mean value at some unknown time, i.e. some year  $a$ . After doing so, a statistical test quantity  $T_a$  is calculated for every  $a$ . The time series of  $T_a$ -values is called a  $T$ -series. The highest value of the  $T$ -series,  $T_{max}$ , marks the year that is most likely to be the year immediately before the break. If  $T_{max}$  is significant above some preferred significance level,  $H_0$  can be rejected. The size of the shift can then be estimated from the  $Q$ -series. After doing so, all data before the break can be corrected by adding the shift size as a constant. These descriptions are valid for the SNHT for single shifts. Since this test can not be used to identify trends, a specific SNHT for trends detects linear trends of arbitrary length from year  $a$  to year  $b$ . It calculates a test value for all combinations of  $a$  and  $b$ ; the maximum value thereof gives the test statistic. The support for a detected break or trend is especially strong, if it coincides with a known modification of measuring conditions (*ibid.*; Moberg and Alexandersson 1997, 38–39). Approaches like SNHT suffer from the limitation of assuming a homogeneous reference series whose reliability, actually, can not be proved (Causinus and Mestre 1996, 63).

The execution of SNHT was eased by the availability of ready-for-use programmed software, which was provided by Anders Moberg (personal communication). The homogenisation routines have been applied here on the monthly temperature series of the most “original” versions UPPo and STO. In a first step, suitable reference stations had to be elected out of the available long-term series from Northern Europe (see Chapter 2.3). Four provisional SNHT operations with varying reference sets were tried until the definitive set was found. The final selection of five reference stations, namely Oslo, Helsinki, Tallinn, Copenhagen and Vilnius, was chosen out of considerations concerning data quality as well as the strength of correlations with the candidate series. Due to the very high correlation among the two candidate records, the same reference was applied to both series (Table 3.2). UPPo and STO themselves were excluded from homogenising each other because the results of such an approach are already known from elsewhere (Bergström and Moberg 2002). A principal test period 1816–2000 arises from considerations of the lengths of

the individual reference records and the constraint that at least three reference stations must be obtainable for each year. When the test was applied and a significant break was detected, the test period was divided into secondary subperiods around the break year. In a number of cases, a further division into tertiary subperiods became necessary. The recognition of any 1853/59 breaks in the results has not been aimed a priori, although breaks at these years were expected.

The primary detected breaks in the monthly temperature series are listed in Table 3.2 and selected results for highly significant ones are shown in Figure 3.2. The dates of all significant breaks, also the secondary and tertiary ones, have been ordered, showing a strong tendency to cluster with each other. In the case of UPPo, the most obvious concentration of negative shifts (7) occurs in the years 1852–64. Far behind, other negative shifts during winter months around 1956–59 (2) and a positive one around 1988–92 (2) appears. The 1852–64 break is highly likely related to the major station relocation in September 1853. The large spread of years into the early 1860s may be caused by an additional minor relocation which happened in 1865. Apparently, the SNHT has difficulties in separating individual close-by events. Regarding the STO series, a major cluster of negative shifts in spring and summer months is revealed around 1858–60 (5) and another one around 1818–20 (3). For three summer and autumn months, a positive temperature break is

**Table 3.2** Reference series utilised in and primary breaks detected by SNHT procedures. Break significance is expressed by three (>97.5 %), two (>95 %), one plus (>90 %) or a minus sign (<90 %).

| candidate series       |              | UPPo      |           |      |       |      | STO       |      |           |      |       |
|------------------------|--------------|-----------|-----------|------|-------|------|-----------|------|-----------|------|-------|
| reference series       | set size     | 5         |           |      |       |      | 5         |      |           |      |       |
|                        | period       | 1816-2000 |           |      |       |      | 1816-2000 |      |           |      |       |
|                        | min set size | 3         |           |      |       |      | 3         |      |           |      |       |
|                        | station      | OSL       | HEL       | TAL  | KOP   | VIL  | OSL       | HEL  | KOP       | TAL  | VIL   |
|                        | correlation  | 0.92      | 0.91      | 0.90 | 0.88  | 0.80 | 0.93      | 0.91 | 0.90      | 0.90 | 0.81  |
|                        |              |           |           |      |       |      |           |      |           |      |       |
|                        |              | a         | shift [K] |      | sign. |      |           | a    | shift [K] |      | sign. |
| primary detected break | J            | 1947      | -0.66     |      | +++   |      |           | 1947 | -0.67     |      | +++   |
|                        | F            | 1852      | -0.81     |      | +++   |      |           | 1956 | -0.65     |      | +++   |
|                        | M            | 1860      | -0.97     |      | +++   |      |           | 1860 | -0.40     |      | +++   |
|                        | A            | 1870      | -0.92     |      | +++   |      |           | 1870 | -0.40     |      | +++   |
|                        | M            | 1854      | -0.97     |      | +++   |      |           | 1858 | -0.75     |      | +++   |
|                        | J            | 1864      | -1.05     |      | +++   |      |           | 1858 | -1.12     |      | +++   |
|                        | J            | 1856      | -0.85     |      | +++   |      |           | 1858 | -0.93     |      | +++   |
|                        | A            | 1863      | -0.67     |      | +++   |      |           | 1859 | -0.59     |      | +++   |
|                        | S            | 1858      | -0.33     |      | +++   |      |           | 1820 | -0.92     |      | +++   |
|                        | O            | 1840      | -0.43     |      | ++    |      |           | 1818 | -1.06     |      | +++   |
|                        | N            | 1847      | -0.27     |      | -     |      |           | 1830 | 0.31      |      | -     |
|                        | D            | 1959      | -0.62     |      | +++   |      |           | 1978 | -0.73     |      | +++   |

indicated in the time from 1915–22. The most important break around 1858–60 corresponds very well to the change of the morning observation hour in 1859. The late 1810s shift may be partly related to systematic temperature data troubles in the early 19<sup>th</sup> century that Moberg *et al.* (2002, 177) have reported. In short, the SNHT with relatively far-distance stations as reference could confirm existing doubts concerning early summer temperatures, by detecting dominant negative shifts for UPPo during the 1850s and for STO in the late 1850s in a strictly methodical approach. Reconsidering metadata, the break dates given by the tests can be interpreted to be directly related to the known changes in observing conditions in September 1853 for UPPo and in January 1859 for STO. To obtain definite temperature corrections, the respective Q-series have been utilised again for all months, in order to determine the size of breaks at these fixed dates. The consequential monthly temperature differences have been rounded down to the first decimal place and were then subtracted from all data before the break time point. By doing so, the UPPh and STOh versions have been completed (Fig. 3.1). The adjustments were, as expected, highest for summer months but are partly surprisingly large for some winter and spring months too. Metadata for Uppsala and Stockholm offer no apparent explanation for that. Such inconsistencies may, however, be caused by

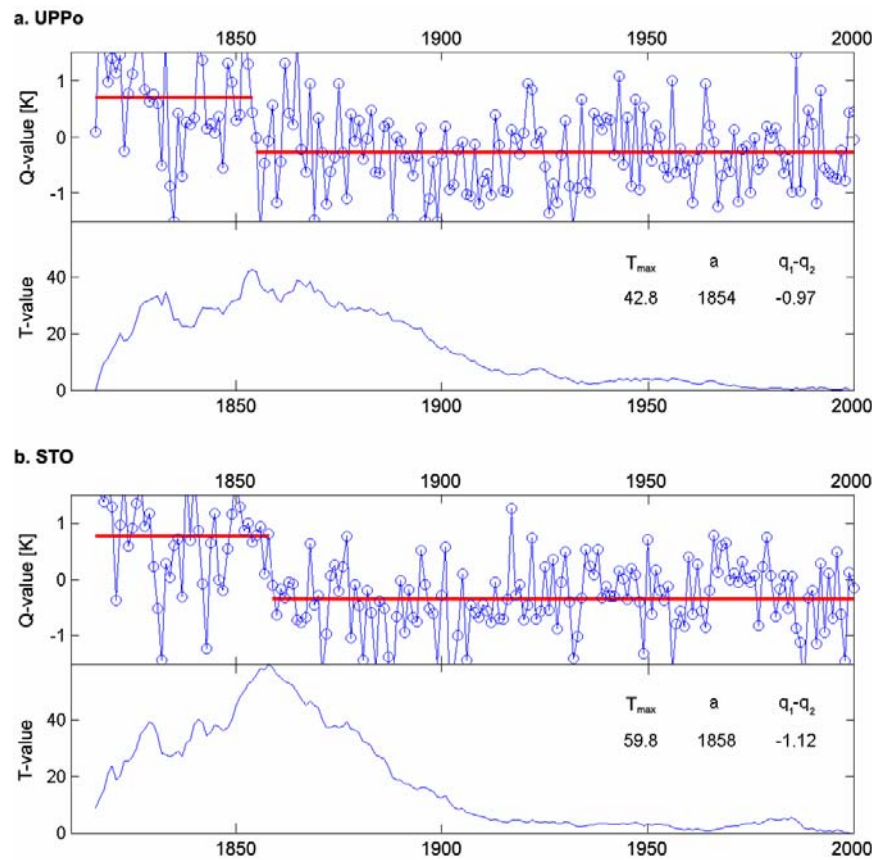


**Figure 3.2** The Q- and T-series for monthly temperature series of May in UPPo (a) and June in STO (b) as example for SNHT results (plot following A. Moberg).

the instance that the reference stations are not homogenous themselves, which can be regarded as a major drawback of the USTh versions.

### 3.4 Creation of atmospheric circulation indices

In order to establish indices related to typical patterns of atmospheric circulation, some basic requirements have been defined in advance. The indices should be monthly resolved and valid for large parts of Europe. As regards the NAO, for instance, the use of a station-based index would be adequate when just winter months would be regarded. But due to the extensive migration of the Icelandic low and the Azores high, the application of just two stations to derive an index of atmospheric circulation is unreliable when other seasons are to be investigated (Portis *et al.* 2001, 71). Principal Component (PC) Analyses, which is an objective and repeatable multivariate statistical method, applied to the ADVICE data set (Chapter 2.6) promises to meet the requirements.

PC Analysis, or EOF Analysis as it is often called in earth sciences, relies on eigenvectors and eigenvalues of correlation or covariance matrices. The method is capable of investigating large data sets in terms of the relationships between the individual data points. By doing so, patterns in multi-dimensional data are identified. Basically, EOF techniques compress the data size by reducing the number of dimensions with a minimal loss of information. To perform the method, the original data has to be put in a matrix with rows indicating temporal development and columns holding variables or spatial points. Then, from each of the data dimensions the mean has to be subtracted, producing a dataset with zero as a mean instead. After that, the covariance matrix between the data's dimensions is calculated. The covariances express how well the data vectors vary together, contrarily or independently from each other. The eigenvectors and eigenvalues of the covariance matrix give information about the pattern in the data; the first eigenvector runs through the middle of the data points (like the line of best fit in a 2-dimensional case), the second one reveals the second most important pattern and so forth. All eigenvectors are sorted by their eigenvalues and the less significant components can be ignored which leads to some information loss, but generally this is assumed to be just noise. The eigenvector with the largest eigenvalue is defined as the leading EOF. The time series out of an EOF is called an expansion coefficient (EC; Smith 2002, 12–20; Stephenson and Benestad 2000, 99–103).

To compute the leading EOFs out of the ADVICE air pressure data, the services of the public climate research website *Climate Explorer* (van Oldenborgh and Burgers 2006) have been exploited. Defined by the temporal coverage of the dataset, the outcome is given for the period 1780–1995.



Because eigenvectors are defined to explain maximum variance, the leading EOFs will expose the regions of highest pressure variability (Hurrell *et al.* 2003, 8–9). For the summer season and the three individual summer months, the four most significant components have been considered more closely. Thereof, the two EOFs that consistently reflect the same modes through all summer months have been chosen. The ECs of these EOFs over the individual months are regarded to constitute the finished, mobile atmospheric circulation indices valid for summer, which are ready for further analysis. The results of the EOF Analysis are presented in Chapter 4.5.

## 4 Results

### 4.1 Early instrumental temperature trends

It is important, when comparing GAR to UST temperature trends, to be aware of the fact that the GAR and UST data are separated by a main difference that has already been pointed out in Chapters 2.1 and 2.2 and that shall be reminded now. The EI subset of HISTALP data analysed in the study consists of 27 series whereas with the Uppsala and Stockholm series only data from two early stations are at hand from Southern Scandinavia. This has important implications for direct comparison since, for instance, the GAR's temperature mean is more smoothed and regionally consistent and the annual temperature range between the individual GAR series becomes much larger compared to the two UST series. For the Alps, a division into subregions is possible; this is not the case for UST. To account for this circumstance, the combined UST series will for some purposes be compared to the CRS (course resolution subregion; see p. 29–30) means rather than to the whole GAR. The central features of the two datasets' temperature climatologies are illustrated in Figure 4.1. The annual temperature trends of the subregions of the GAR (Fig. 4.1a) agree closely. With a correlation coefficient over their whole length between 0.85 and 0.98 among the CRS pairs, the five subregions display rather similar temperature variability, even if the differences become slightly larger before around 1860. The year to year range of the differences between the lowest and highest annual temperature of all incoming series is, due to the high number of 27 stations, quite large. The reduced range before 1830 has to be interpreted as a result of the smaller station number then. The Uppsala and Stockholm series (Fig. 4.1b), on the other hand, shows very little difference, or none at all, as the two series have nearly constantly identical variations ( $r = 0.97$ ). Moreover, the UST series consists exclusively of Uppsala before 1756. The year to year temperature variability of the GAR and UST means is, however, larger in UST than in the GAR because the latter has been averaged over many more single series. Nevertheless, keeping these data related differences in mind a fruitful analysis is possible by means of comparisons of these far back-reaching climate data bases, as the following results will show. In this manner, the question concerning how Alpine and Swedish temperature climate in the EI period is related to each other over the distance of about 1,500 km shall be addressed.

In a first step, Figure 4.1 shall be regarded again, this time in terms of temperature evolution. The two annual trend curves have overall similarities in their main features; decreasing trends

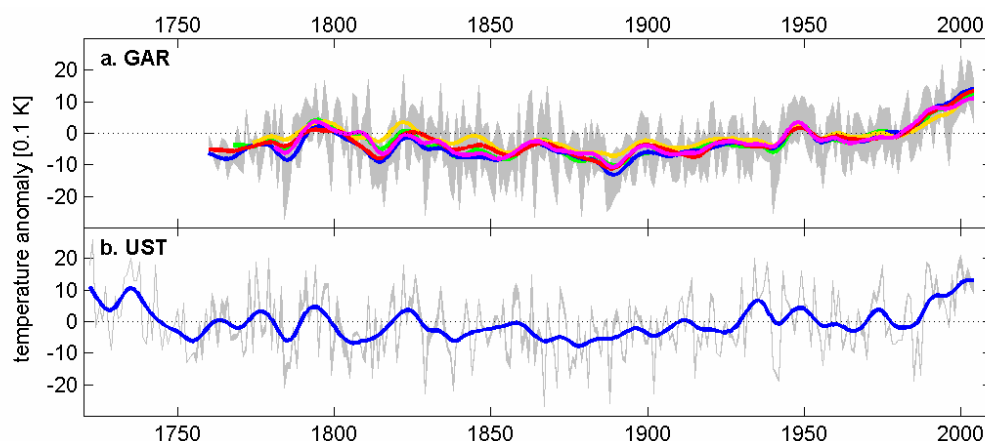


**Figure 4.1** Mean annual temperature evolution and variability in the different subregions of the GAR 1760/81–2005 (a) and UST 1722–2004 (b) (anomalies from 1961–1990). The lines show 20-years Gaussian low-pass filtered trends of temperature anomalies (green – CRS-NE, blue – CRS-NW, yellow – CRS-SE, red – CRS-SW, lilac – CRS-high; see Chapter 2.1); the grey background area contains the range between the minimum and maximum single station value of each year.

from the warm late 18<sup>th</sup> century to the cold mid-19<sup>th</sup> century with large interdecadal variability, small interdecadal variability during a period of low temperature level from then on until about 1930 and finally increased interdecadal variability again with a temperature rising trend that is enhanced after about 1980. Considering the annual GAR average solely, this final rising trend stands out over the warm early episode around 1800. For the UST mean, however, temperature about as warm as the post-1980 conditions are seen in the very first 34 years that base completely on Uppsala data. The 1720s and 1730s were warm above average due to notably maritime climate conditions with mild winters. Yet, the actual level of warmth is not certain due to various problems connected with the fact that the thermometer was placed indoors in an unheated and well ventilated room before 1739 and because temperature data from another site was used and extrapolated to the Uppsala level (see p. 30–31; Moberg and Bergström 1997, 684–686). The annual values and running trends of the seasonal mean temperatures as well as of a continentality index of the GAR and UST are directly drawn against each other in Figure 4.2. In addition, the trend of the USTh series (the version of UST that has been produced by relative homogeneity testing and is generally cooler than the standard UST series before the 1859; see p. 46–50), is plotted. Paying special attention to the evolution of summer temperature since 1722/60 (Fig. 4.2c), the generally high values of UST from the beginning until about 1860 stand out. This warm period is also seen in the GAR data, even if the abnormally warm intervals are less pronounced, not as long-lasting and more concentrated around 1800 there. Accordingly, summers in Sweden until around 1860 seem to have been generally warmer than in the Alps, with respect to respective standard climate. From 1860 until the beginning of the 20<sup>th</sup> century, summer temperatures in the Alps and Southern

Sweden were generally cool and variations occurred within a similar range. Despite of this, the 20<sup>th</sup> century's summer warming trends did not proceed simultaneously; fairly warm summers observed in Sweden in the 1930s and around 1970 did not occur in the Alps. The steep summer temperature rise during the last 25–30 years initiated some years earlier in the GAR, but is, nevertheless, a common feature to both regions. In short, some extended episodes of similar temperature evolutions do exist in both the GAR and UST but the relations are not constant and, in some cases, summer temperature trends seem to be decoupled. The application of the homogenised USTh version lowers the Swedish pre-1860 summer temperatures considerably to a level that, in the main, matches better with the GAR series and reduces the differences in long-term trends between the regions. Nevertheless, this simple lowering of summer temperatures does

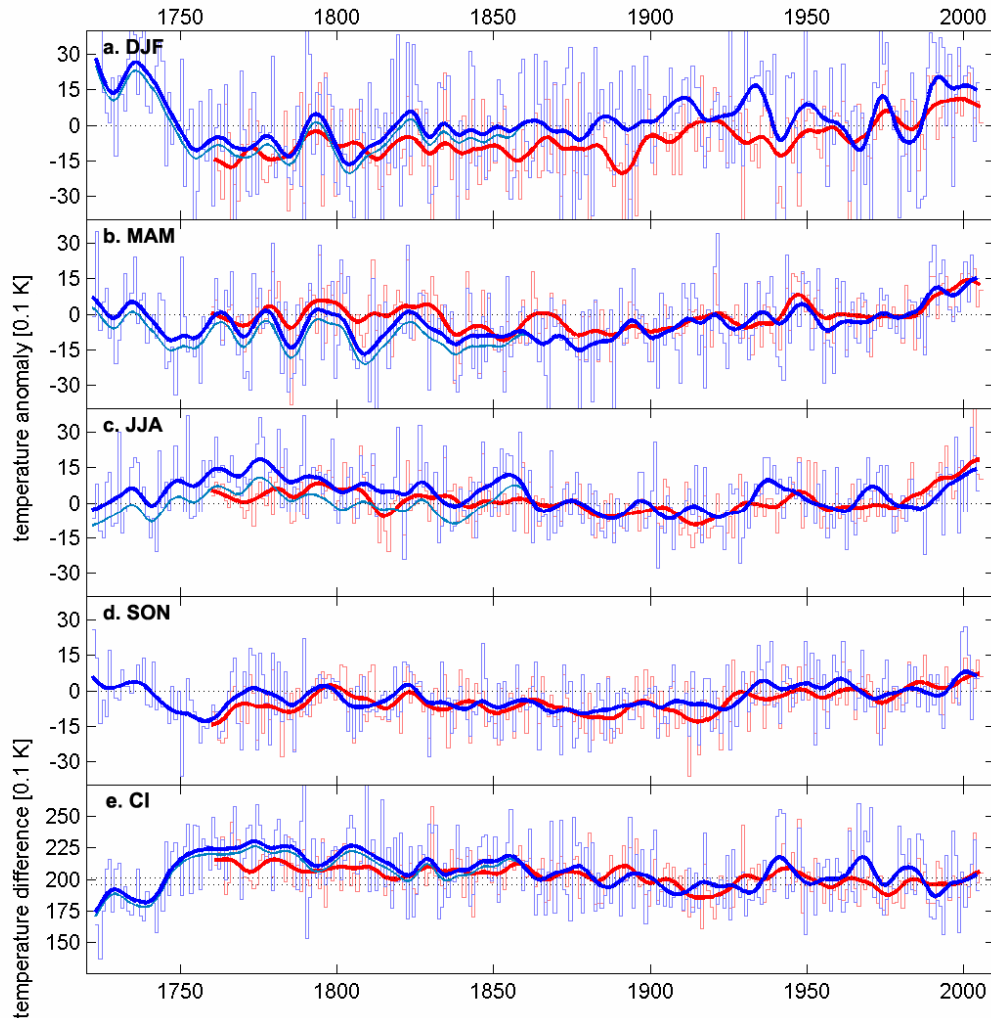


**Figure 4.2** Comparison of mean winter (a), spring (b), summer (c) and autumn (d) temperature evolution and a continentality index (e) in the GAR (red) 1760–2005 and for UST (blue) 1722–2004. Continentality is defined as the difference between January and July mean temperatures (1961–90 average is 19.6 K for the GAR and 20.1 K for UST). Shown are anomalies from the 1961–90 average (stairs) and their 20-years Gaussian low-pass filtered trends (lines); the light blue line illustrates the USTh version.

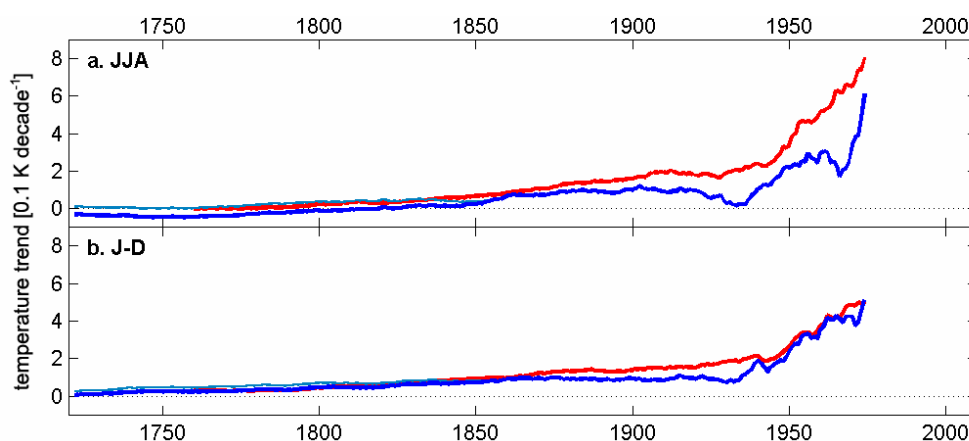
naturally not cause the details in the UST temperature series to better fit GAR temperatures. The other subplots of Figure 4.2 intend to set the coming analyses, which largely concentrate on summer and annual results, in relation to the other seasons. Interannual variability is largest during winter months. The correlation between the GAR and UST is quite strong in winter ( $r = 0.49$  for the entire common data period 1760–2004), but the strongest correlation is found for spring ( $r = 0.60$ ), followed by autumn ( $r = 0.53$ ). For the non-summer seasons, the visual comparison shows partly long-lasting phases of strong agreement between Alpine and Swedish temperature trends. Actually, the strength of correlation is lowest for the summer season (see Table 4.3). This can be traced back to the fact that large-scale atmospheric circulation over Europe is weakest during the warm season, an outcome that will be regarded more closely later on (especially in Chapter 4.5).

Table 4.1 provides a description of the temperature evolution in a more standardised and numeric form, namely in terms of trends derived from linear regression for different time periods. The left half of the table contains summer, the right one annual temperature trends. For both parts, trends for the entire period of existing data and for two subperiods separating the EI period from the modern observation period and for six roughly 50-year subperiods are specified. Each trend rate value is complemented by the respective absolute temperature change. The noted highly significant overall annual temperature trend for the GAR is  $0.03 \text{ K decade}^{-1}$ , which gives a total temperature increase of  $0.69 \text{ K}$  over 245 years. In UST, the averaged temperature rose by only  $0.17 \text{ K}$  over the 283 years, resulting from a small positive trend of  $0.01 \text{ K decade}^{-1}$ . Because of its lower EI temperatures, the USTh version raises the overall trend to be comparable to the GAR's. In both regions, annual temperature declined somewhat during the EI period, followed by an increase after 1860. Regarding summer temperatures only, it has been mentioned in the introductory chapter that a surprising zero or even slightly negative trend had been found for the entire GAR series (Matulla *et al.* 2005, 40). As expected, this feature is also evident for the 27 longest GAR series, where the summer trend diminishes to about zero and the absolute temperature change from 1760–2004 was  $-0.06 \text{ K}$ . During the EI period, the trend was negative over the whole GAR ( $-0.05 \text{ K decade}^{-1}$ ) implying an average temperature drop by about half a degree. The strongest cooling trend was observed in the high-elevation subregion CRS-high, where the temperature declined by nearly one degree ( $-0.12 \text{ K decade}^{-1}$  for 1781–1860), the weakest one in the southwestern subregion CRS-SW ( $-0.02 \text{ K decade}^{-1}$  for 1760–1860). After 1860, summer temperatures in the Alps had a positive trend of  $0.09 \text{ K decade}^{-1}$  leading to a total warming of  $1.22 \text{ K}$ . Despite some warm summers in Scandinavia recently, the trend for the whole data period is significantly negative ( $-0.03 \text{ K decade}^{-1}$ ), which means a summer cooling by  $-0.78 \text{ K}$  since 1722. During the EI period, the summer trend was approximately balanced ( $0.01 \text{ K decade}^{-1}$ ), whereas since 1860 the

**Table 4.1** Long-term change of mean summer and annual temperature in the GAR in different subperiods and subregions, and for UST in different subperiods and different versions. The upper italic values indicate the respective trends [K decade<sup>-1</sup>] derived from linear regression, the lower roman numbers give the absolute temperature change [K] during the respective periods. Underscored trends are significant at the 95 % level, double underscored trends at the 99 % level.

|                    |                                    | JJA                      |                          |               |             |                               |             |               |             | J-D           |                          |                          |               |              |                               |              |               |             |               |
|--------------------|------------------------------------|--------------------------|--------------------------|---------------|-------------|-------------------------------|-------------|---------------|-------------|---------------|--------------------------|--------------------------|---------------|--------------|-------------------------------|--------------|---------------|-------------|---------------|
|                    | starting<br>year (a <sub>1</sub> ) | a <sub>1</sub> –<br>2004 | a <sub>1</sub> –<br>1860 | 1861–<br>2004 | 1722–<br>60 | 1761/a <sub>1</sub> –<br>1810 | 1811–<br>60 | 1861–<br>1910 | 1911–<br>60 | 1961–<br>2004 | a <sub>1</sub> –<br>2004 | a <sub>1</sub> –<br>1860 | 1861–<br>2004 | 1722–<br>60  | 1761/a <sub>1</sub> –<br>1810 | 1811–<br>60  | 1861–<br>1910 | 1911–<br>60 | 1961–<br>2004 |
| number of<br>years |                                    | 224–<br>283              | 80–139                   | 144           | 39          | 30–50                         | 50          | 50            | 50          | 44            | 224–<br>283              | 80–139                   | 144           | 39           | 30–50                         | 50           | 50            | 50          | 44            |
| GAR                | 1760                               | 0.00                     | -0.05                    | <u>0.09</u>   | -           | 0.08                          | 0.06        | <u>-0.12</u>  | <u>0.20</u> | <u>0.52</u>   | <u>0.03</u>              | -0.02                    | <u>0.10</u>   | -            | <u>0.16</u>                   | -0.10        | -0.08         | <u>0.11</u> | <u>0.39</u>   |
|                    |                                    | -0.06                    | -0.47                    | 1.22          | -           | 0.42                          | 0.32        | -0.59         | 0.98        | 2.28          | 0.69                     | -0.24                    | 1.42          | -            | 0.79                          | -0.48        | -0.40         | 0.56        | 1.71          |
| CRS-NE             | 1767/8                             | -0.01                    | <u>-0.09</u>             | <u>0.08</u>   | -           | 0.08                          | -0.01       | <u>-0.16</u>  | <u>0.20</u> | <u>0.51</u>   | <u>0.02</u>              | <u>-0.07</u>             | <u>0.10</u>   | -            | 0.16                          | <u>-0.15</u> | -0.10         | 0.11        | <u>0.37</u>   |
|                    |                                    | -0.18                    | -0.87                    | 1.12          | -           | 0.34                          | -0.06       | -0.82         | 1.01        | 2.23          | 0.53                     | -0.65                    | 1.41          | -            | 0.67                          | -0.77        | -0.49         | 0.53        | 1.64          |
| CRS-NW             | 1760                               | 0.00                     | -0.04                    | <u>0.09</u>   | -           | 0.08                          | 0.17        | <u>-0.14</u>  | <u>0.20</u> | <u>0.56</u>   | <u>0.04</u>              | -0.02                    | <u>0.11</u>   | -            | <u>0.16</u>                   | -0.05        | -0.11         | 0.11        | <u>0.44</u>   |
|                    |                                    | 0.06                     | -0.43                    | 1.32          | -           | 0.40                          | 0.87        | -0.68         | 0.98        | 2.48          | 0.90                     | -0.24                    | 1.60          | -            | 0.79                          | -0.24        | -0.53         | 0.54        | 1.94          |
| CRS-SE             | 1774                               | -0.01                    | <u>-0.07</u>             | <u>0.07</u>   | -           | -0.02                         | -0.03       | <u>-0.08</u>  | <u>0.19</u> | <u>0.43</u>   | <u>0.01</u>              | <u>-0.06</u>             | <u>0.07</u>   | -            | 0.08                          | <u>-0.14</u> | -0.04         | 0.08        | <u>0.29</u>   |
|                    |                                    | -0.14                    | -0.59                    | 0.97          | -           | -0.09                         | -0.15       | -0.38         | 0.93        | 1.87          | 0.30                     | -0.48                    | 1.02          | -            | 0.29                          | -0.69        | -0.20         | 0.40        | 1.26          |
| CRS-SW             | 1760                               | 0.00                     | -0.02                    | <u>0.09</u>   | -           | 0.08                          | 0.07        | <u>-0.08</u>  | <u>0.20</u> | <u>0.53</u>   | <u>0.03</u>              | -0.02                    | <u>0.10</u>   | -            | <u>0.12</u>                   | -0.06        | -0.04         | <u>0.14</u> | <u>0.39</u>   |
|                    |                                    | 0.03                     | -0.21                    | 1.29          | -           | 0.39                          | 0.33        | -0.42         | 0.98        | 2.33          | 0.66                     | -0.19                    | 1.43          | -            | 0.58                          | -0.30        | -0.21         | 0.69        | 1.72          |
| CRS-high           | 1781                               | 0.00                     | <u>-0.12</u>             | <u>0.10</u>   | -           | 0.17                          | 0.02        | <u>-0.08</u>  | <u>0.19</u> | <u>0.49</u>   | <u>0.03</u>              | <u>-0.10</u>             | <u>0.09</u>   | -            | 0.20                          | -0.13        | -0.10         | 0.10        | <u>0.39</u>   |
|                    |                                    | 0.07                     | -0.95                    | 1.38          | -           | 0.52                          | 0.11        | -0.40         | 0.96        | 2.15          | 0.62                     | -0.84                    | 1.31          | -            | 0.60                          | -0.63        | -0.49         | 0.52        | 1.71          |
| USTo               | 1722                               | <u>-0.03</u>             | 0.00                     |               | 0.31        | <u>-0.22</u>                  | 0.12        |               |             |               | 0.00                     | <u>-0.07</u>             |               | <u>-0.51</u> | -0.13                         | -0.04        |               |             |               |
|                    |                                    | -0.87                    | 0.06                     |               | 1.20        | -1.09                         | 0.61        |               |             |               | -0.10                    | -0.91                    |               | -1.97        | -0.67                         | -0.20        |               |             |               |
| UST                | 1722                               | <u>-0.03</u>             | 0.01                     | <u>0.07</u>   | 0.31        | -0.22                         | 0.13        | -0.08         | 0.12        | <u>0.31</u>   | 0.01                     | <u>-0.05</u>             | <u>0.09</u>   | <u>-0.48</u> | -0.13                         | -0.02        | 0.07          | 0.06        | <u>0.37</u>   |
|                    |                                    | -0.78                    | 0.12                     | 0.99          | 1.22        | -1.09                         | 0.63        | 0.42          | 0.60        | 1.34          | 0.17                     | -0.74                    | 1.31          | -1.88        | -0.67                         | -0.10        | 0.37          | 0.30        | 1.63          |
| USTm               | 1722                               | 0.00                     | 0.02                     |               | 0.31        | -0.22                         | 0.18        |               |             |               | <u>0.01</u>              | -0.05                    |               | <u>-0.48</u> | -0.13                         | 0.00         |               |             |               |
|                    |                                    | 0.06                     | 0.23                     |               | 1.22        | -1.09                         | 0.90        |               |             |               | 0.42                     | -0.71                    |               | -1.88        | -0.67                         | -0.02        |               |             |               |
| USTh               | 1722                               | 0.01                     | 0.01                     |               | 0.30        | <u>-0.22</u>                  | 0.19        |               |             |               | <u>0.03</u>              | -0.05                    |               | <u>-0.49</u> | -0.13                         | 0.01         |               |             |               |
|                    |                                    | 0.30                     | 0.15                     |               | 1.18        | -1.09                         | 0.94        |               |             |               | 0.73                     | -0.71                    |               | -1.91        | -0.67                         | 0.05         |               |             |               |

summers have become warmer by about one degree ( $0.07 \text{ K decade}^{-1}$ ). The lowering of early summer temperatures introduced by the correction applied to the USTm version approximately equalises the overall trend. USTh even leads to a small trend reversal to a warming by  $0.01 \text{ K decade}^{-1}$  or an absolute change of  $0.3 \text{ K}$  from 1722–2004. Going into shorter temporal segments of about 50 years, the only subperiod with a negative trend in the GAR is from 1861–1910 ( $-0.12 \text{ K decade}^{-1}$ ). The EI subperiods from 1761–1810 and 1811–1860 show small positive trends. The summer temperature trend for the most recent subperiod is large and significant ( $0.52 \text{ K decade}^{-1}$  for 1961–2004), where CRS-NW is the most affected Alpine subregion. The recent summer trend is somewhat less expressed in the UST ( $0.31 \text{ K decade}^{-1}$ ), but is larger than the trends of all preceding 50-year subperiods, except for 1722–60, which shows a warming trend of the same size. For the three subperiods during 1811–1960, the UST trends fit quite well with the Alpine ones. Yet, the early subperiod 1761–1810 is, in contrast to the GAR, characterised by a negative trend of  $-0.22 \text{ K decade}^{-1}$ . To put early Alpine and Swedish temperature trends into another context, Figure 4.3 provides an interesting alternative. It compares the GAR, UST and USTh summer and annual temperature trends and illustrates their changes over time. To this end, the trend has been calculated starting at each year on the abscissa to the common final year 2004. Therefore, the trend length varies from right to left from 30 to 283 or 245 years. The annual temperature trends from the Alps and Sweden (Fig. 4.3b) agree very well. The internal difference between UST and USTh is negligible too. The trends over the longest periods are close to zero, they grow continuously with decreasing length until about 55 years (1950–2004) and rise largely from then on. The general picture is the same for summer trends (Fig. 4.3a). One important difference are the zero and even



**Figure 4.3** Comparison of the change of summer (a) and annual (b) temperature trends with different length for the GAR (red), UST (blue) and USTh (light blue). The abscissa holds the trends' starting year (1722/60–1974), the common final year is 2004. Therefore, the trend length from left to right varies from 283/245–30 years.

negative trends over the long periods for the GAR and UST. The USTh version, however, lifts these long UST trends by about  $0.04 \text{ K decade}^{-1}$  to a slightly positive level.

Besides the analysis of long-term averages, single extreme values may provide insight into temperature variability and into the supraregional extension of outstanding events. Table 4.2 lists the coldest and warmest summer month (among June, July and August) and seasonal (JJA mean) and annual means for both the GAR and UST. The lowering of summer temperature induced to the EI data in the USTh version affects warm values in the years prior to 1859 to appear less warm and the cold values to appear more extreme. To illustrate the effect of the USTh correction, results are shown for both UST and USTh. The only extreme event that happened to lie at top position in both the GAR and UST is June 1923 ( $-3.5$  and  $-4.7 \text{ K}$  respectively, expressed as anomalies from the 1961–90 average), which was the coolest summer month over the whole data period in both study regions. June 1871 is evident in both regions too. June 2003, which had the largest positive summer temperature anomaly of all months in the Alps since observations started ( $+5.7 \text{ K}$  in the GAR,  $+6.6 \text{ K}$  in CRS-high), was not unusual at all in UST ( $+0.6 \text{ K}$ ) where the six hottest Junes took place during the EI period instead. In a similar manner, seven of the ten most positively deviating July months occurred before 1860 in UST, whereas in the Alps more recent Julies (1983, 1994) dominate. However, the correction applied to USTh moves July 1994 forward to the fourth position. The ranking of cool August months shows a wider distribution over the data period. 1833 was very cool both in the GAR ( $-2.5 \text{ K}$ ) and UST ( $-2.9 \text{ K}$ ). On the other end of the rank, 1846 appears as the very hottest August month in UST ( $+5.5 \text{ K}$ ); USTh downgrades it to the second place, being exceeded by 2002 ( $+5.1 \text{ K}$ ). August 2003, which stood out in the Alps ( $+5.4 \text{ K}$ ), was again not very special in Sweden ( $+1.6 \text{ K}$ ). Concerning the summer season as a whole, the coolest UST summer, 1902 ( $-2.8 \text{ K}$ ), is not particular from an Alpine point of view ( $-0.9 \text{ K}$ ), but the third coolest one – and according to USTh even the coolest, the summer of 1821 ( $-2.4 \text{ K}$ ) – can be found among the ten coolest Alpine ones ( $-1.4 \text{ K}$ ). Conversely, the coolest GAR summer, the in Central Europe well noted “year without a summer” 1816 ( $-2.1 \text{ K}$ ) – which, interestingly enough, is not as evident concerning single monthly values – had a totally different character in Sweden ( $+0.5 \text{ K}$ ). The ranking of the warmest UST summers is remarkable; 24 of the 30 Swedish summers with the largest positive anomalies took place during the EI period; the USTh version, however, reduces this concentration in early years (to 17 of 30) and even puts 2002 on the top of the list ( $+3.2 \text{ K}$ ). The hottest UST summer 1752 ( $+3.7 \text{ K}$ ) lies beyond the coverage available for Alpine instrumental data, but for 2002 a quite strong positive anomaly was observed ( $+1.7 \text{ K}$ ). The extraordinary hot summer of 2003 ( $+4.4 \text{ K}$ ) in the GAR was by far not as extreme in UST ( $+2.0 \text{ K}$ ). The comparison of the coldest and warmest annual means reveals some similarities. Nevertheless, drawing valuable conclusions from the comparison of extreme monthly and seasonal summer extreme events



**Table 4.2** List of the negative and positive monthly (June, July or August), seasonal (JJA mean) and annual extreme values (as anomalies [K] from the 1961–90 period’s mean) at single stations, subregions and the entire regions of the GAR and UST. For UST, no division into subregions is possible, but results are shown for both the UST and USTh versions.

|                  |      | Jun/Jul/Aug |         |      |      |         |      | JJA  |      |      |      | J–D  |      |      |      |      |      |      |      |
|------------------|------|-------------|---------|------|------|---------|------|------|------|------|------|------|------|------|------|------|------|------|------|
|                  |      | min         |         |      | max  |         |      | min  |      | max  |      | min  |      | max  |      |      |      |      |      |
| single stations  | GAR  | -7.7        | 1839-08 | INN  | +7.2 | 2003-06 | ZUR  | -3.0 | 1816 | KAR  | +5.4 | 2003 | MUN  | -2.7 | 1784 | KAR  | +2.4 | 2000 | MUN  |
|                  |      | -4.8        | 1884-06 | VER  | +6.8 | 2003-06 | BAS  | -2.8 | 1816 | BAS  | +5.1 | 2003 | ZUR  | -2.7 | 1864 | RGB  | +2.3 | 2002 | MUN  |
|                  |      | -4.7        | 1833-08 | MUN  | +6.8 | 2003-06 | MUN  | -2.7 | 1816 | NIC  | +5.1 | 2003 | BAS  | -2.6 | 1879 | STU  | +2.3 | 2003 | PAD  |
|                  | UST  | -4.9        | 1923-06 | UPP  | +5.8 | 1752-07 | UPP  | -2.8 | 1902 | STO  | +4.1 | 1789 | STO  | -2.7 | 1867 | UPP  | +2.6 | 1723 | UPP  |
|                  |      | -4.6        | 1923-06 | STO  | +5.5 | 1846-08 | UPP  | -2.8 | 1902 | UPP  | +3.7 | 1752 | UPP  | -2.7 | 1867 | STO  | +2.1 | 2000 | UPP  |
|                  |      | -4.4        | 1928-06 | UPP  | +5.4 | 1846-08 | STO  | -2.6 | 1928 | UPP  | +3.6 | 1826 | STO  | -2.6 | 1888 | UPP  | +2.0 | 1735 | UPP  |
|                  | USTh | -4.9        | 1923-06 | UPP  | +5.1 | 1997-08 | STO  | -3.2 | 1821 | UPPh | +3.3 | 2002 | UPP  | -2.7 | 1829 | STOh | +2.3 | 1723 | UPPh |
|                  |      | -4.6        | 1821-06 | STOh | +5.1 | 2002-08 | STO  | -3.0 | 1821 | STOh | +3.2 | 1789 | STOh | -2.7 | 1867 | UPP  | +2.1 | 2000 | UPP  |
|                  |      | -4.6        | 1923-06 | STO  | +5.1 | 2002-08 | UPP  | -2.8 | 1902 | STO  | +3.1 | 1752 | UPPh | -2.7 | 1867 | STO  | +2.0 | 1934 | UPP  |
| subregions (CRS) | GAR  | -4.1        | 1919-07 | high | +6.6 | 2003-06 | high | -2.7 | 1816 | NW   | +4.8 | 2003 | NW   | -2.3 | 1829 | NE   | +2.0 | 1994 | NW   |
|                  |      | -3.8        | 1923-06 | NE   | +6.3 | 2003-06 | NW   | -2.3 | 1913 | NE   | +4.7 | 2003 | high | -2.2 | 1879 | NW   | +2.0 | 1994 | NE   |
|                  |      | -3.8        | 1884-06 | high | +5.7 | 2003-08 | NW   | -2.2 | 1816 | SW   | +4.6 | 2003 | SW   | -2.1 | 1864 | NE   | +1.9 | 2000 | NE   |
|                  |      | -3.7        | 1913-07 | high | +5.6 | 2003-06 | SW   | -2.2 | 1913 | high | +4.1 | 2003 | SE   | -2.1 | 1829 | NW   | +1.9 | 2000 | NW   |
|                  |      | -3.7        | 1871-06 | high | +5.5 | 2003-08 | SW   | -2.1 | 1813 | NW   | +4.0 | 2003 | NE   | -2.1 | 1879 | NE   | +1.9 | 2000 | SW   |
| versions         | UST  | -4.7        | 1923-06 |      | +5.8 | 1752-07 |      | -2.8 | 1902 |      | +3.7 | 1752 |      | -2.7 | 1867 | UST  | +2.6 | 1723 |      |
|                  |      | -4.3        | 1928-06 |      | +5.5 | 1846-08 |      | -2.6 | 1928 |      | +3.7 | 1789 |      | -2.4 | 1888 | UST  | +2.0 | 1735 |      |
|                  |      | -3.8        | 1871-06 |      | +5.1 | 2002-08 |      | -2.4 | 1821 |      | +3.6 | 1775 |      | -2.2 | 1829 | UST  | +2.0 | 2000 |      |
|                  |      | -3.5        | 1821-06 |      | +5.0 | 1997-08 |      | -2.2 | 1987 |      | +3.3 | 1826 |      | -2.2 | 1902 | UST  | +2.0 | 1934 |      |
|                  |      | -3.3        | 1865-06 |      | +4.9 | 1752-08 |      | -2.1 | 1742 |      | +3.2 | 1819 |      | -2.1 | 1871 | UST  | +1.9 | 1779 |      |
|                  | USTh | -4.7        | 1923-06 |      | +5.1 | 2002-08 |      | -3.1 | 1821 | USTh | +3.2 | 2002 |      | -2.7 | 1867 |      | +2.3 | 1723 |      |
|                  |      | -4.4        | 1821-06 |      | +5.1 | 1752-07 |      | -2.8 | 1902 |      | +3.1 | 1752 |      | -2.6 | 1829 | USTh | +2.0 | 2000 |      |
|                  |      | -4.3        | 1928-06 |      | +5.0 | 1997-08 |      | -2.8 | 1742 | USTh | +3.0 | 1789 |      | -2.5 | 1838 | USTh | +2.0 | 1934 |      |
|                  |      | -3.8        | 1871-06 |      | +4.9 | 1846-08 |      | -2.6 | 1928 |      | +2.8 | 1997 |      | -2.4 | 1888 |      | +1.8 | 1989 |      |
|                  |      | -3.8        | 1832-07 |      | +4.7 | 1914-07 |      | -2.5 | 1832 | USTh | +2.8 | 1775 |      | -2.2 | 1902 |      | +1.8 | 1938 |      |
| region           | GAR  | -3.5        | 1923-06 |      | +5.7 | 2003-06 |      | -2.1 | 1816 | GAR  | +4.4 | 2003 |      | -1.8 | 1879 | GAR  | +1.8 | 1994 |      |
|                  |      | -3.4        | 1913-07 |      | +5.4 | 2003-08 |      | -1.9 | 1913 | GAR  | +2.4 | 1807 |      | -1.7 | 1829 | GAR  | +1.7 | 2000 |      |
|                  |      | -3.4        | 1919-07 |      | +4.4 | 1807-08 |      | -1.7 | 1813 | GAR  | +2.4 | 1994 |      | -1.7 | 1864 | GAR  | +1.6 | 2003 |      |
|                  |      | -3.2        | 1884-06 |      | +4.3 | 1822-06 |      | -1.5 | 1918 | GAR  | +2.1 | 1846 |      | -1.6 | 1785 | GAR  | +1.6 | 2002 |      |
|                  |      | -3.1        | 1896-08 |      | +3.7 | 1992-08 |      | -1.5 | 1882 | GAR  | +2.1 | 1834 |      | -1.6 | 1816 | GAR  | +1.2 | 1822 |      |

between the Alps and Sweden is only possible in some cases and provides no consistent insights, as no steady coincidence could be found.

Correlation analysis is expected to be more useful. This has been accomplished for the subregions of the GAR and the versions of the UST series over the entire common data period, the EI and the modern observational period (Table 4.3). All correlation coefficients among subregions and different versions take positive values, implying a main common dependence of temperature

evolution in the two regions, even if the strengths of correlations differ quite a lot. Due to long calculation periods, the bulk of the resulting values is characterised by very high significance. Not surprisingly, the correlations among the GAR's subregions are especially large and significant. Anyhow, the key value in Table 4.3 is  $r = 0.36$ , describing the moderate (not to say weak) positive correlation between the summer temperature means of the GAR and UST during 1760–2004. Similar calculations applied to the more homogenised versions USTm and USTh result in somewhat lower correlations. As already suggested, the seasonal changes in large-scale circulation strength over Europe trigger the correlation to be weakest during the summer and considerably higher during other seasons. This gives rise to an annual correlation of as much as 0.62 over the far distance between the Alps and Southern Sweden. As regards the Alpine subregions, the annual correlation with UST weakens from the north-east (0.64 for CRS-NE) to the south-west (0.54 for CRS-SW). Considering the EI and modern observational periods separately, the correlation is somewhat weaker prior to 1860 (0.59) than from 1861 onwards (0.63), but significant in both subperiods. On the contrary, the correlation of summer temperatures was slightly higher during the EI period (0.37) compared to afterwards (0.30). As regards the period 1760–1860, the correlation between the GAR and UST is unimportantly weakened if the USTm and USTh versions (0.36) are employed (as expected because the applied corrections were constant over time). Furthermore, the discrepancy in temperature correlations between UST and the subregions north and south of the Alpine main chain respectively is enhanced during summers compared to the whole year. For the period 1760–2004, the summer correlations between UST and CRS-NE (0.43) and CRS-NW (0.37) are noticeably stronger than between UST and CRS-SE (0.29) and CRS-SW (0.21). The high-elevation subregion CRS-high achieves a correlation of 0.29 with UST for the period 1781–1860. Similar correlations between the Alpine subregions and UST are obtained for the whole period 1760–2004.

Recently, Efthymiadis *et al.* (2006) handled a similar issue. They calculated correlation fields between GAR winter (DJF) and summer (JJA) temperatures and broader European temperatures. Whereas Alpine temperatures are stronger correlated to Northern Europe during winter, the coherence is markedly lowered during summer, when Alpine temperatures rather link towards Northern Africa. Furthermore, GAR high-elevation temperatures show higher correlation with Scandinavia during winter.

**Table 4.3** (p. 61) *Correlation table of the mean summer (left half) and annual (right half) temperature series of the GAR and its subregions with different versions of the UST temperature series for the overall common period of existing data (upper part) and the periods of EI (middle part) and modern (lower part) measurements. Underscored correlations are significant at the 99.5 % level, double underscored correlations at the 99.9 % level.*

| JJA                  |             |             |             |             |             |             |             |             |             |             | J-D         |  |             |             |             |             |             |             |             |             |             |             |             |
|----------------------|-------------|-------------|-------------|-------------|-------------|-------------|-------------|-------------|-------------|-------------|-------------|--|-------------|-------------|-------------|-------------|-------------|-------------|-------------|-------------|-------------|-------------|-------------|
|                      |             | GAR         | CRS-NE      | CRS-NW      | CRS-SE      | CRS-SW      | CRS-high    | USTo        | UST         | USTm        | USTh        |  |             | GAR         | CRS-NE      | CRS-NW      | CRS-SE      | CRS-SW      | CRS-high    | USTo        | UST         | USTm        | USTh        |
| 1760/a,<br>-<br>2004 | GAR         | -           | <u>0.95</u> | <u>0.97</u> | <u>0.93</u> | <u>0.92</u> | <u>0.97</u> | <u>0.36</u> | <u>0.36</u> | <u>0.34</u> | <u>0.33</u> |  |             | -           | <u>0.97</u> | <u>0.98</u> | <u>0.93</u> | <u>0.94</u> | <u>0.94</u> | <u>0.61</u> | <u>0.62</u> | <u>0.62</u> | <u>0.62</u> |
|                      | CRS-NE      | <u>0.95</u> | -           | <u>0.90</u> | <u>0.88</u> | <u>0.78</u> | <u>0.92</u> | <u>0.43</u> | <u>0.43</u> | <u>0.41</u> | <u>0.40</u> |  |             | <u>0.97</u> | -           | <u>0.93</u> | <u>0.91</u> | <u>0.85</u> | <u>0.90</u> | <u>0.64</u> | <u>0.64</u> | <u>0.64</u> | <u>0.63</u> |
|                      | CRS-NW      | <u>0.97</u> | <u>0.90</u> | -           | <u>0.84</u> | <u>0.85</u> | <u>0.94</u> | <u>0.37</u> | <u>0.37</u> | <u>0.36</u> | <u>0.36</u> |  |             | <u>0.98</u> | <u>0.93</u> | -           | <u>0.87</u> | <u>0.89</u> | <u>0.93</u> | <u>0.59</u> | <u>0.60</u> | <u>0.61</u> | <u>0.61</u> |
|                      | CRS-SE      | <u>0.93</u> | <u>0.88</u> | <u>0.84</u> | -           | <u>0.88</u> | <u>0.89</u> | <u>0.30</u> | <u>0.29</u> | <u>0.27</u> | <u>0.25</u> |  |             | <u>0.93</u> | <u>0.91</u> | <u>0.87</u> | -           | <u>0.89</u> | <u>0.86</u> | <u>0.60</u> | <u>0.60</u> | <u>0.59</u> | <u>0.57</u> |
|                      | CRS-SW      | <u>0.92</u> | <u>0.78</u> | <u>0.85</u> | <u>0.88</u> | -           | <u>0.87</u> | <u>0.21</u> | <u>0.21</u> | <u>0.18</u> | <u>0.17</u> |  |             | <u>0.94</u> | <u>0.85</u> | <u>0.89</u> | <u>0.89</u> | -           | <u>0.87</u> | <u>0.54</u> | <u>0.54</u> | <u>0.54</u> | <u>0.54</u> |
|                      | CRS-high    | <u>0.97</u> | <u>0.92</u> | <u>0.94</u> | <u>0.89</u> | <u>0.87</u> | -           | <u>0.29</u> | <u>0.29</u> | <u>0.27</u> | <u>0.26</u> |  |             | <u>0.94</u> | <u>0.90</u> | <u>0.93</u> | <u>0.86</u> | <u>0.87</u> | -           | <u>0.59</u> | <u>0.59</u> | <u>0.59</u> | <u>0.58</u> |
|                      | USTo        | <u>0.36</u> | <u>0.43</u> | <u>0.37</u> | <u>0.30</u> | <u>0.21</u> | <u>0.29</u> | -           |             |             |             |  |             | <u>0.61</u> | <u>0.64</u> | <u>0.59</u> | <u>0.60</u> | <u>0.54</u> | <u>0.59</u> | -           |             |             |             |
|                      | UST         | <u>0.36</u> | <u>0.43</u> | <u>0.37</u> | <u>0.29</u> | <u>0.21</u> | <u>0.29</u> |             | -           |             |             |  |             | <u>0.62</u> | <u>0.64</u> | <u>0.60</u> | <u>0.60</u> | <u>0.54</u> | <u>0.59</u> |             | -           |             |             |
|                      | USTm        | <u>0.34</u> | <u>0.41</u> | <u>0.36</u> | <u>0.27</u> | <u>0.18</u> | <u>0.27</u> |             |             | -           |             |  |             | <u>0.62</u> | <u>0.64</u> | <u>0.61</u> | <u>0.59</u> | <u>0.54</u> | <u>0.59</u> |             |             | -           |             |
| USTh                 | <u>0.33</u> | <u>0.40</u> | <u>0.36</u> | <u>0.25</u> | <u>0.17</u> | <u>0.26</u> |             |             |             |             | -           |  | <u>0.62</u> | <u>0.63</u> | <u>0.61</u> | <u>0.57</u> | <u>0.54</u> | <u>0.58</u> |             |             |             | -           |             |
| 1760/a,<br>-<br>1860 | GAR         | -           | <u>0.94</u> | <u>0.96</u> | <u>0.88</u> | <u>0.87</u> | <u>0.94</u> | <u>0.37</u> | <u>0.37</u> | <u>0.36</u> | <u>0.36</u> |  |             | -           | <u>0.97</u> | <u>0.97</u> | <u>0.92</u> | <u>0.91</u> | <u>0.95</u> | <u>0.60</u> | <u>0.59</u> | <u>0.59</u> | <u>0.59</u> |
|                      | CRS-NE      | <u>0.94</u> | -           | <u>0.88</u> | <u>0.83</u> | <u>0.70</u> | <u>0.92</u> | <u>0.44</u> | <u>0.44</u> | <u>0.44</u> | <u>0.44</u> |  |             | <u>0.97</u> | -           | <u>0.93</u> | <u>0.89</u> | <u>0.81</u> | <u>0.92</u> | <u>0.63</u> | <u>0.62</u> | <u>0.61</u> | <u>0.61</u> |
|                      | CRS-NW      | <u>0.96</u> | <u>0.88</u> | -           | <u>0.79</u> | <u>0.79</u> | <u>0.91</u> | <u>0.38</u> | <u>0.38</u> | <u>0.38</u> | <u>0.38</u> |  |             | <u>0.97</u> | <u>0.93</u> | -           | <u>0.84</u> | <u>0.84</u> | <u>0.93</u> | <u>0.60</u> | <u>0.60</u> | <u>0.59</u> | <u>0.59</u> |
|                      | CRS-SE      | <u>0.88</u> | <u>0.83</u> | <u>0.79</u> | -           | <u>0.80</u> | <u>0.83</u> | <u>0.29</u> | <u>0.29</u> | <u>0.28</u> | <u>0.28</u> |  |             | <u>0.92</u> | <u>0.89</u> | <u>0.84</u> | -           | <u>0.87</u> | <u>0.84</u> | <u>0.56</u> | <u>0.55</u> | <u>0.54</u> | <u>0.54</u> |
|                      | CRS-SW      | <u>0.87</u> | <u>0.70</u> | <u>0.79</u> | <u>0.80</u> | -           | <u>0.76</u> | 0.16        | 0.16        | 0.15        | 0.15        |  |             | <u>0.91</u> | <u>0.81</u> | <u>0.84</u> | <u>0.87</u> | -           | <u>0.82</u> | <u>0.52</u> | <u>0.51</u> | <u>0.50</u> | <u>0.50</u> |
|                      | CRS-high    | <u>0.94</u> | <u>0.92</u> | <u>0.91</u> | <u>0.83</u> | <u>0.76</u> | -           | <u>0.29</u> | <u>0.29</u> | 0.29        | 0.29        |  |             | <u>0.95</u> | <u>0.92</u> | <u>0.93</u> | <u>0.84</u> | <u>0.82</u> | -           | <u>0.58</u> | <u>0.58</u> | <u>0.57</u> | <u>0.56</u> |
|                      | USTo        | <u>0.37</u> | <u>0.44</u> | <u>0.38</u> | <u>0.29</u> | 0.16        | <u>0.29</u> | -           |             |             |             |  |             | <u>0.60</u> | <u>0.63</u> | <u>0.60</u> | <u>0.56</u> | <u>0.52</u> | <u>0.58</u> | -           |             |             |             |
|                      | UST         | <u>0.37</u> | <u>0.44</u> | <u>0.38</u> | <u>0.29</u> | 0.16        | <u>0.29</u> |             | -           |             |             |  |             | <u>0.59</u> | <u>0.62</u> | <u>0.60</u> | <u>0.55</u> | <u>0.51</u> | <u>0.58</u> |             | -           |             |             |
|                      | USTm        | <u>0.36</u> | <u>0.44</u> | <u>0.38</u> | <u>0.28</u> | 0.15        | 0.29        |             |             | -           |             |  |             | <u>0.59</u> | <u>0.61</u> | <u>0.59</u> | <u>0.54</u> | <u>0.50</u> | <u>0.57</u> |             |             | -           |             |
| USTh                 | <u>0.36</u> | <u>0.44</u> | <u>0.38</u> | <u>0.28</u> | 0.15        | 0.29        |             |             |             |             | -           |  | <u>0.59</u> | <u>0.61</u> | <u>0.59</u> | <u>0.54</u> | <u>0.50</u> | <u>0.56</u> |             |             |             | -           |             |
| 1861<br>-<br>2004    | GAR         | -           | <u>0.96</u> | <u>0.97</u> | <u>0.95</u> | <u>0.95</u> | <u>0.98</u> |             | <u>0.30</u> |             |             |  |             | -           | <u>0.97</u> | <u>0.98</u> | <u>0.95</u> | <u>0.96</u> | <u>0.94</u> |             | <u>0.63</u> |             |             |
|                      | CRS-NE      | <u>0.96</u> | -           | <u>0.93</u> | <u>0.91</u> | <u>0.85</u> | <u>0.92</u> |             | <u>0.38</u> |             |             |  |             | <u>0.97</u> | -           | <u>0.95</u> | <u>0.93</u> | <u>0.87</u> | <u>0.90</u> |             | <u>0.65</u> |             |             |
|                      | CRS-NW      | <u>0.97</u> | <u>0.93</u> | -           | <u>0.87</u> | <u>0.89</u> | <u>0.97</u> |             | <u>0.34</u> |             |             |  |             | <u>0.98</u> | <u>0.95</u> | -           | <u>0.90</u> | <u>0.92</u> | <u>0.93</u> |             | <u>0.61</u> |             |             |
|                      | CRS-SE      | <u>0.95</u> | <u>0.91</u> | <u>0.87</u> | -           | <u>0.93</u> | <u>0.92</u> |             | <u>0.24</u> |             |             |  |             | <u>0.95</u> | <u>0.93</u> | <u>0.90</u> | -           | <u>0.91</u> | <u>0.88</u> |             | <u>0.62</u> |             |             |
|                      | CRS-SW      | <u>0.95</u> | <u>0.85</u> | <u>0.89</u> | <u>0.93</u> | -           | <u>0.93</u> |             | 0.18        |             |             |  |             | <u>0.96</u> | <u>0.87</u> | <u>0.92</u> | <u>0.91</u> | -           | <u>0.89</u> |             | <u>0.55</u> |             |             |
|                      | CRS-high    | <u>0.98</u> | <u>0.92</u> | <u>0.97</u> | <u>0.92</u> | <u>0.93</u> | -           |             | <u>0.25</u> |             |             |  |             | <u>0.94</u> | <u>0.90</u> | <u>0.93</u> | <u>0.88</u> | <u>0.89</u> | -           |             | <u>0.59</u> |             |             |
|                      | UST         | <u>0.30</u> | <u>0.38</u> | <u>0.34</u> | <u>0.24</u> | 0.18        | <u>0.25</u> |             | -           |             |             |  |             | <u>0.63</u> | <u>0.65</u> | <u>0.61</u> | <u>0.62</u> | <u>0.55</u> | <u>0.59</u> |             | -           |             |             |

The correlations of summer temperatures between the Alps and Southern Sweden have not been stable over time, as Figure 4.4a explains by means of 21-year running correlations. Considering the fact that Northern Alpine temperatures match Southern Swedish temperatures better than Southern Alpine regions do, correlations have been calculated between CRS-NE-NW (mean of the individual series in CRS-NE and CRS-NW) and UST this time. The longest episode of quite a constant positive relationship lasted between around 1800 and 1870. Thereafter, a period followed

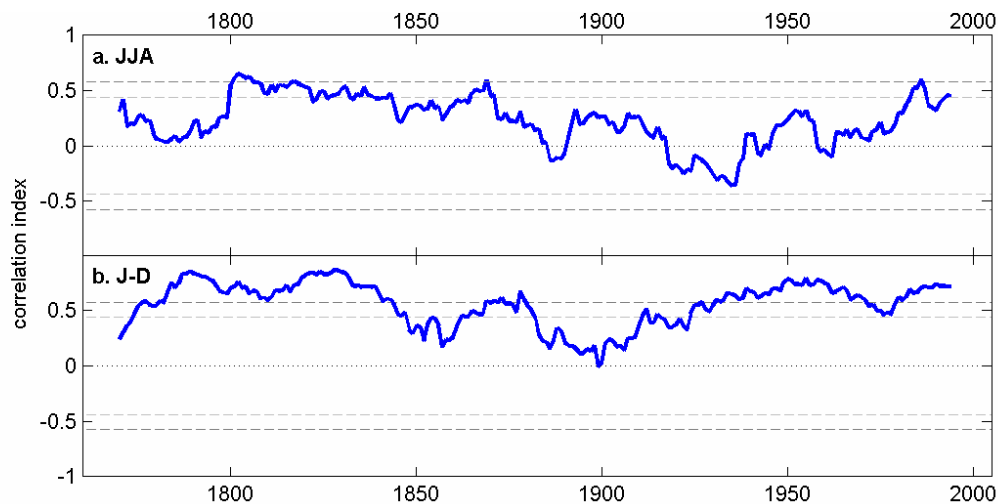


**Figure 4.4** Running correlations over a 21-year window of mean summer (a) and annual (b) temperature between the GAR and UST 1760–2004. The first and last ten years are not plotted. The light grey and dark grey dashed lines indicate the 95 % and 99 % significance levels.

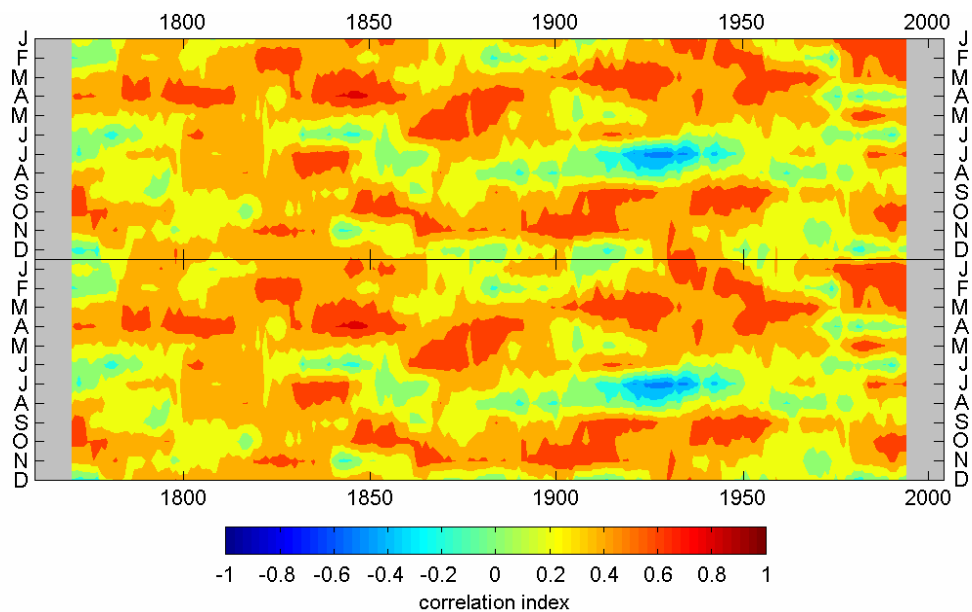


**Figure 4.5** Isopleth diagram showing seasonal differences and temporal evolution of the running correlations (21-year window) between the Alpine subregions CRS-NE-NW and UST 1760–2004. The first and last ten years are not plotted.

when summer temperature correlations vanished or even took negative values. The minimum point of this development occurred in the 1930s; from then on, the correlation has recovered continuously. To conclude the correlation analysis, Figure 4.5 demonstrates the relationship between CRS-NE-NW and UST for both time and seasons. The interregional temperature connection varies within positive values in all seasons and is most pronounced in spring and autumn. Even for the winter, a major decline in correlations between around 1870 and 1920 has been noticed. However, the episode of zero and inverted temperature correlations for the summer months, especially July, from the end of the 19<sup>th</sup> to the middle of the 20<sup>th</sup> century is exceptional and visualised very well by the diagram. The episode's minimum point during the 1930s may be connected to the particularly warm Swedish summers.

With the background information from the trend, extreme value and correlation analyses, the investigation of early summer temperatures shall be refocused on similarities and differences between the Alps and Sweden. To this end, the summer temperature evolution will be considered again by different temporal filtering and compared to annual temperatures (Fig. 4.6). This time, the

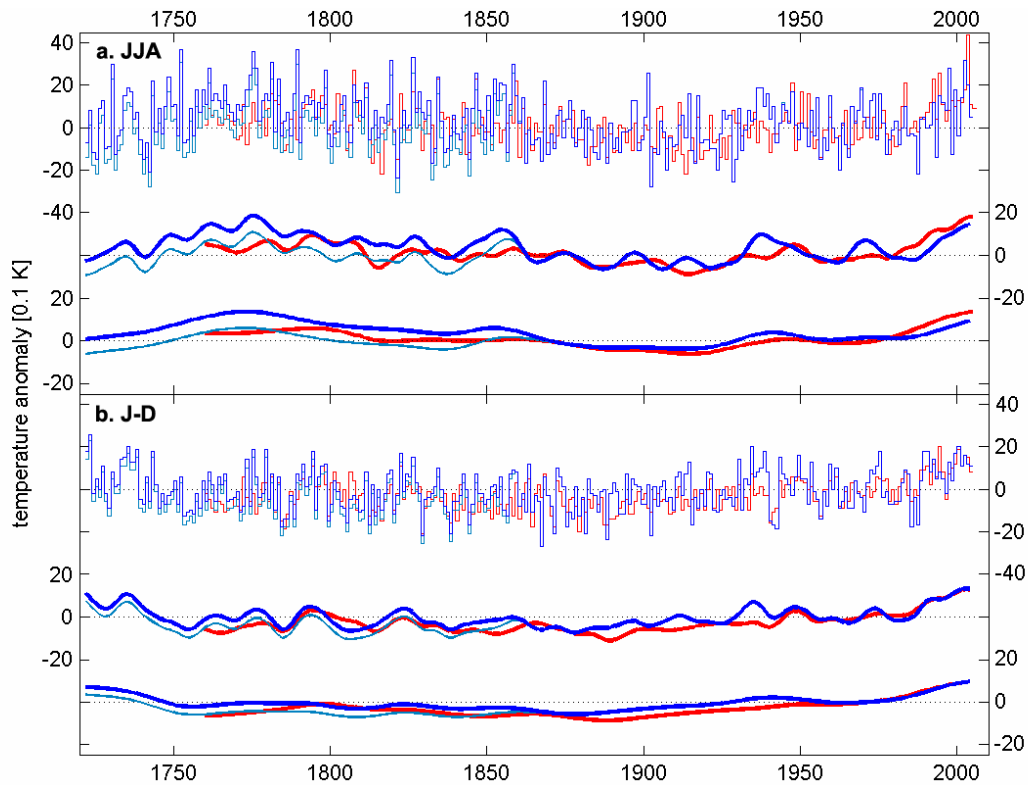


**Figure 4.6** Comparison of mean summer (a) and annual (b) temperature evolution in the Alpine subregions CRS-NE-NW (red) 1760–2005, UST (blue) and USTh (light blue) 1722–2004 at different temporal scales. Shown are the annual anomalies from the 1961–90 average (stairs in the upper third of each subplot), their 20-years (lines in the middle third) and their 50-years (lines in the lower third) Gaussian low-pass filtered trends.

mean of the North Alpine subregions CRS-NE and CRS-NW is compared to UST (and USTh respectively). The same general features of agreement (EI warmth around 1800, enduring cool episode 1860–1930) and disagreement (duration and intensity of EI warmth, different behaviour during the 1930s and around 1970) of summer temperature trends already discussed earlier in this chapter are visible again. The, with respect to Alpine conditions, outstandingly warm early summers in UST before around 1860 are obvious from the 50-years filtered trends in the lower subplot of Figure 4.6a. The application of the correction used in the USTh version before 1860 forces the Swedish trend to the level of the Alpine trend or even a somewhat lower one.

To further analyse the similarities and dissimilarities between the North Alpine subregions and Sweden, differences between CRS-NE-NW and UST have been calculated, averaged over subperiods and are visible from Figure 4.7. Results are also displayed in Table 4.4. The differences in annual temperature have been in general slightly negative ( $-0.2$  to  $-0.4$  K for subperiods of 50 years), denoting a somewhat warmer UST climate in relative terms before 1960, when directly compared to GAR. For annual data, the values vary within a rather small range of temperature differences. For summer data, however, the differences between the Northern Alpine regions and UST are fairly balanced only in the period of modern observations, whereas a break-like rise around 1860 shifts the differences to notably lower values during the EI period ( $-0.6$  K for subperiods of 50 years), i.e. the early summers were clearly warmer in UST in relation to the Northern Alpine regions. The differences between Southern Sweden and the Alps reduce to near zero, if USTh is applied instead of UST. This speaks in favour of the USTh version. Two main reasons are possible: Either the Alpine or UST data are biased before around 1860 or a major shift

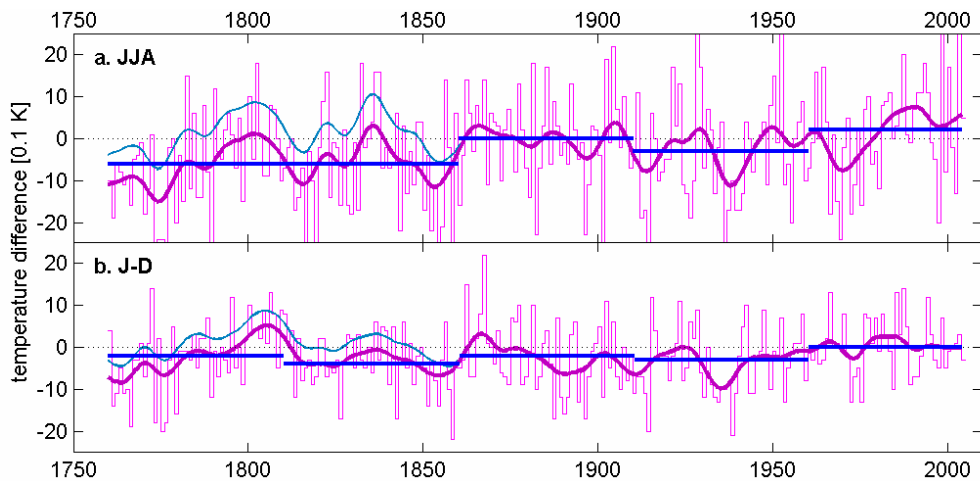


**Figure 4.7** Differences (CRS-NE-NW minus UST) of mean summer (a) and annual (b) temperature between the Alpine subregions CRS-NE-NW and UST 1760–2004. Shown are the year to year values (stairs), their 20-years Gaussian low-pass filtered trends (line) and the means of five subperiods (horizontal lines); the light blue line illustrates the difference trend to the USTh version.

**Table 4.4** Differences of mean summer and annual temperature [K] between the Alpine subregions CRS-NE-NW and UST and USTh respectively in different subperiods from 1760–2004.

| period    | years | JJA             |                  | J-D             |                  |
|-----------|-------|-----------------|------------------|-----------------|------------------|
|           |       | CRS-NE-NW - UST | CRS-NE-NW - USTh | CRS-NE-NW - UST | CRS-NE-NW - USTh |
| 1760–1810 | 51    | -0.6            | 0.1              | -0.2            | 0.2              |
| 1811–1860 | 50    | -0.6            | 0.1              | -0.4            | 0.0              |
| 1861–1910 | 50    | 0.0             | 0.0              | -0.2            | -0.2             |
| 1911–1960 | 50    | -0.3            | -0.3             | -0.3            | -0.3             |
| 1961–2004 | 44    | 0.2             | 0.2              | 0.0             | 0.0              |

in circulation occurred around 1860. Again, a hint to Chapter 4.5 is given. Before the analysis of early summer temperatures comes to that point, instrumental data will set in relation to air pressure observations, proxy evidence and climate model runs.

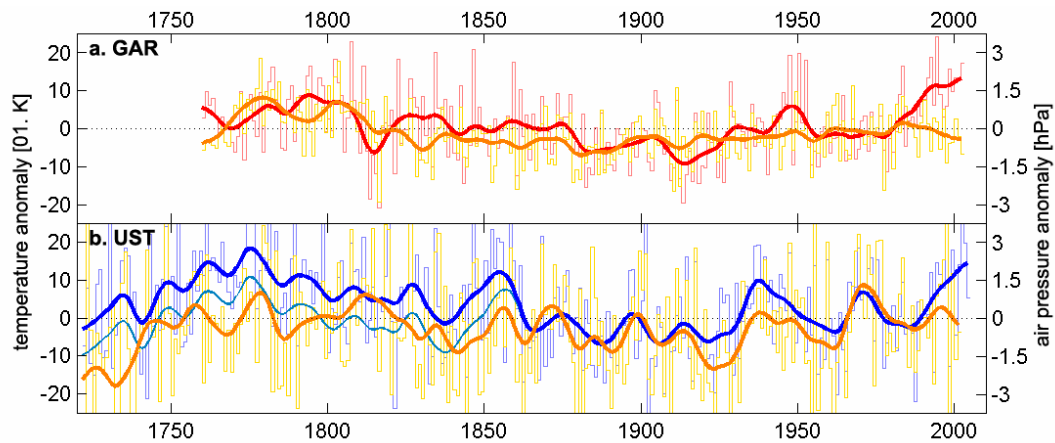
## 4.2 Comparison with instrumental air pressure data

Two effects are responsible for close similarity between the two elements air temperature and air pressure; local ones caused by incoming short wave radiation (heat gain on cloudless summer days, conversely heat loss in winters) and the large-scale advection of air masses (Auer *et al.* 2001, 121; Böhm *et al.* 1998). This relationship, that is especially strong during the summer half-year, must not remain unused in the study. The comparison with another element like sunshine duration, which is also correlated with temperature, is not possible during the EI period because of too short time series. The existing similarities of the parameters air pressure, sunshine duration and temperature, however, point at an existing plausible causal chain (e.g. Auer *et al.* 2006, 17–18).

For the GAR, pressure time series have been selected from those 27 stations where temperature has been measured already before 1830 too. The longest pressure record starts in 1760 in Basel. Already during the 1760s the number increases to four and, from 1830 onwards, 13 series are considered. From this data set with increasing number of stations, the GAR air pressure mean arises. To allow for better comparability, a GAR temperature mean has been recalculated for these 13 instead of 27 stations. This recalculated GAR temperature series is used, whenever related to air pressure data. For UST, the situation is less difficult. Both the Uppsala and the Stockholm pressure records started simultaneously with temperatures in 1722 and 1756 respectively. Both in the Alpine region and in UST, summer temperature and air pressure variations are significantly correlated, with somewhat higher values found for the Swedish region (Table 4.5). Differences in correlations between EI and modern observational times are not pronounced. Whereas a positive relationship

**Table 4.5** Correlations between the mean temperature and air pressure series of the GAR and UST and USTh respectively in different periods. Double underscored correlations are significant at the 99.9 % level.

| period          | JJA         |             |             | J–D         |       |       |
|-----------------|-------------|-------------|-------------|-------------|-------|-------|
|                 | GAR         | UST         | USTh        | GAR         | UST   | USTh  |
| 1722/60–2001/02 | <u>0.45</u> | <u>0.54</u> | <u>0.55</u> | <u>0.39</u> | -0.03 | -0.04 |
| 1722/60–1860    | <u>0.46</u> | <u>0.49</u> | <u>0.49</u> | <u>0.41</u> | 0.03  | 0.03  |
| 1861–2001/02    | <u>0.39</u> | <u>0.65</u> | <u>0.65</u> | <u>0.38</u> | -0.09 | -0.09 |

**Figure 4.8** Comparison between instrumental summer (JJA) temperature and air pressure time series. **a.** GAR temperature (red) and air pressure (orange) 1760–2002 **b.** UST (blue) and USTh (light blue) temperature and air pressure (orange) 1722–2001/04. Shown are annual anomalies from the 1961–90 average (bars) and their 20-years Gaussian low-pass filtered trends (lines).

holds over the whole year in the Alps, a negative correlation in Scandinavian winters cause the annual-correlations to be around zero in UST. The use of the USTh instead of the UST temperature version does not change the results. In any case, the close similarity between the two elements in summer in early times raises the hopes for a clearer answer concerning the uncertainty of early warm summers.

The data are presented in Figure 4.8. As regards the Alpine region (Fig. 4.8a), the comparison of the temperature and pressure trends demonstrates strong qualitative similarities. In fact, also the warm temperatures around 1800 are in large parts reflected by a higher level in pressure data. However, during other periods (around 1950, since 1980) warming occurred without any obvious pressure change. The most remarkable disagreement appears during the most recent warming which is not at all accompanied by a pressure rise and hence might be a sign of an anthropogenic cause for this warming (Auer *et al.* 2001a, 122; Auer *et al.* 2006, 18). Interestingly, a similar behaviour can be found in the recent UST data (Fig. 4.8b). But there, also the high levels of summer temperatures around 1940 and during EI times are not reflected in pressure evolution – in spite of



the agreement in general trend behaviour. The outcome of the temperature-pressure comparison is far from simple to interpret. If the pressure data are believed to be sufficiently homogenised and more reliable than the temperature data, they imply cooler early UST summers. To conclude, the incorporation of pressure long-time series into the study leads to a corroboration of the high summer temperatures around 1800 for the GAR, but provides more inconsistent evidence for UST.

### 4.3 Comparison with proxy data

As previously mentioned, the EI paradox is manifested in the comparison of instrumental with proxy temperature information and it is also in this context where the discrepancy is clearest. However, there is some disagreement among the proxy series. In this subchapter, no interregional evaluations are accomplished, but proxies targeting at Alpine on the one hand and Southern Scandinavian summer temperatures on the other hand are considered separately. Table 4.6 presents long-term summer temperature trends from the Alps (except for the glacier length reconstruction; GL) and Southern Scandinavia in a way that is similar to Table 4.1 (p. 56). The observed temperature series have been seasonally averaged here to match the targets of the offered proxies. Besides the standard summer season (JJA), a weighted spring to early autumn temperature series (growing season temperature; Chapter 2.4) has been computed to meet the target of ice-core reconstructions from Colle Gnifetti (CG). An unweighted monthly mean from April to August is assumed to correspond best to the Scandinavian harvest-based proxy series (AUS, VES). To begin with the GAR instrumental data, it has been pointed out previously that the overall summer temperature trend is practically zero, although there is a temperature decrease before and an increase after 1860. The general century-scale cooling-warming behaviour is broadly reproduced by all three available proxy series, at least in the sense that zero or even negative trends appear during the EI period while larger trends appear during the modern observation period. Large differences between the proxy-series, however, exist in terms of the long-term trends since 1760. The CG reconstruction (Wagenbach *et al.* 2001), built on three ice-cores ( $0.01 \delta^{18}\text{O}$  decade<sup>-1</sup>), fits best with the corresponding instrumental GAR series ( $-0.01 \text{ K decade}^{-1}$ ) over the whole instrumental period. Marked differences to the GAR series are, however, found for the tree-ring (TR) reconstruction of Büntgen *et al.* (2005) where a long-term change by  $0.08 \text{ K decade}^{-1}$  leads to an absolute summer temperature increase by 1.85 K. This significantly positive trend of dendrochronological evidences, which is in considerable conflict to the observed temperature data, is not due to stronger recent warming but due to cooler estimated early summers (Fig. 4.9) and, therefore, a manifestation of the EI paradox. As regards temperature changes within the EI period (1760–1860), the uncertainties of different temperature reconstructions are notable too. The

**Table 4.6** Long-term change of observed and reconstructed proxy summer temperature in the GAR (upper half) and Southern Scandinavia (lower half) in different subperiods. The upper italic values indicate the respective trends [K decade<sup>-1</sup>] derived from linear regression, the lower roman numbers give the absolute temperature change [K] during the respective periods. Underscored trends are significant at the 95 % level, double underscored correlations at the 99 % level. For the analyses, Alpine tree-ring (TR) and ice-core (CG) reconstructions as well as Southern Scandinavian harvest date reconstructions (AUS, VES) are employed (see Chapter 2.4).

|   | starting<br>year (a <sub>1</sub> ) | last<br>year (a <sub>n</sub> ) | 1760–<br>a <sub>n</sub> | 1760–<br>1860         | 1861–<br>a <sub>n</sub> | 1761–<br>1810       | 1811–<br>60         | 1861–<br>1910         | 1911–<br>60         | 1961–<br>a <sub>n</sub> |
|---|------------------------------------|--------------------------------|-------------------------|-----------------------|-------------------------|---------------------|---------------------|-----------------------|---------------------|-------------------------|
| years (n)                                     |                                    |                                | 236–243                 | 101                   | 139–142                 | 50                  | 50                  | 50                    | 50                  | 39–42                   |
| <b>GAR</b><br>(JJA)                           | 1760                               | 2002                           | -0.01<br>-0.19          | -0.05<br>-0.47        | <u>0.07</u><br>1.02     | 0.08<br>0.42        | 0.06<br>0.32        | <u>-0.12</u><br>-0.59 | <u>0.20</u><br>0.98 | <u>0.43</u><br>1.83     |
| <b>GAR</b><br>(w. MAMJJAS)                    | 1760                               | 1999                           | <u>-0.01</u><br>-0.35   | <u>-0.06</u><br>-0.57 | <u>0.06</u><br>0.81     | 0.10<br>0.50        | -0.08<br>-0.39      | <u>-0.15</u><br>-0.75 | <u>0.16</u><br>0.81 | <u>0.33</u><br>1.27     |
| <b>TR</b><br>(JJA)                            | 951                                | 2002                           | <u>0.08</u><br>1.85     | <u>-0.08</u><br>-0.76 | <u>0.10</u><br>1.37     | -0.11<br>-0.54      | <u>0.42</u><br>2.12 | 0.02<br>0.11          | 0.08<br>0.42        | <u>0.83</u><br>3.47     |
| <b>CG</b> [δ <sup>18</sup> O]<br>(w. MAMJJAS) | 1751                               | 1999                           | 0.01<br>0.29            | 0.00<br>-0.03         | <u>0.10</u><br>1.37     | <u>0.29</u><br>1.47 | 0.09<br>0.46        | <u>-0.35</u><br>-1.75 | 0.14<br>0.69        | 0.33<br>1.29            |

|                        | starting<br>year (a <sub>1</sub> ) | last<br>year (a <sub>n</sub> ) | a <sub>1</sub> –<br>a <sub>n</sub> | a <sub>1</sub> –<br>1860 | 1861–<br>a <sub>n</sub> | a <sub>1</sub> –<br>1760 | 1761–<br>1810         | 1811–<br>60    | 1861–<br>1910  | 1911–<br>60  | 1961–<br>a <sub>n</sub> |
|------------------------|------------------------------------|--------------------------------|------------------------------------|--------------------------|-------------------------|--------------------------|-----------------------|----------------|----------------|--------------|-------------------------|
| years (n)              |                                    |                                | 253–283                            | 112–139                  | 141–144                 | 39                       | 50                    | 50             | 50             | 50           | 41–44                   |
| <b>UST</b><br>(AMJJA)  | 1722                               | 2004                           | -0.01<br>-0.27                     | -0.01<br>-0.15           | <u>0.09</u><br>1.32     | 0.08<br>0.31             | <u>-0.22</u><br>-1.11 | 0.05<br>0.25   | -0.02<br>-0.12 | 0.09<br>0.47 | <u>0.32</u><br>1.43     |
| <b>USTh</b><br>(AMJJA) | 1722                               | 2004                           | <u>0.02</u><br>0.68                | -0.01<br>-0.10           |                         | 0.07<br>0.28             | <u>-0.22</u><br>-1.12 | 0.10<br>0.52   |                |              |                         |
| <b>AUS</b><br>(AMJJA)  | 1749                               | 2001                           | <u>0.07</u><br>1.75                | 0.05<br>0.58             | <u>0.11</u><br>1.50     |                          | -0.01<br>-0.03        | 0.12<br>0.62   | 0.12<br>0.59   | 0.15<br>0.75 | 0.18<br>0.72            |
| <b>VES</b><br>(AMJJA)  | 1734                               | 2004                           | <u>0.05</u><br>1.26                | 0.02<br>0.29             | <u>0.07</u><br>1.06     |                          | -0.09<br>-0.45        | -0.02<br>-0.09 | 0.00<br>0.00   | 0.19<br>0.93 | <u>0.25</u><br>1.08     |

instrumental trend of -0.05 or -0.06 K decade<sup>-1</sup> agrees best with the findings from the tree-ring study (-0.08 K decade<sup>-1</sup>), whereas isotope data shows no trend at all. However, the ice-core records reproduce the observed 19<sup>th</sup> century temperature decrease (-0.10 K decade<sup>-1</sup>) very well (-0.12 δ<sup>18</sup>O decade<sup>-1</sup>). The accordance among the different data types is better during the post-1860 period, when sign and general magnitude of the last 145 years' summer temperature changes are correctly represented by the proxies. Trends during the 1761–1810 period disagree remarkably from each other and range from -0.11 K decade<sup>-1</sup> in the tree-ring to 0.29 δ<sup>18</sup>O decade<sup>-1</sup> in the ice-core chronology.

Turning the focus to the instrumental UST records, these suggest an insignificant negative temperature trend in the April to August season during 1722–2004 (-0.01 K decade<sup>-1</sup>). The USTh version converts this long-term change into a significant positive one (0.02 K decade<sup>-1</sup>). A minor cooling trend prior to 1860 and a major warming trend afterwards is a common feature of both

UST and USTh. In terms of the AUS proxy series (Nordli 2001b), the overall temperature change is apparently larger ( $0.07 \text{ K decade}^{-1}$ ), even when compared to the USTh version, resulting in a total warming which is more than two and a half times larger ( $1.75 \text{ K}$ ). Although the AUS and VES series (Nordli *et al.* 2003) represent temperature in more western regions within Scandinavia, they have a late spring and summer temperature trend that is similar to the UST records from 1861 onwards. Nevertheless – similarly to Alpine proxies – they contradict the observed temperature climate evidence during EI times, implying a warming trend already from the mid-18<sup>th</sup> century to 1860 ( $0.05$  and  $0.02 \text{ K decade}^{-1}$  respectively). Having a closer look at the subperiods of about 50 years, it becomes apparent that both AUS and VES show a smaller cooling trend during 1761–1810 than the instrumental UST and USTh data. While AUS captured the warming trend of UST and USTh during the subsequent half century (1811–1860) quite well, VES witnesses a small cooling. Both harvest-based proxy records reveal a smaller warming trend in the last subperiod (1961–2001/04) compared to UST. This is, to some degree, likely connected to the fact that they do not represent the same climate region.

Correlations between instrumental and proxy time series can only be meaningfully calculated for proxies with annual resolution. Results from such calculations are shown in Table 4.7. The correlations between the observed GAR and reconstructed dendrochronological and ice-core summer temperatures for the Alpine region are statistically highly significant but not very strong, with coefficients of 0.33 and 0.20 respectively. Yet, the difference between EI and modern observational times is remarkable. Whereas the agreement between GAR and TR is modest during the first century of instrumental observations (0.32), the correlation coefficient is much stronger after 1860 (0.62). On a lower level, the same is true for GAR and CG (0.13 for the period 1760–1860, 0.23 for 1861–1999). In line with the geographical location of the bulk of the tree-ring data by Büntgen *et al.* (2005), the correspondence is best with the Western subregions CRS-NW and CRS-SW and worst with the South-eastern subregion CRS-SE. The correlations between the UST record and Scandinavian AUS and VES proxies are rather stronger over the entire period, but weaker

**Table 4.7** Correlations between instrumental (GAR subregions and UST versions) and proxy data time series for the Alps and Southern Scandinavia. Underscored correlations are significant at the 99.5 % level, double underscored correlations at the 99.9 % level.

|           |    | GAR         | CRS-NE      | CRS-NW      | CRS-SE      | CRS-SW      | CRS-high    |          |     | USTo        | UST         | USTm        | USTh        |
|-----------|----|-------------|-------------|-------------|-------------|-------------|-------------|----------|-----|-------------|-------------|-------------|-------------|
| 1760–     | TR | <u>0.33</u> | <u>0.30</u> | <u>0.35</u> | <u>0.26</u> | <u>0.32</u> | <u>0.31</u> | 1734/49– | AUS | <u>0.55</u> | <u>0.58</u> | <u>0.67</u> | <u>0.72</u> |
| 1999/2002 | CG | <u>0.20</u> | <u>0.20</u> | <u>0.19</u> | <u>0.19</u> | <u>0.20</u> | 0.18        | 2001/04  | VES | <u>0.42</u> | <u>0.45</u> | <u>0.53</u> | <u>0.57</u> |
| 1760–     | TR | <u>0.32</u> | <u>0.32</u> | <u>0.35</u> | 0.26        | <u>0.28</u> | 0.28        | 1734/49– | AUS | <u>0.62</u> | <u>0.62</u> | <u>0.63</u> | <u>0.63</u> |
| 1860      | CG | 0.13        | 0.13        | 0.10        | 0.16        | 0.17        | 0.14        | 1860     | VES | <u>0.45</u> | <u>0.45</u> | <u>0.46</u> | <u>0.46</u> |
| 1861–     | TR | <u>0.62</u> | <u>0.58</u> | <u>0.59</u> | <u>0.54</u> | <u>0.62</u> | <u>0.59</u> | 1861–    | AUS |             | <u>0.87</u> |             |             |
| 1999/2002 | CG | 0.23        | 0.24        | 0.24        | 0.19        | 0.22        | 0.19        | 2001/04  | VES |             | <u>0.73</u> |             |             |

correlations before 1860 are seen also in this region. As expected, the overall correlation between UST and the AUS series (0.58) is somewhat stronger than between UST and the more remote VES series (0.45). Notably, the temperature corrections that have been applied to the USTh version enhance the coefficients in both cases and, consequently, indicate fairly strong correlations of 0.72 (AUS) and 0.57 (VES) respectively. The very close relationships between the instrumental records and proxies from 1861 onwards (0.87 and 0.73 respectively) is not seen during the time of early measurements (0.62 and 0.45 respectively). In any case, AUS shows the stronger climatic connection to UST and is, therefore, considered to be the more meaningful evidence for direct comparison with the Southern Swedish series.

In a similar comparison between instrumental and proxy data, Frank *et al.* (2006) recently showed a substantial divergence between warmer EI observations and colder tree-ring reconstructions for the NH and the Alps too. There, also a discussion of the shortcomings of both homogenised instrumental data and uncertain proxy data can be found.

A study of the temporal evolution of instrumental versus proxy time series allows for a more qualitative assessment of the EI paradox. Because the time series of the GAR and its subregions are very similar, the common overall GAR mean is chosen for this kind of study. As Figure 4.9a shows, the concurrence of observed and reconstructed tree-ring summer temperatures is excellent after about 1860, despite minor deviations like the estimation of the most recent warming. Before this year and, to an increased extent, before around 1840, unreasonably large departures occur. These differences, which constitute the EI paradox, are largest between around 1810 and 1830 and decrease somewhat further back in time towards the beginning of instrumental measurements. In spite of these disagreements, the qualitative evolution of the two times series shows large similarities even during EI times. The most obvious one is the sudden drop of summer temperatures that uniformly – but on different levels – occurred during the 1810s. Subplot 4.9b confronts the growing season temperatures of the GAR and the CG ice-core record. Because of the uncertainties that are typical for isotope records (calibration, dating, external fluctuations etc.; see p. 37), the comparability is reduced in this case. A highly similar evolution of the two curves can only be found during the 20<sup>th</sup> century. The warm 1940s, for instance, are pleasingly replicated by the ratio of stable water isotopes. Marked positive deviations in the CG record can be seen around 1825 and 1880, negative ones around 1895 when actual cool summers are underestimated. On the other hand, the curves match fairly closely during other times of the 19<sup>th</sup> century. Nevertheless, the trend of isotope data temperatures lies systematically below the instrumental record around 1760–1840 and, therefore, partly contradicts the observed warm summers around 1800, even if the EI bias is smaller than the one against TR. This is in conflict to previous findings, which compared an older version of the CG data to temperature observations, when the high instrumental summer

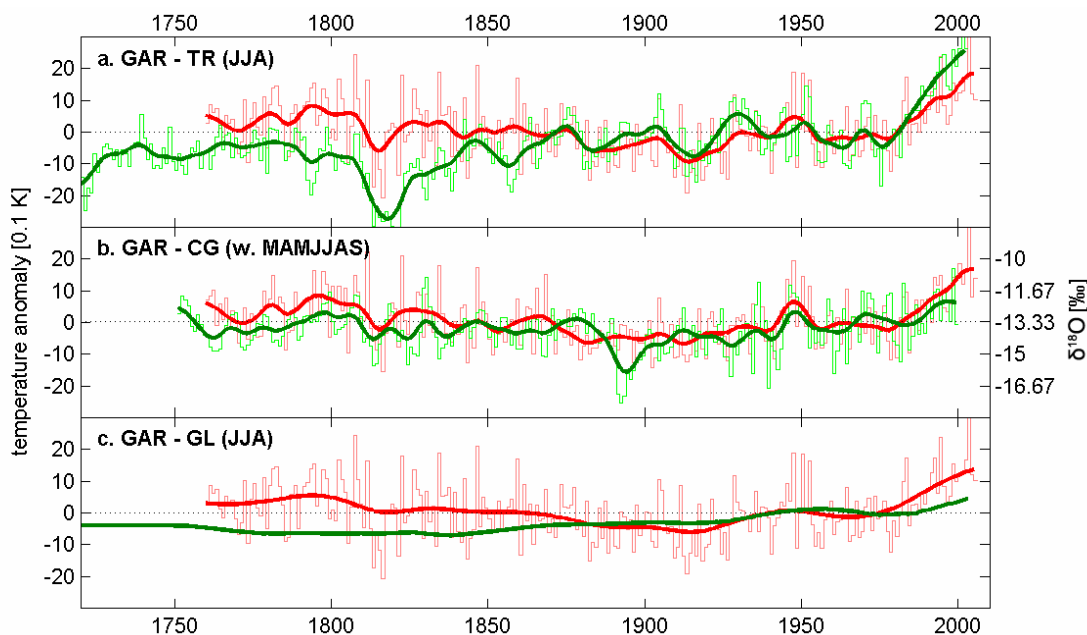


**Figure 4.9** Comparison between instrumental and proxy data for the Alpine region. **a.** Summer (JJA) temperature anomalies of observational (red) versus tree-ring width data (green; Büntgen et al. 2005) 1720/60–2002/05. **b.** Monthly weighted summer half-year (March–September) temperature anomalies of observational (red) versus isotope temperature data from Colle Gnifetti (green; Wagenbach et al. 2001) 1751/60–1999/2005. Shown are anomalies from the 1961–90 average (stairs) and their 20-years Gaussian low-pass filtered trends (lines). **c.** Summer (JJA) temperature anomalies of observational (red; anomalies from the 1961–90 average (stairs) and 50-years Gaussian low-pass filtered trends (line)) versus glacier data (green; Oerlemans 2005, interpolated and smoothed with the Stineman method, anomalies from 1950) 1720/60–2003/05.

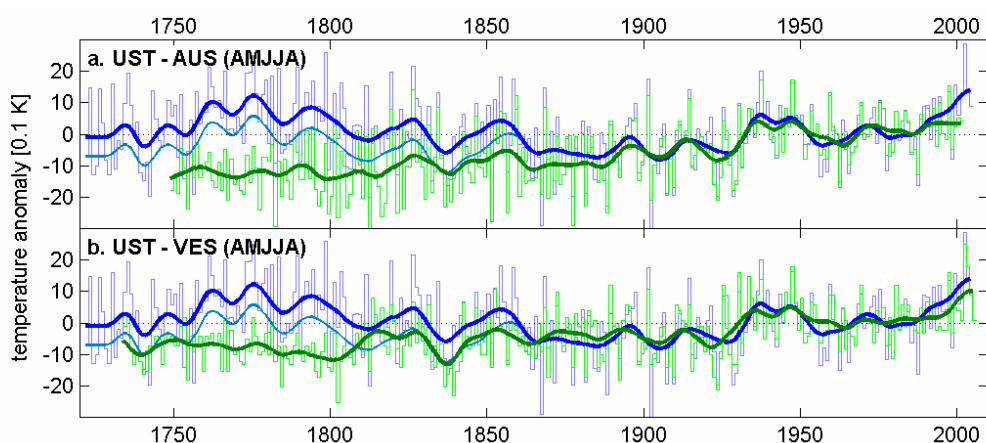


**Figure 4.10** Comparison between instrumental and proxy data for Southern Scandinavia. **a.** Late spring and summer (April–August) temperature anomalies of UST observational (blue) versus grain harvest data from Austlandet (green; Nordli 2001c) 1722/49–2001/04. **b.** Late spring and summer (April–August) temperature anomalies of UST observational (blue) versus grain harvest and terminal moraine data from Vestlandet (green; Nordli et al. 2003) 1722/34–2004/05. Shown are anomalies from the 1961–90 average (stairs) and their 20-years Gaussian low-pass filtered trends (lines).

temperature level at the end of the 18<sup>th</sup> century was confirmed (see p. 38; Wagenbach *et al.* 2001, 103–104). Anyhow, the large range of methodological uncertainties related to isotope ice-core data does not allow for definite conclusions as regards summer temperatures at the turn to the 19<sup>th</sup> century. Turning the focus to the GL proxy data, this record is related to a comparable 50 years filtered trend of GAR summer temperatures (Fig. 4.9c). Besides the observed temperature rise after about 1980, the GL record replicates the GAR temperature curve very well back until around 1870. Prior to this time and especially around 1800, a large discrepancy in suggested summer temperature climate emerges. Consequently, the EI paradox is also evident in the temperature proxy based on glacier lengths. Moreover, no signal of any abrupt temperature drop in the 1810s is visible in the reconstruction curve. Similarly to the other two proxy comparisons, the differences between instrumental and proxy data diminish somewhat back in time towards 1760. It has to be taken into consideration that also larger inconsistencies between the TR and GL curves are evident. The strong warming of TR by 2 K from around 1820 to 1850, for instance, does not exist in the GL record and contradicts fundamentally the fact that Alpine glaciers reached a maximum extent in 1850.

The temporal evolutions of the two proxy records accessible for Southern Scandinavia, from Austlandet and Vestlandet, look alike for the most parts (Fig. 4.10). Both agree with the evolution of the UST April to August temperature curve nearly identically from the 1860s onwards. However, particularly before about 1810, a large difference between the observed and reconstructed temperature curves becomes apparent, which decreases to some extent from around 1760 backwards. This episode of diverging instrumental and proxy summer temperature evolutions is the Scandinavian manifestation of the EI paradox. But also during this uncertain phase, similarities are visible among the trends. The appliance of the USTh version not only reduces the differences between the instrumental and reconstructed data but also shortens its temporal extension.

In order to subsume this central subchapter of the thesis, all five proxy records that could be obtained from the Alpine region and Southern Scandinavia contradict the observed regional temperature trends as evidenced by the GAR and the UST series. Using these proxy records for reconstructed temperature, a discrepancy to instrumental data around 1800, the so-called EI paradox, becomes apparent. General similarities in the onset, the duration and the ending of the paradox can be detected, in spite of the specific uncertainties that come along with the use of the individual proxy techniques. The assessment of proxy evidence in terms of the EI paradox is – among other things – part of the discussion (see p. 90–92).

## 4.4 Comparison with model run

The concept of climate modelling has been outlined in Chapter 1.3 and its practical realisation by the ECHO-g model has been summarised in Chapter 2.5. There, ECHO-g's potential to simulate seasonal means and interannual variability of temperature (Min *et al.* 2005a) as well as the broad patterns of temperature deviations during the last 500 years (Zorita *et al.* 2004) has been outlined. In this thesis, ECHO-g is used to investigate how the model simulates temperature variability over Europe since the start of climatological observations. In particular, the behaviour of early summer temperatures after 1722 over the Alps and in Southern Sweden will be regarded. The model run Erik2 (see p. 41) was employed for the analysis. As already described, the model operates on basis of a  $3.75 \times 3.75^\circ$  grid. Three grid points, which match the GAR best, were chosen to calculate a mean Alpine temperature series. For the UST, instrumental data are best covered by one ECHO-g grid point. The locations of the areas that are associated to the relevant grid points are highlighted in e.g. Figure 4.11.

Model data overlaps with instrumental series during the period 1722/60–1990 for UST and the GAR. For further analyses, these 269 years were divided into six subperiods for which analyses were made. Figures 4.11 and 4.12 show maps with simulated temperature anomalies in Europe relative to the period 1901–29 (see p. 43) averaged over subperiods, for the summer season and the whole year respectively. In both cases, cold temperature conditions at the Alpine grid points and about average conditions at the Southern Swedish one until 1910 were followed by a beginning warming during the subperiod 1911–60 leading to strong positive anomalies in the last subperiod 1961–90. Table 4.8 contains the figures of these main model results and confronts them with the instrumental counterparts. To begin with the GAR, high early instrumental summer temperature anomalies (+0.5 to +1.0 K) that can be related to the EI paradox are not reproduced by Erik2. On the contrary, the simulation results into even negative deviations (-0.4 K). After 1860, the overall

**Table 4.8** Comparison between observed instrumental and simulated model mean summer and annual temperature anomalies (with respect to 1901–29) for six subperiods.

| period    | years | JJA          |             |              |            | J–D          |             |              |            |
|-----------|-------|--------------|-------------|--------------|------------|--------------|-------------|--------------|------------|
|           |       | instrumental | erik2       | instrumental | erik2      | instrumental | erik2       | instrumental | erik2      |
|           |       | GAR          | grid points | UST          | grid point | GAR          | grid points | UST          | grid point |
| 1722–1760 | 39    |              | -0.4        | 0.9          | -0.3       |              | -0.4        | 0.5          | -0.5       |
| 1761–1810 | 50    | 1.0          | -0.4        | 1.6          | 0.2        | 0.2          | -0.4        | 0.2          | 0.1        |
| 1811–1860 | 50    | 0.5          | -0.4        | 1.1          | 0.2        | 0.0          | -0.4        | 0.1          | 0.2        |
| 1861–1910 | 50    | 0.2          | -0.1        | 0.2          | 0.5        | -0.1         | 0.0         | -0.2         | 0.5        |
| 1911–1960 | 50    | 0.3          | 0.1         | 0.6          | 0.6        | 0.2          | 0.1         | 0.3          | 0.4        |
| 1961–1990 | 30    | 0.5          | 0.6         | 0.5          | 1.7        | 0.5          | 0.9         | 0.3          | 2.0        |

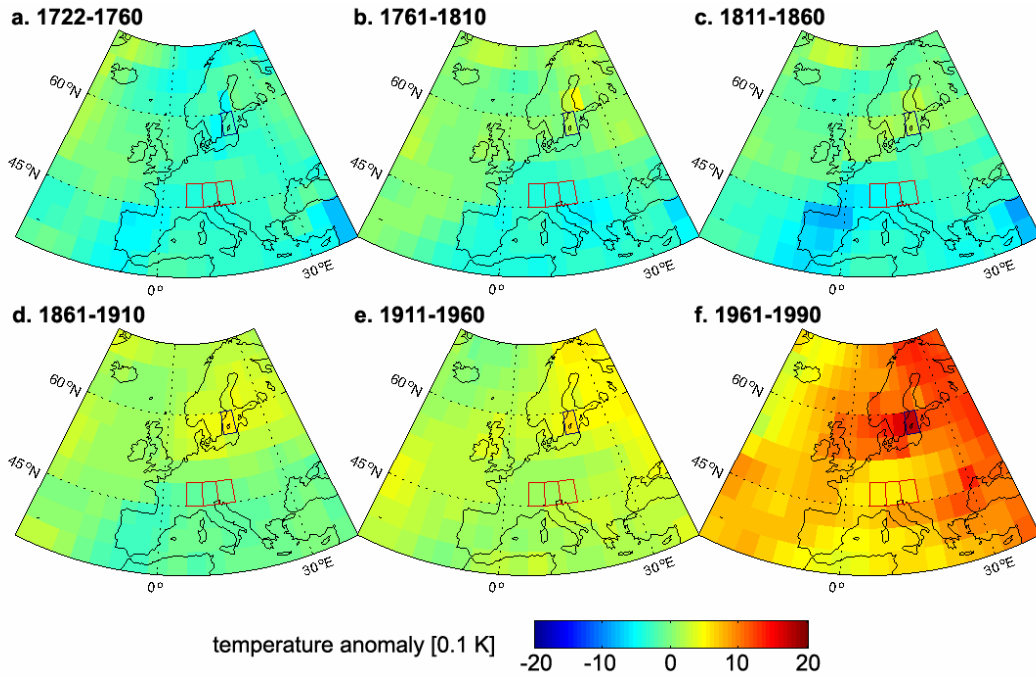


**Figure 4.11** Mean summer temperature anomalies (with respect to 1901–29) during six subperiods from 1722–1990 over Europe as simulated by Erik2. The areas pertaining to the grid point(s) corresponding to the location of the GAR and UST are framed.

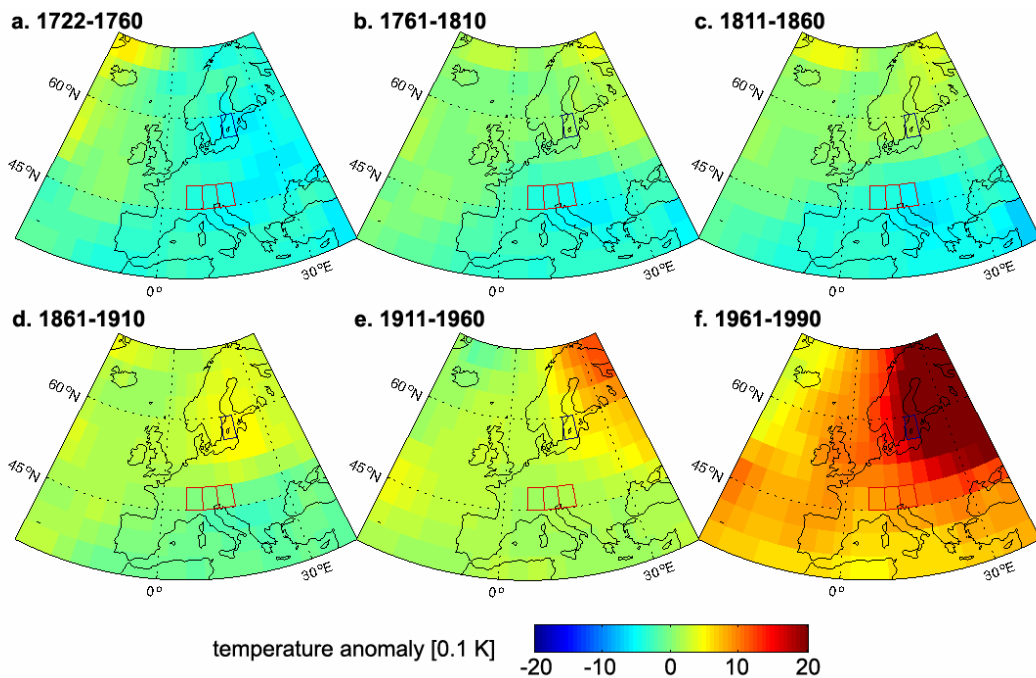


**Figure 4.12** The same as in Figure 4.11 but for mean annual temperature.

agreement between instrumental and model data is reasonable. During EI times, the difference to between observational and Erik2 data is large in UST too, which results from instrumental



observations producing even warmer summer averages. Thereafter, model simulations agree well with real world temperature averages, apart from the last subperiod whose warming is fairly exaggerated. With regard to annual temperatures, the Erik2 simulation computes early temperatures that are too cold, whereas the last three subperiods are overall captured well. The model performance for annual means is generally better over Southern Sweden, despite of the overrated recent warming.

The time series of modelled temperatures are displayed in Figure 4.13a and b for the GAR and UST grid points. It is notable that no enduring positive anomalies around 1800 can be found neither for the GAR nor for the UST model temperature series. According to Erik2, temperatures decline abruptly during the 1810s (due to a decrease in external forcing). This drop is more expressed at the Swedish grid point than at the Alpine ones. In reality, the corresponding

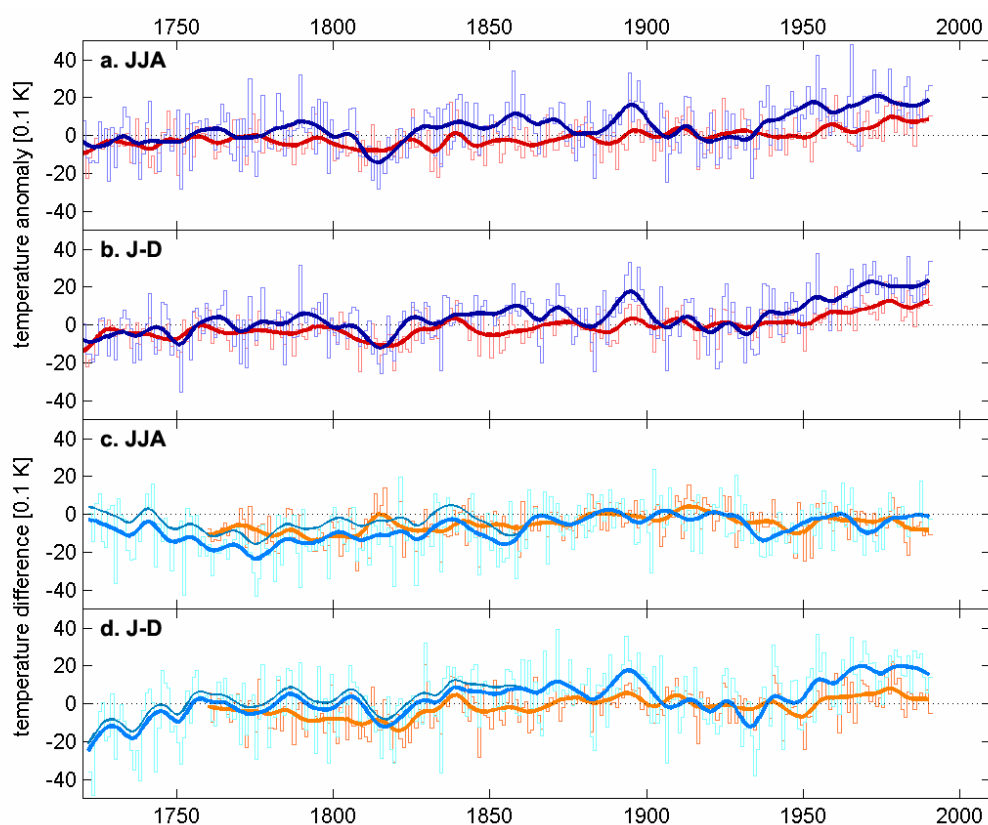


**Figure 4.13** Comparison of mean summer (a) and annual (b) temperature evolution 1720–1990 as simulated by Erik2 for three grid points corresponding with the location of the GAR (mean thereof dark red) and one grid point corresponding with the location of UST (dark blue). Shown are anomalies from the 1901–29 average (stairs) and their 10-years Gaussian low-pass filtered trends (lines). – Differences (model minus instrumental data) between simulated temperature by Erik2 (mean of the three grid points) and the observed GAR temperature (orange) and between simulated temperature by Erik2 (one grid point) and the observed UST temperature (turquoise) 1722/60–1990 for the summer season (c) and the whole year (d). Shown are the year-to-year values (stairs) and their 10-years Gaussian low-pass filtered trends (line); the light blue line illustrates the difference trend to the USTh version.

peculiarity of observed summer temperature evolution triggered by volcanic and solar forcing was, in fact, more apparent in Central compared to Northern Europe. A short temperature increase near the end of the 19<sup>th</sup> century in Erik2 does not match the observations. Moreover, the simulated temperature rise towards the end of the 20<sup>th</sup> century sets off too early and is overestimated, particularly for the UST grid point. The temperature there rises more gradually from the mid-18<sup>th</sup> to the end of the 20<sup>th</sup> century for the Alps. Given that there is a large similarity between the model output for summer and annual means, the above statements are broadly also true for the whole year's temperature evolution. To depict the differences between Erik2 and instrumental temperature trends, they have been plotted in Figure 4.13c and d for summer and annual values. Positive or negative temperature differences indicate that the model has interpreted too warm or too cold temperature conditions, respectively, compared to measured data. Underestimated temperatures before around 1860 and overestimated warming at the end of the analysis period are the most distinctive features. When compared to the USTh version (also shown), the early discrepancy is somewhat mitigated. To recapitulate the central finding, the ECHO-g model run does not produce any especially warm early summers as indicated by instrumental series.

## 4.5 Linkage to atmospheric circulation

The results from EOF Analysis of the ADVICE air pressure dataset 1780–1995 described in Chapter 3.4 are plotted in Figure 4.14, where the patterns of the four leading EOFs (rows 1–4) for the average of the whole summer (column 1) and the three single summer months (columns 2–4) are shown. In order to keep this subchapter's extent within reasonable limits, the following investigation confines to the two most apparent detected circulation modes.

The first pattern of the summer season describes an intense centre of action across the British Isles, the North Sea and Southern Norway that reveals strong air pressure variations in this region. This mode can be interpreted as reflecting the preferred path of intense low-pressure systems in over Europe as well as a waxing and waning high-pressure centre over the same region. In whichever case, this region of variations between high and low pressure (L/H) is the most influential feature of atmospheric circulation over the European region during summer. When the single months are regarded separately, this pressure pattern is very similar to the pattern of the second component of June and to the patterns of the first components of July and August. The centre of action near the British Isles could also be interpreted as the Western part of the Eurasian pattern, although the spatial coverage of ADVICE is far from capturing this circulation mode.

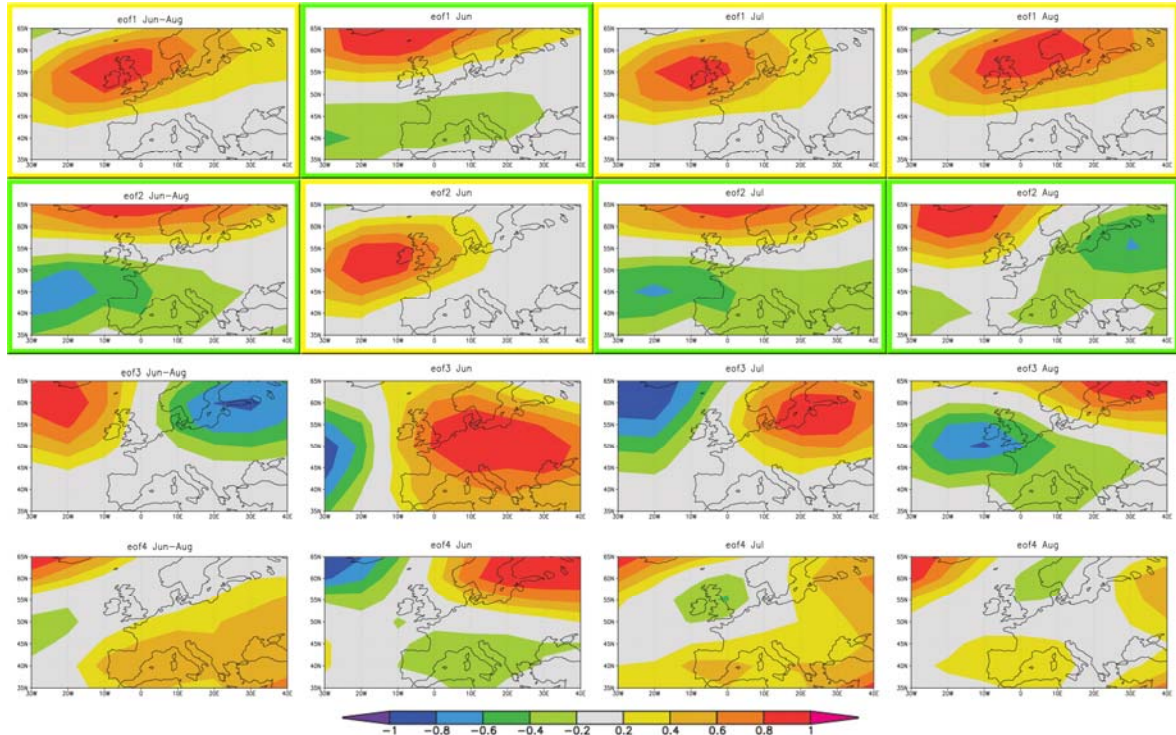


**Figure 4.14** The four leading EOFs out of the ADVICE air pressure dataset 1780–1995 for the average of the whole summer season and the individual summer months. EOFs-maps, which are regarded to reflect the L/H-mode, are yellowish framed; NAO-like EOF-maps are greenish framed.

**Table 4.9** Explained variance and cumulative explained variance [%] of air pressure variability according to the ADVICE dataset 1780–1995 by the four leading EOFs shown in Figure 4.14 for the average of the whole summer season and the individual summer months.

|      | JJA        |                 | Jun        |                 | Jul        |                 | Aug        |                 |
|------|------------|-----------------|------------|-----------------|------------|-----------------|------------|-----------------|
|      | expl. var. | cum. expl. var. | expl. var. | cum. expl. var. | expl. var. | cum. expl. var. | expl. var. | cum. expl. var. |
| EOF1 | 32.6       | 32.6            | 27.4       | 27.4            | 34.7       | 34.7            | 38.2       | 38.2            |
| EOF2 | 21.4       | 54.0            | 25.0       | 52.4            | 22.1       | 56.8            | 23.6       | 61.7            |
| EOF3 | 18.2       | 72.2            | 20.1       | 72.5            | 19.2       | 76.0            | 18.1       | 79.8            |
| EOF4 | 11.0       | 83.2            | 12.9       | 85.4            | 8.4        | 84.4            | 8.5        | 88.3            |

An EOF that signifies a typical NAO-related mode, as it has been shown in Figure 1.2 (p. 8) is actually found for the second EOF of summer principal components. It shows opposite polarities of pressure anomalies over the northern parts of the European region compared to more southerly parts of the North Atlantic Ocean and Southern Europe. For June, a pattern of air pressure distribution representing the NAO appears as the first EOF and for July as the second most important one. Considering August, the determination of a NAO-related pattern has not been as well-defined; both EOF2 and EOF3 provide options that possibly but not necessarily reflect the NAO-mode. A clear NAO-pattern is not present in any of the August EOFs. For continued

analyses here, EOF2 has been chosen to represent the NAO. The EOF2 is preferred to EOF3 due to the instance that EOF3 interprets the centres of action exceedingly far in the North. In how far the spatial coverage of the ADVICE data, especially due to its extension towards the North, captures the NAO as a whole has to be questioned again at this point.

Another well reproduced pattern can be found in the third component of June. Its dominant centre of action lies across large parts of the core of the European continent. It can be interpreted as reflecting variations between situations with low-pressure activity caused by ascending air above the overheated land masses that frequently occurs at that time of the year (“European monsoon”) and other situations when high-pressure conditions prevail over Central Europe. The other, less important EOFs are not as clear to classify, less persistent through the months and characterised by less pronounced contrasts.

The fractioned of the total variances of sea level air pressure variability explained by the leading EOFs that are shown in Figure 4.14 are specified in Table 4.9. The described L/H-pattern over the North Sea explains around a third of seasonal summer air pressure variability, whereas the NAO-pattern explains another fifth. As regards the single summer months, the L/H-modes are responsible for an increasing fraction of explained variance from June to August, while the NAO-related EOFs account for around a fourth. Together, the first two EOFs explain, in any case, more than 50 % of air pressure variability over Europe according to the ADVICE data.

The first two seasonal and monthly EOFs, reflecting L/H- and NAO-modes, were selected for further analyses to obtain flexible atmospheric circulation indices which are favourably representative for summer. For the L/H-mode, the centre of action has been interpreted to reveal strong variations of low- and high-pressure anomalies in an area concentrated over the British Isles. In the case of low-pressure (high-pressure) anomalies in the centre of action, it can be assumed that the summer temperatures in Uppsala and Stockholm are somewhat cooler (warmer) than average. On the other hand, the L/H-mode is not expected to have any evident influence on GAR summer temperatures (especially not in the southern subregions).

Those EOFs, which have been interpreted as NAO-like circulation patterns, illustrate air pressure variations between northern and southern parts of Europe. The summer NAO-EOFs, with positive and negative signs as shown in Figure 4.14, imply positive pressure anomalies towards the north (i.e. the low-pressure there is weakened compared to the average pressure field) and negative deviations towards the south (i.e. the high-pressure there is weakened). This situation corresponds to a negative NAO-phase. Higher-than-average summer temperatures in UST and lower ones in GAR are expected. If this pattern is reversed in a certain year (accompanied by a negative EC-value then), a positive NAO-phase is instead occurring. Accordingly, Southern Scandinavia would be located within the influence of low-pressure anomalies (with strengthened

westerly winds), whereas the Alpine region (in particular the Southern subregions) would benefit from high-pressure anomalies over the Mediterranean Sea. Consequently, the negative NAO-phase is expected to lead to cooler-than-average summer temperatures in UST and warmer ones in the (southern) GAR.

The ECs of the putative L/H- and NAO-indices are depicted in the left and right half of Figure 4.15, respectively, together with the Alpine and Southern Swedish temperature trends. In Figure 4.15a, it can be seen that the overall relationship between the L/H-EC and UST temperatures is inconstant in the summer season, coinciding well during some episodes (e.g. around 1930–1980) and disagreeing (as expected) during others (e.g. around 1860–1890). The peculiarities of warm Swedish summers around 1940 and even more around 1970 are interestingly evident in the L/H-EC rather than in the NAO-EC. GAR summer temperatures, however, evolve much independently from the L/H-mode over the British Isles in both the seasonal and monthly investigations. The assumed cooling impact of the L/H-pattern on UST temperatures is partly more noticeable and marked in terms of the monthly analyses for June and July (Fig. 4.15b and c) than for the summer season as a whole. In these two months, the extension of the relevant centres of actions is more confined compared to JJA (and August) when the L/H-mode reaches far to the east (Fig. 4.14).

To allow for the instance that a positive NAO-phase is reflected by a negative EC-value, the abscissas in Figures 4.15e–h have been inverted for the ECs. As argued above, rather negatively (positively) deviating summer temperatures are expected in UST (in the GAR) in this case. In fact, it can be seen that UST summer temperature trends from 1780 to around 1930 for the most part reacted reversely to changes in the NAO-circulation, i.e. a strongly positive NAO-phase often caused Swedish temperatures to decline (Fig. 4.15e). This simultaneous divergence is, however, of qualitative nature and sometimes hardly noticeable. Particularly during the 1940s, for instance, Southern Swedish temperatures have evolved totally independently from any NAO-related forcing. Also during later times of the 20<sup>th</sup> century, an apparent relation has not been found. The dependence of Alpine summer temperature evolution on the supposed NAO-index is not as clear. If possible, some episodes of converse trend development between GAR temperatures and variations in the EOF2 pattern (e.g. 1780–1840, 1930–1960) can rather be revealed than phases of concurrent evolution. In the main, no noteworthy similarities between Alpine temperatures and a NAO-related circulation mode are existent. The post-1980 summer temperature rise in both UST and the GAR is not reflected by any corresponding NAO-episode. However, the ADVICE SLP dataset ends in 1995, which is too early to allow for an investigation of the most recent years. Anyway, the most important message of Figure 4.15 is that any negative summer NAO-phase in the EI period, which possibly could account for the high temperature level in UST around 1800, is

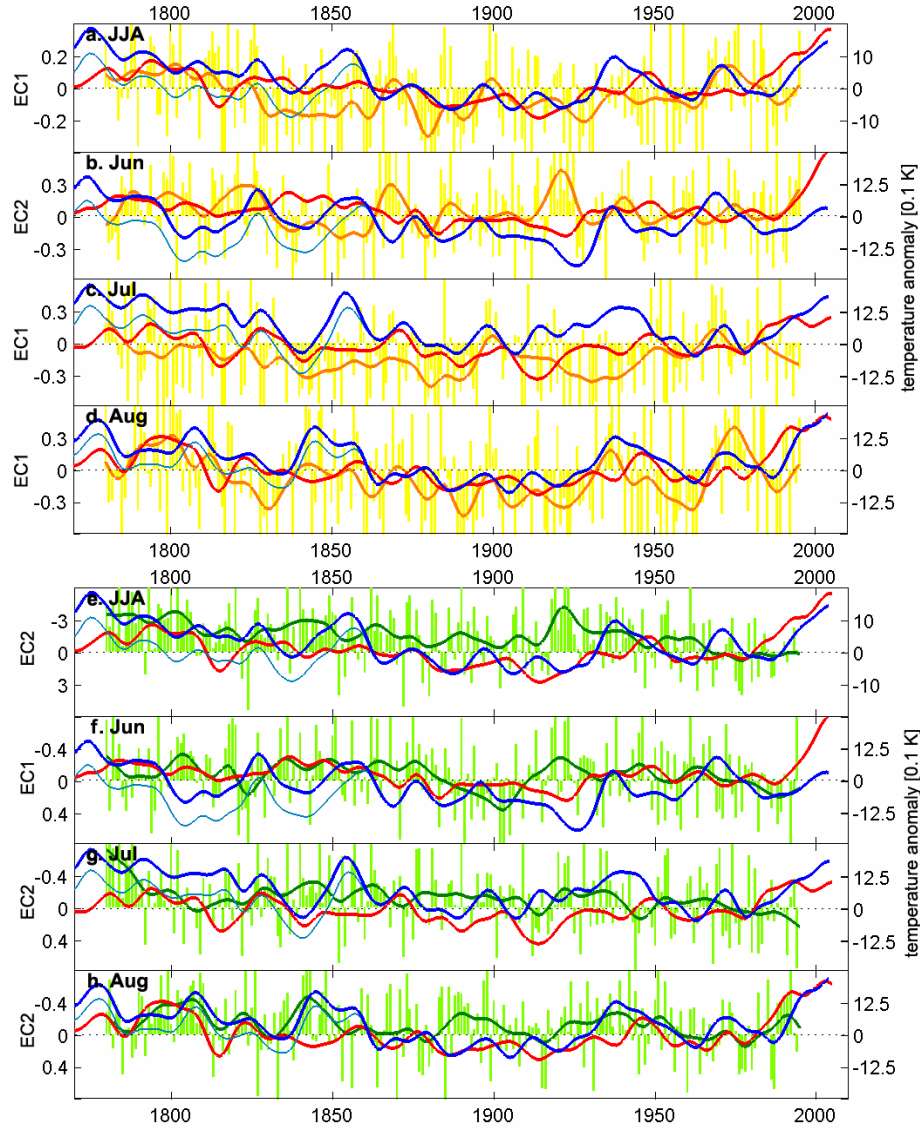


**Figure 4.15** Temporal evolution of the L/H-like (yellow bars, upper half) and NAO-like ECs (green bars, lower half) and their 20-years Gaussian low-pass filtered trends (lines) in comparison to the 20-years Gaussian low-pass filtered trends of GAR (red line), UST (blue line) and USTh (light blue line) temperatures 1770/80–1995/2005 for the average of the whole summer season (a, e) and the individual summer months June (b, f), July (c, g) and August (d, h). Shown are anomalies from the 1961–90 average. To allow for the instance that a positive EC-value in the subplots e–h reflects a negative NAO-phase, the abscissas for the ECs have been inverted there.

not reproduced according to the ADVICE data. Actually, the assumed NAO-indices point towards a positive phase before and around 1800.

The weak connection of summer temperatures to atmospheric circulation in general, and to the NAO in particular, causes problems in drawing significant conclusions in this subchapter. To test the reliability of the chosen method itself, it has been applied in exactly the same manner for the winter season, when the relationship between atmospheric circulation and air temperature are

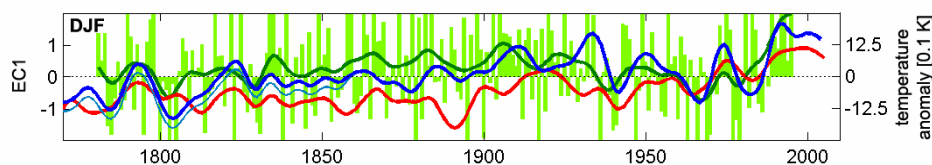


**Figure 4.16** Temporal evolution of the NAO-like EC (green bars) and its 20-years Gaussian low-pass filtered trend (green line) in comparison to the 20-years Gaussian low-pass filtered trends of GAR (red line), UST (blue line) and USTh (light blue line) temperatures 1770/80–1995/2005 for the winter season. Shown are anomalies from the 1961–90 average.

expected to be more pronounced. For the winter season, the first EOF of air pressure data, which explains 46.1 % of the variance, represents a (positive) NAO-like mode (Fig. 1.2a, p. 8). This NAO-behaviour is supposed to bring about milder temperature conditions in both Southern Swedish and Alpine winters. The relevant EC corresponds broadly rather well to the evolution of seasonal temperatures for the Swedish part, but there are also clear signs of decadal temperature variations that are not related to simultaneous changes in NAO-phase (Fig. 4.16). For the GAR winter temperatures, several stages of NAO-relation occurred, but these are not clearly marked. The recent winter warmth in both study regions is visibly connected to a strong positive NAO-episode (up to the end of the ADVICE dataset in 1995). The correlation between UST winter temperatures and the putative NAO-EC over the common data period (1781–1995) is strong and highly significant (0.68). The winter temperatures of the GAR correlate at 0.36 with the leading pressure EC. The North Alpine subregions CRS-NE and CRS-NW and the high-elevation subregion CRS-high (0.47) are evidently closer connected to the NAO than the South Alpine CRS-SE (0.15) and CRS-SW.

The correlations between the summer circulation indices and GAR and UST temperatures are given in Table 4.10. Over the whole ADVICE data period, the summer L/H-mode (EC1) correlates weakly, but significantly with GAR temperatures (0.19) as well as with UST temperatures (0.24). In contrast, practically no relationship between NAO-forced air circulation and summer temperatures can be verified for the Alpine region and its subregions. The official UST records show a weak correlation (0.15). This value increases to some extent, if USTm (0.21) or USTh (0.23) are applied instead of UST. In terms of these versions, the correlations are also featured by a high significance. Concerning the two subperiods 1780–1860 and 1861–1995, only small differences between the EI and the modern observational period are detectable. Generally, the circulation dependency of summer temperature – regardless of whether the L/H- or NAO-mode is taken – is higher in the Southern Swedish than in the Alpine region. For monthly resolution, the picture becomes more diffuse and less expressive. The strongest and even significant correlations are seen between August's NAO-mode (EC2) and GAR (0.41) and UST (0.40) but the representativity of EC2 in terms



**Table 4.10** Correlation table of the mean temperature series of the GAR subregions and UST versions with the L/H-like and NAO-like ECs for the whole summer season and the individual summer months. Underscored correlations are significant at the 99.5 % level, double underscored correlations at the 99.9 % level.

|           |     |     | GAR          | CRS-NE       | CRS-NW       | CRS-SE       | CRS-SW       | CRS-high     | USTo         | UST          | USTm         | USTh         |
|-----------|-----|-----|--------------|--------------|--------------|--------------|--------------|--------------|--------------|--------------|--------------|--------------|
| 1780–1995 | EC1 | JJA | <u>0.19</u>  | <u>0.20</u>  | <u>0.29</u>  | 0.07         | 0.04         | <u>0.21</u>  | <u>0.24</u>  | <u>0.24</u>  | <u>0.23</u>  | <u>0.22</u>  |
|           | EC2 | Jun | -0.16        | <u>-0.22</u> | -0.11        | -0.15        | -0.12        | -0.16        | -0.11        | -0.11        | -0.12        | -0.12        |
|           | EC1 | Jul | <u>0.27</u>  | <u>0.22</u>  | <u>0.34</u>  | 0.17         | <u>0.20</u>  | <u>0.29</u>  | 0.07         | 0.07         | 0.06         | 0.06         |
|           | EC1 | Aug | 0.16         | 0.17         | <u>0.28</u>  | 0.02         | 0.01         | 0.16         | <u>0.36</u>  | <u>0.36</u>  | <u>0.36</u>  | <u>0.35</u>  |
|           | EC2 | JJA | -0.03        | 0.02         | 0.02         | -0.07        | -0.13        | -0.04        | 0.15         | 0.15         | <u>0.21</u>  | <u>0.23</u>  |
|           | EC1 | Jun | <u>-0.25</u> | <u>-0.18</u> | <u>-0.19</u> | <u>-0.28</u> | <u>-0.34</u> | <u>-0.24</u> | -0.04        | -0.04        | -0.02        | -0.01        |
|           | EC2 | Jul | 0.00         | 0.05         | 0.02         | -0.04        | -0.10        | 0.00         | <u>0.29</u>  | <u>0.29</u>  | <u>0.33</u>  | <u>0.33</u>  |
|           | EC2 | Aug | <u>-0.41</u> | <u>-0.48</u> | <u>-0.36</u> | <u>-0.38</u> | <u>-0.29</u> | <u>-0.39</u> | <u>-0.40</u> | <u>-0.40</u> | <u>-0.39</u> | <u>-0.38</u> |
| 1780–1860 | EC1 | JJA | 0.18         | 0.22         | 0.26         | 0.10         | -0.01        | 0.22         | 0.20         | 0.20         | 0.19         | 0.18         |
|           | EC2 | Jun | -0.20        | -0.28        | -0.14        | -0.12        | -0.13        | -0.22        | -0.09        | -0.09        | -0.11        | -0.11        |
|           | EC1 | Jul | 0.24         | 0.20         | <u>0.31</u>  | 0.14         | 0.17         | 0.26         | 0.02         | 0.02         | 0.03         | 0.03         |
|           | EC1 | Aug | 0.26         | <u>0.30</u>  | <u>0.33</u>  | 0.15         | 0.09         | 0.21         | <u>0.38</u>  | <u>0.38</u>  | <u>0.37</u>  | <u>0.37</u>  |
|           | EC2 | JJA | -0.13        | -0.06        | -0.10        | -0.16        | -0.23        | -0.15        | 0.24         | 0.24         | 0.25         | 0.25         |
|           | EC1 | Jun | <u>-0.29</u> | -0.23        | -0.23        | <u>-0.30</u> | <u>-0.40</u> | -0.27        | -0.05        | -0.05        | -0.04        | -0.05        |
|           | EC2 | Jul | -0.13        | -0.06        | -0.10        | -0.19        | -0.26        | -0.12        | 0.23         | 0.23         | 0.23         | 0.23         |
|           | EC2 | Aug | <u>-0.52</u> | <u>-0.59</u> | <u>-0.46</u> | <u>-0.52</u> | <u>-0.36</u> | <u>-0.48</u> | <u>-0.45</u> | <u>-0.45</u> | <u>-0.44</u> | <u>-0.44</u> |
| 1861–1995 | EC1 | JJA | 0.17         | 0.16         | <u>0.29</u>  | 0.01         | 0.04         | 0.19         |              | <u>0.25</u>  |              |              |
|           | EC2 | Jun | -0.14        | -0.19        | -0.08        | -0.19        | -0.11        | -0.11        |              | -0.13        |              |              |
|           | EC1 | Jul | <u>0.28</u>  | <u>0.23</u>  | <u>0.35</u>  | 0.20         | <u>0.22</u>  | <u>0.31</u>  |              | 0.08         |              |              |
|           | EC1 | Aug | 0.08         | 0.04         | <u>0.24</u>  | -0.08        | -0.05        | 0.11         |              | <u>0.32</u>  |              |              |
|           | EC2 | JJA | 0.11         | 0.16         | 0.15         | 0.06         | 0.00         | 0.10         |              | <u>0.24</u>  |              |              |
|           | EC1 | Jun | -0.20        | -0.13        | -0.14        | <u>-0.24</u> | <u>-0.28</u> | -0.19        |              | 0.00         |              |              |
|           | EC2 | Jul | 0.10         | 0.14         | 0.11         | 0.09         | 0.02         | 0.08         |              | <u>0.41</u>  |              |              |
|           | EC2 | Aug | <u>-0.31</u> | <u>-0.37</u> | <u>-0.27</u> | <u>-0.28</u> | <u>-0.23</u> | <u>-0.32</u> |              | <u>-0.33</u> |              |              |

of the NAO is quite unsure. However, the monthly correlations seem to be more affected by the actual positions of centres of action as derived by monthly EOF than by any more consistent circulation pattern.

As two subperiods can not really resolve the correlations' temporal evolution, running correlations using a 21-year window have been calculated and illustrated in Figure 4.17. The relationship between UST summer temperatures and the L/H-mode was strongest during the 20<sup>th</sup> century when also some evolutionary agreement has already been observed (Fig. 4.17a). The linkage of UST summer temperatures to the NAO is stronger compared to the GAR over nearly the entire period (Fig. 4.17e). In the GAR, a relationship is hardly visible, as reflected by the alternately



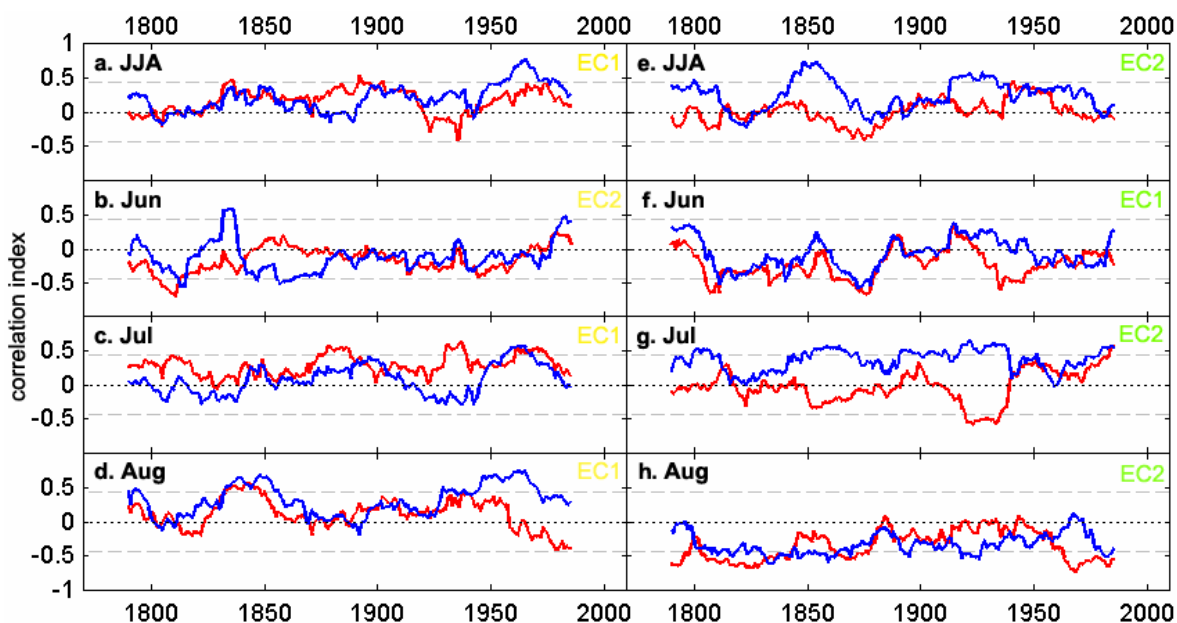


**Figure 4.17** Running correlations over a 21-year window between the L/H-like and NAO-like ECs and GAR (red) and UST (blue) temperatures respectively 1780–1995 for the average of the whole summer season (a, e) and the individual summer months June (b, f), July (c, g) and August (d, h). The first and last ten years are not plotted. The light grey dashed lines indicate the 95 % significance levels.

positive and negative, but always weak correlations. The high instability of correlations ranging from near zero-values (e.g. around 1825) to quite good correspondence (e.g. around 1850) are a clear feature of the connection of UST temperature to the NAO during summer. Again, the correlations between single month ECs and monthly temperature series are influenced by the actual positions of the centres of action as derived from the EOF-analysis (Fig. 4.17b–d, f–h). Anyhow, the generally relatively low correlations between circulation indices and observed temperatures around 1800 limit the potential for significant conclusions on the existence of EI warm summers from reconstructed atmospheric circulation.

To subsume this subchapter on summer temperature linkage to atmospheric circulation, it can be stated that only a weak relationship between air pressure variations over the North Sea and GAR as well as UST temperatures is existent. Furthermore, GAR temperatures are not at all linked to a NAO-mode during summers. As regards the UST records, a rather weak overall NAO-correlation, which slightly increases by the appliance of the USTh version, is detectable. But even in the Swedish case, the relationships are too unstable in time to draw any reliable conclusions from the fact that an actually occurring prolonged positive NAO phase around 1800 puts the observed warm summers into question. Therefore, no efforts to reinterpret the warm early Alpine and Scandinavian summers in relation to the temporal evolution of a NAO index as it has been constructed here can be undertaken.

## 5 Discussion

### 5.1 Natural temperature variability

The majority of scientific contributions to the current climate warming debate based on instrumental evidence confine to the most recent 150 years, due to the fact that area-wide data amount and data quality increased considerably with the introduction of national meteorological services in the mid-19<sup>th</sup> century. These findings, however, are derived from a period, whose beginning just coincides with the full spread of industrialisation in Europe and North America, leading to the instance that most climate observations are potentially affected by anthropogenic influences related to industrial activities (especially the emission of greenhouse gases and aerosols in the atmosphere). An interesting subject is to relate this – at least partly anthropogenic forced – climate state into longer-term pre-industrial – natural – climate variability. Integration of another century of instrumental data back in time may considerably change the size and partly even the sign of observed temperature long-term trends (cf. Table 4.1, p. 56). Even if another century of instrumental information are added, as is possible at least on a regional scale by means of the HISTALP and UST datasets, the period under investigation is still too short for the estimation of the natural range of climate and, for example, temperature variability on a decadal to centennial scale. The already presented Figure 4.6 (p. 63) shows annual and summer seasonal year-to-year variability in the Alpine and Southern Scandinavian regions. But since temperature also fluctuates over decades and centuries, the climatically even more interesting time scales are the longer-term ones (also shown in Fig. 4.6). The coolest consecutive ten summers in the GAR record occurred from 1909–18 (–0.9 K with respect to 1961–90), the warmest ones from 1994–2003 (+1.5 K). In UST, 1902–11 (–0.9 K) was the coolest and 1772–81 (+1.9 K) the warmest summer decade. The USTh version moves these outstanding periods into (–1.0 K from 1832–41) and out of (+1.3 K from 1994–2003) the EI period and decreases the total range of observed temperature variability. Larger positive than negative anomalies (with respect to the standard climate period) seem to be a common feature of variability in both regions. As already shown by several examples, the value and sign of long-term temperature change in UST is additionally dependent on which record version is regarded to be the most reliable one. This insecurity in data homogeneity makes it more difficult to capture real temperature variability and, furthermore, the underlying causes for

changes. The following possible factors are capable of driving decadal to century temperature variability:

- Variations in solar activity, like changes in radiation intensity over the solar cycles, vary the amount of incoming energy at the top of the atmosphere. Both the so-called Late Maunder Minimum, a phase with nearly no sunspots just before the onset of instrumental measurements in the study regions (1680–1715), and the following Dalton Minimum (around 1820) brought along some of the coldest climate episodes of the last half-millennium and have been regarded to be responsible for a global-scale cooling (Lean *et al.* 1995; Cubasch and Voss 2000). The latter one is evident in the records from the two study regions, being more expressed in the GAR than in UST and also more in annual than in summer temperature. 1813, 1815, 1816 and 1821 appear among the coolest summers in the Alps, whereas in Southern Scandinavia only 1821 was extremely cool (see Table 4.2, p. 59).
- Volcanic activity can alter summer temperature in one direction and over short time periods only. The net effect of volcanic eruptions, taking into account the interaction of incoming solar radiation, outgoing infrared emission and sulphate aerosols in the lower stratosphere on the atmosphere's radiation balance, is a cooling of near surface temperatures. Whereas volcanoes exert the largest climate effects during summers, regionally even positive deviations are thinkable during winters (Matulla *et al.* 2005, 43–44). Within the instrumental period, the Tambora eruption of 1815, which coincided with the ongoing Dalton Minimum, was the most prominent volcanic event. The cool Alpine summer of 1816 within the extraordinarily cool decade of the 1810s is only understandable in terms of this event. According to UST, this actually globally noticeable forcing was much less effective. In return, another event, i.e. the (still high-levelled) short-term drop of UST annual temperatures after 1783 may be related to the outbreak of the Lakagígar in Iceland in this year (Nordli *et al.* 2003, 1834).
- The influence of atmospheric circulation on temperature in the Alpine region and Southern Sweden has been exhaustively examined in the thesis. This resulted in the insight that its impact is weak and inconstant during summer (at least when the ADVICE data and the EOF method are applied; see Chapter 4.5). In order to cope with the inconstancy of the temporal relationships of summer temperatures to the temporal evolutions (ECs) of atmospheric patterns (EOFs), a final attempt is undertaken here, to at least identify typical periods of higher circulation-temperature linkage in order to eventually draw valuable conclusions for some climate episodes. Figure 5.1 plots the running correlations between GAR and UST summer temperatures against the evolution of the L/H-like and NAO-like ECs (see p. 76–79), in order to study whether the interregional temperature linkage is related to phases of prevailing atmospheric modes or not. However, no such connection can be found. Similarly, the effort to

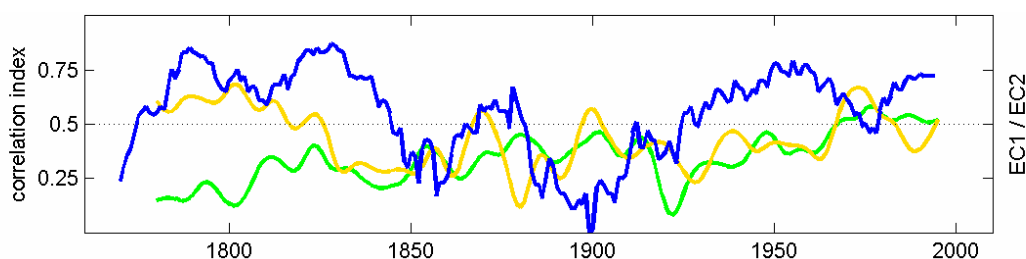


**Figure 5.1** Running correlations over a 21-year window of mean summer temperatures between the GAR and UST (blue) against the temporal evolution of 20-years Gaussian low-pass filtered trends of the L/H-like (yellow) and NAO-like ECs (green) 1760/80–1995/2004 (differently scaled anomalies from the 1961–90 average).

determine if periods of high or low circulation-temperature correlations overlap with periods of relatively warm or cool summer temperatures ended in no clear result. Due to the weak circulation impact, it is assumed that atmospheric circulation plays a minor roll in varying summer temperatures on a decadal scale too. Anyway, it has to be kept in mind that reducing the atmosphere's complexity to just a few indices, which have been studied separately in this thesis, explains only a fraction of the total variability and results from such an approach can be misleading (Hurrell *et al.* 2003, 14–15). One way to partially come around this problem is to combine several circulation indices in a multivariate approach. Moberg *et al.* (2003) demonstrated that such a procedure, combined with the addition of local air pressure and cloud cover information, can rather successfully explain summer temperature variations in UST (statistically as much as 65 %). Cloud amounts, however, were found by these authors to be more important than the circulation indices.

- In addition to these natural driving factors of decadal to century temperature variability, the human factor has to be accounted for during the last about 150 years. The anthropogenic emission of carbon dioxide, methane and other trace gases into the atmosphere results in the excessive concentration of these gases in the stratosphere, which constrains terrestrial long-wave radiation back into space by enhanced absorption and emission of infrared radiation. The resulting enrichment of energy within the lower part of the atmosphere is referred to as the anthropogenic greenhouse effect. Even if it might not be causal to recent climate warming exclusively, it is indisputable that it at least serves as an enforcing factor in the last one and a half centuries' and, especially, the recent decades' temperature warming (IPCC 2001, 93).

The potential of an interregional comparison of instrumental data reaching back into the pre-industrial 18<sup>th</sup> century is to provide insight in how the recent warming is to be placed in perspective to the pre-greenhouse climate's natural temperature variability. Even if 250 years are still a short time period for estimating natural variability – the question appears if the recent warming reached above the natural background of temperature variability, taking the additional

100 years from 1722/60–1860 into consideration? The answer has to be differentiated by study region and data reliability. To begin with, the warm summers around 1800 are taken for real. In general, it has clearly been seen that large temperature variability is a main climate feature of both the Alpine and Southern Scandinavian region during all observationally captured times. As regards the GAR solely, the most recent annual and summer warmth is unprecedented in course of the entire instrumental period; especially, the summer of 2003 remains unique within at least the last 250 years. Due to the recognised summer warmth around 1800, which has been surpassed only slightly so far, the recent years are not significantly out of range. However, there are main differences between the outstandingly warm periods around 1800 and around 2000: (1) While the 1800 warmth is concentrated on summer months, the 2000 warmth is virtually observed all year round. (2) Even if the warm summers around 1800 are a common feature to the Alps as well as to Scandinavia, they are not evident in global temperature reconstructions and long-time series from other regions, which might indicate that they might still have been a regionally confined climate characteristic. The present warming is, however, labelled as a global one. (3) Finally, the temporal scattering of the positive summer temperature anomalies around 1800 distinguishes between the warmth then and the contemporaneous one (Luterbacher *et al.* 2004, 1503). Particularly in case of the UST records, the decision concerning whether the warm summer temperatures are believed to reflect real climate (i.e. version UST is taken for real) or to be a result of an observational bias (i.e. version USTm or USTh is assumed to be more true than the UST version) strongly affects the overall conclusions on natural variability. As regards the UST version, the knowledge of younger climate history puts the recent evolution into perspective as the positive anomalies during the late 18<sup>th</sup> century are about as large as or even above the recent ones. Concerning the USTh version, however, analogous assumptions to the GAR can be made.

Regardless of these assertions on temperature variability as indicated by instrumental records, it is not the extent of the recently observed temperature rise per se but the warming rate and the predictions by the bulk of climate models (quasi-linear continuation of temperature trends into the 21<sup>st</sup> century) that are alarming.

## **5.2. Reliability of results**

Having exploited a variety of climate information from different sources, where data extends back to the EI period, both the data's weaknesses and strengths have to be kept in mind. In addition to the instrumentally recorded temperatures from the GAR and UST regions, which constitute the main focus in this thesis, a number of various other types of climate data have been analysed. A

common positive property of these data is the extension into pre-industrial times. Since a comprehensive discussion of the problems related to the application of all various kinds of proxy, model and gridded air pressure data, on the one hand, goes beyond the scope of this thesis and, on the other hand, such problem have been mentioned in Chapters 2.4–2.6 and 5.3, this review concentrates on reliability issues regarding the two instrumental core data collections HISTALP and UST.

Highly homogenised instrumental data like the HISTALP data collection allow for a study of pre-industrial climate on a regional scale, thanks to the relatively high spatial coverage that data they provide. This is a major advantage over global and continental datasets like CRU, which are limited temporally and in spatial resolution (Auer *et al.* 2006, 2). Even the EI station density in HISTALP is still high enough to catch major temperature variability signs. Similar data exists also for other European region, although most data are less well explored. In this regard, Europe stands out as the only region with sufficient data coverage, which has not completely been exploited yet. Another benefit of adding EI data is a longer calibration period for proxy records of reconstructed climate; calibration data that are less influenced by greenhouse climate and may help diminish errors when linking and adjusting proxy information to observational data. The most important disadvantage in the usage of EI data is related to the quality and homogeneity issue. Before the build-up of national and international meteorological networks, individual observations showed a low degree of standardisation, owing to a variety of routines and different instrumental equipment. In addition, non-climate signals, also known from more recent instrumental temperature series (e.g. urbanisation, relocation etc.) induce inhomogeneities to the data. To overcome this problem, three principal paths can be taken: (1) The application of relative homogeneity tests (cf. p. 47–50) that statistically incorporate information from other neighbouring stations can be a reasonable solution, but may be a problem during the EI period because of the scarcity of potential reference records. (2) The interpretation of metadata on station history is more frequently applied to EI temperature records. (3) Finally, the more qualitative consideration and checking of EI climate information in respect to proxy evidence enlarge the understanding of natural climate variability (cf. Chapter 4.3). Mutual comparison and comparison with other climate elements including circulation indices are other possible approaches (cf. Chapters 4.2 and 4.5). Great efforts in this context have already been made both in the GAR and UST, which have remarkably reduced the problem of data quality. The heavy homogenisation work that has already taken place was retraced in Chapters 2.1 and 2.2. As temperature is regarded to be the most well developed of all observational climate variables, the disadvantage of inhomogeneities has to large extent been erased. Still, concerns in respect to the applied homogenisation remain. The most well-known uncertainty, actually, is the EI paradox. The homogenisation of temperature data in the HISTALP database revealed, in the mean, negative inhomogeneities during the EI period, due to

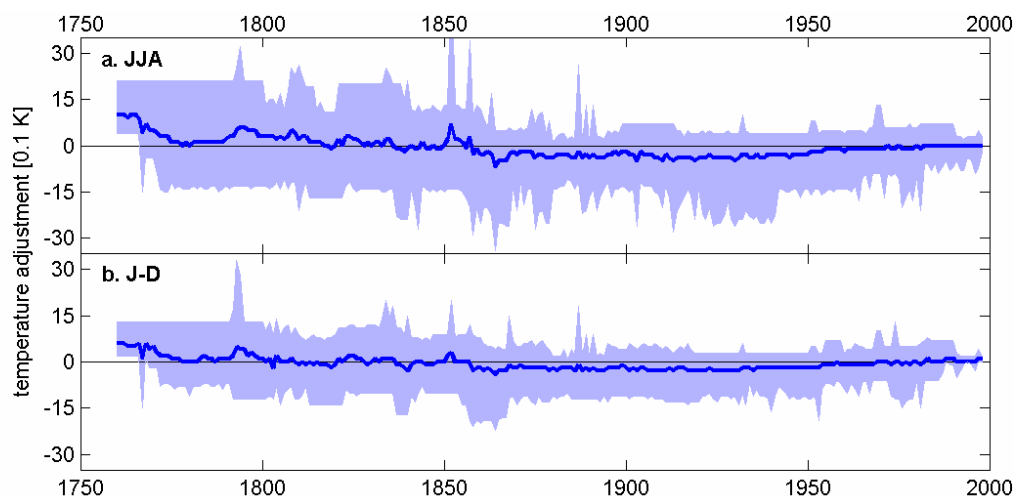


**Figure 5.2** Difference series between homogenised and original temperature data 1760–1998 from 19 of the 27 EI temperature series out of the HISTALP dataset for the summer season (a) and the whole year (b). The line denotes the mean over the sample, the shading shows the total range of adjustments.

the specific conditions at the different stations (see p. 29; Böhm *et al.* 2001, 1783–1785). As Figure 5.2a shows, the mean series of applied temperature adjustments is nearly continuously positive prior to 1835, i.e. most original series have been corrected towards warmer temperatures then. Problematically, the adjustment size is as large as typical real climate trends. As the comparison with the mean adjustments of annual temperature (Fig. 5.2b) illustrates, the bulk of positive adjustments seems to have been applied to summer temperatures. One may ask if the constantly positive mean values of summer temperature adjustments at the time of the early warmth around 1800 could eventually have lead to an artificially induced, too high temperature level. However, mean adjustments reach too low values at that time (typically +0.4 K during 1791–1810) to be solely responsible for the offset with Alpine proxy evidence (e.g. on average +1.5 K during 1791–1810 compared to TR). This means that, even if the questioned adjustments were exaggerated, the EI paradox would remain. Generally, the total range of adjustments proves that, without these homogenisations, any result would be superimposed by a large size of non-climate signals.

In case of the UST records, the homogeneity of early summer temperatures is more uncertain. To overcome this problem, a further homogenisation of the EI part of the record has been undertaken here and all analyses in this study have been accomplished in terms of various record versions. Applying the USTh version, indeed, brings results with better agreement in some analyses but, by including far away reference stations to derive this version, real spatial climate variance could possibly have been erased rather than leading to a homogenised series (Nordli 2001a, 214). Another drawback of USTh is that most reference stations are not homogeneous or

homogenised themselves. The corrections deriving from relative homogeneity testing for summer months seem reliable and can be explained by metadata. However, relatively large adjustments have been suggested and also applied for winter months, when no metadata explanation can be offered. Nevertheless, it has been decided for the purpose of the thesis to treat all months similarly in order to guarantee methodological consistency. However, another UST version regarding only provable, i.e. summer, corrections shall be suggested at this point. In any case, the dangers arising from these problems have absolutely to be borne in mind whenever employing USTh.

### 5.3 The early instrumental paradox reconsidered

The conclusive reassessment of the EI paradox connects directly to Chapter 1.4.2. The study at hand is – except for Moberg *et al.*'s (2003) work – the first comprehensive report solely concentrated on this issue, which has to date often been mentioned in passing but not been regarded in detail. Figure 5.3 qualitatively compares all analyses that have been undertaken on the matter so far. On the left side of the chart, the somewhat abstract term of significance is included. It has been interpreted as the respective analysis' validity in terms of the EI paradox and consists not only of the method's reliability but also of its relevance. The framing of the single investigations implies their degree of consideration in this thesis. The HISTALP instrumental observations (Auer *et al.* 2006) and the multiple regression model of other climate variables (Moberg *et al.* 2003) have been constructed and described in the particular papers and have only been referred to or been used as a basis in the thesis; their implications in connection with the EI paradox are known from Chapter 1.4.2. Besides, already existing data and approaches have been developed further or considered in greater detail; these analyses shall be recapitulated now:

- In addition to the “official” UST versions (Bergström and Moberg 2002; Moberg *et al.* 2002), five independent Northern European long-time instrumental temperature series have been employed in the SNHT to derive a further summer homogenised version of the temperature series. The resultant USTh version corresponds more closely to GAR temperature, UST air pressure, proxy and model data series. Even if USTh is not at all at the final stage (see p. 89–90) and the size of adjustments is up to discussion, most analyses clearly support the too high level of the official UST version's summer temperatures. This is in line with the finding of Moberg *et al.* 2003. By lowering early UST summer temperatures, at least a fraction of the EI paradox for the Swedish part could be resolved.



- The high summer temperatures around 1800 could be verified by the investigation of concurrent air pressure long-time series for the GAR. This finding can not be seen in case of the UST records.
- The Alpine tree-ring proxy record (Büntgen *et al.* 2005) is in drastic contrast to the GAR instrumental series as far as warm early summer temperatures are concerned. Potential sources for this discrepancy may be found in proxy insecurities. It is not fully understood yet to what extent the temperature in individual months actually contributes to annual tree-ring growth. Furthermore, not only temperature but also precipitation and snow cover duration in spring modify the tree-ring's climate signal. Relatively high summer precipitation before around 1830 could partly explain "cool" tree-ring temperatures (Böhm 2005).
- The ice-core proxy from Colle Gnifetti (Wagenbach *et al.* 2001) does – unlike earlier investigations – not reproduce an episode of warm summers around 1800 but is troubled by insecurities. Besides the doubts concerning the highly variable conserved fractions of annual precipitation, upstream correction and dating are rather uncertain. Even the single core records partly point in opposite directions.
- The glacier length and mass balance reconstructions (Oerlemans 2005; Schöner and Böhm 2007) do not indicate any signal of warm EI summers either. However, rough estimates of the climate sensitivity and the response times of the single glaciers and a small sample size at the beginning of the record are factors that constrain its representativity. Moreover, it is speculated that wet summers during the first half of the 19<sup>th</sup> century could compensate for high temperatures (Matulla *et al.* 2005, 61). On the other hand, a local study of historical glacier extent in the Austrian Hohe Tauern mountain chain (Slupetzky and Slupetzky 1995) brings up noticeably reduced glacier coverage during the 1810s, which would better fit to the instrumentally observed warm summers.
- Böhm (2005) provided a possible explanation for the Alpine EI paradox between warmer instrumental summer temperatures and cooler tree-ring temperatures that has not been further regarded in this thesis. All tree-ring data around 1800 originate from high-elevation sites near the tree line, whereas the corresponding instrumental temperature data at that time are available from lowland stations only. Therefore, a decoupling of summer temperatures at cooler high elevations and warmer low elevations around 1800 may have existed. Relatively high observed precipitation during the EI period support this theory, since a higher vertical temperature gradient (low – warm, high – cold) would have caused more labile thermal conditions and, thus, lead to enhanced convective precipitation. By that means, a reason for weak tree-ring growth as well as glacier advance at high Alpine sites despite of warm lowland

temperatures would be found. Nevertheless, this solution, which indicates that both instrumental and proxy data are true, is not plausible either, because later measurements never indicated signs of a similar decoupling again (R. Böhm, ZAMG, personal communication).

- Both the AUST and the VES harvest (and in VES also terminal moraine stands) proxy series (Nordli 2001b; Nordli *et al.* 2003) may be affected by inhomogeneities (e.g. long-term trends in harvest data) and insecure modelling estimates (e.g. glacier equilibrium line altitudes, moraine dates). Furthermore, the rather long distance to UST may play a major role in case of comparison with VES.

Whereas these analyses were based on previously existing thoughts, also several new approaches were chosen to assess the nature of the EI paradox. In general, they both confirm and oppose warm early summers but are also among the less significant analyses:

- The direct comparison of GAR and UST summer temperatures around 1800 has revealed that, despite individual peculiarities, the overall trends are in good agreement. However, it could be shown that UST summer temperatures are disproportionately high before the mid-19<sup>th</sup> century in comparison with the GAR. The GAR and UST summer temperatures are significantly

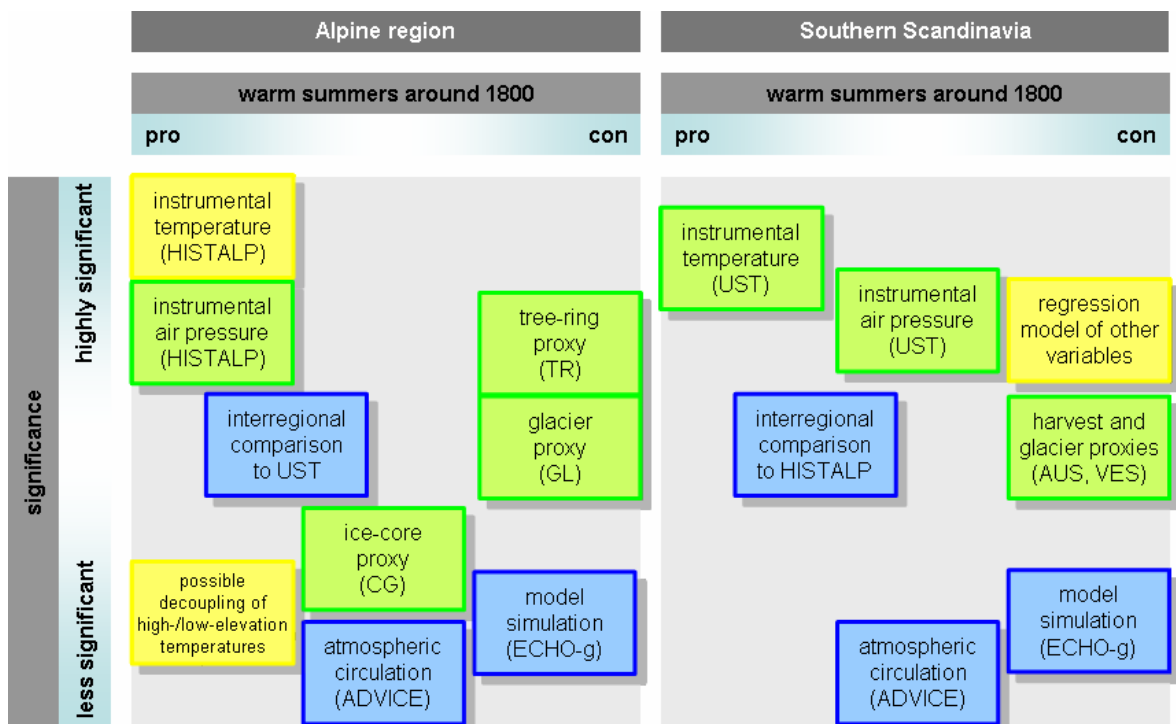


**Figure 5.3** Overview over accomplished analyses in connection with the EI paradox. Yellowish framing signifies previously undertaken investigations, greenish framing denotes existing approaches that have been deepened and bluish framing indicates new analyses.

statistically connected by a correlation coefficient of 0.36 over the whole data period; however this climatic linkage is not at all temporally stable and seasonally weakest during summer.

- The analysed ECHO-g model run does not simulate any especially warm summers around 1800 as suggested by instrumental series. The model, indeed, is regarded to reproduce broad temperature deviation patterns reliably but its sensitivity is lowered by uncertain external driving factors. Moreover, only one model simulation has been analysed. Another simulation, starting from other initial conditions, may very well have given a somewhat different evolution of regional temperatures (e.g. due to a different path of storm tracks).
- Due to the too weak and unstable linkage of summer temperature to atmospheric circulation patterns as calculated from gridded air pressure data, no final conclusions from analyses of circulations patterns can be drawn with regard to the observed warm summers around 1800.

It has to be concluded that the EI paradox could not be resolved. In return, deeper insights in interregional summer temperature connection, in comparability of instrumental and proxy data and in temperature linkage to atmospheric circulation during summer have been obtained. That the remaining paradox solely is a result of inhomogeneous instrumental data, for instance, due to deficient measuring techniques, is not credible. Other, data-related reasons for the appearance of the EI paradox are more probable: As already pointed out, the official UST records are most likely still positively biased during summers before around 1850. But in order to explain the larger fraction of the discrepancy, homogenisation, calibration and dating techniques to develop proxy records should be re-evaluated to reduce insecurities and erase errors in proxy data. Furthermore, totally independent proxies like stalagmites (e.g. Vollweiler *et al.* 2006), lake sediments (e.g. Danis *et al.* 2003) or historical documents might provide further evidence to better estimate the actual temperature level during the recent centuries.

For the future, the possibilities to improve the homogeneity of early HISTALP and UST data are still not exhausted. Large potential and a lot of climatological work awaits in the form of numerous, still inhomogeneous long-time instrumental temperature series from other European countries. Hopefully, responsible researchers there will become inspired by pioneer projects, not only to improve data quality but also to create regional or once even European-wide networks. Then, insecurities like the EI paradox may be solved once and for all.

## 6 Conclusions

To end with, the central outputs of the thesis are summarised and evaluated in terms of a short overview. The general idea to use historical climatology in order to assess the natural and anthropogenic fractions of recent climate warming has been introduced in the beginning of the study. In this thesis, the Alpine region and Southern Scandinavia were chosen because of the unique opportunity of interregional comparison of pre-industrial temperature trends as indicated by highly homogenised observational data provided in these regions. In a multi-data-type approach, the instrumental core datasets, HISTALP and the UST records, as well as proxy, model and gridded air pressure data were analysed using various methods. To outline the most important findings, the introductory research questions are responded to, following their order in Chapter 1.5 (see p. 24–25):

- The interregional climatic linkage between summer temperatures from the two totally independent and highly homogenised instrumental datasets is described by a moderate correlation coefficient (0.36 for the entire data period). Yet, the correlation is neither temporally nor seasonally stable and usually weakest during summer. General summer temperature evolution proceeded – in spite of individual peculiarities like the warm 1930s in UST and the warm 1940s in the GAR – rather similarly in both regions. A multi-decadal period of positive EI summer temperature deviations (with respect to the reference period 1961–90) is evident in both datasets. In fact, warm summers around 1800 can be found in the GAR as well as in UST instrumental data and, in both cases, only the summer season was affected by the warming. Whereas the warm episode lasted for about two decades in the Alps, it seems to have been more prolonged in UST. Several investigations imply that the level of GAR summer temperatures before the mid-19<sup>th</sup> century is reliable, whereas the EI summer temperatures are most likely positively biased in UST. A further homogenised version (based on relative homogeneity testing against other North European long-time instrumental temperature series) of UST temperatures provides an alternative (USTh) to the official records.
- Summer temperature and air pressure development is significantly correlated in both regions (GAR:  $r = 0.45$ , UST:  $r = 0.54$ ). The high level of GAR pressure measurements in summers around 1800 strengthens the reliability of warm early summers in the Alps. As regards UST, however, temperatures seem to be somewhat too high in view of the pressure records.

- The available proxy records (GAR: tree-ring widths, stable ice-core isotopes, glacial evidence; Southern Scandinavia: harvest dates, moraine stands) do not support summer warmth around 1800. Even if the relative temperature evolution is captured rather well by most reconstructions, temperature levels before around 1850 differ partly substantially. Nevertheless, all proxy reconstructions are to some extent complicated by specific insecurities in underlying data quality, exact climatic signal, calibration techniques and statistical editing.
- The ECHO-g climate model run Erik2 does not simulate any warm summers around 1800, neither in the Alpine region nor in Southern Sweden. The value of comparing regional instrumental data with results from a single model simulation is, however, quite limited.
- In addition, it has been shown that, due to a generally low pressure gradient over Europe, temperature evolution is only very weakly linked to fluctuations in atmospheric circulation during summers. As EOF analyses of gridded air pressure fields over Europe back to 1780 indicate, the influence of low-pressure activity over the North Sea is somewhat noticeable in UST temperatures but an NAO-related impact is barely evident. No valuable insights in a possible circulation dependency of the early summer warmth could be obtained.
- To assess recent climate warming in perspective of the last 250 years, it has been noted that the contemporary temperature rise in the Alps has slightly exceeded the limits of instrumentally observed variability. The same is true for Southern Sweden, if the USTh version is considered, while EI and present summer temperature deviations are of about the same size according to the official UST records. Nevertheless, the observed warmth around 1800 was confined to the summer season, to parts of Europe, was temporally scattered and, hence, differs from the warmth around 2000, which is an all-year, global-scale and apparently temporally continuing climatic feature.

On the whole, the thesis leaves the EI paradox more well-defined and more closely examined than ever before, but – as contradictory results derive from the analyses undertaken – it could in the main not be removed. Since the instrumental records are regarded to be generally reliable in comparison with proxy data, a really existent relatively high summer temperature level around 1800 seems probable. Future efforts should concentrate on the build-up of high-quality instrumental databases from other European regions and the improvement of proxy methods.

## Used abbreviations

### General terms

|     |  |
|-----|--|
| EI  | early instrumental                       |
| GAR | greater Alpine region (43°N4°E–49°N19°E) |
| NH  | Northern Hemisphere                      |
| UST | Uppsala and Stockholm                    |

### Series acronyms

For single instrumental series acronyms see Tables 2.1 (p. 28) and 2.2 (p. 33)!

|             |   |
|-------------|---|
| AUS         | harvest dates proxy record from South-Eastern Norway, Austlandet (Nordli 2001b; see p. 38–39)   |
| CG          | stable ice-core isotopes proxy from the Monte Rosa massif, Colle Gnifetti (Wagenbach <i>et al.</i> 2001; see p. 37–38)  |
| CRS         | course resolution subregion (GAR subregion, as defined by Matulla <i>et al.</i> 2005; see p. 29–30)   |
| GAR         | greater Alpine region, 27 longest instrumental records from HISTALP (Auer <i>et al.</i> 2006; see p. 26–30)   |
| GL          | glacier lengths proxy from all over the Alps (Oerlemans 2005; see p. 38)  |
| STO         | official version of the Stockholm instrumental temperature record (Moberg <i>et al.</i> 2002; see p. 32–33, 45–46)  |
| STOm        | summer temperature homogenised version of the Stockholm instrumental record (as discussed in Moberg <i>et al.</i> 2003 and implemented in Moberg <i>et al.</i> 2005a; see p. 45–46) |
| STOh        | further summer temperature homogenised version of the Stockholm instrumental record (present study; see p. 46–50)   |
| TR          | tree-ring width proxy record from the Western and Central Alps (Büntgen <i>et al.</i> 2005; see p. 36–37)   |
| UPP         | official version of the Uppsala instrumental temperature record (Moberg and Bergström 2002; see p. 31–32, 45–46)  |
| UPPo        | “original” version of the Uppsala instrumental temperature record, i.e. no correction has been applied for data before September 1853 (see p. 45)                                   |
| UPPm        | summer temperature homogenised version of the Uppsala instrumental record (as discussed in Moberg <i>et al.</i> 2003 and implemented in Moberg <i>et al.</i> 2005a; see p. 45–46)   |
| UPPh        | further summer temperature homogenised version of the Uppsala instrumental record (present study; see p. 46–50)   |
| UST(/o/m/h) | mean of instrumental Uppsala and Stockholm records, using the different UPP- and STO-versions (see p. 30–34, 45–46)   |
| VES         | harvest dates and terminal moraines proxy record from Western Norway, Vestlandet (Nordli <i>et al.</i> 2003; see p. 39–40)  |

### Climatological terms

|       |   |
|-------|---|
| AMJJA | late spring and summer temperature (mean April to August) |
| AOGCM | atmosphere-ocean coupled general circulation model        |
| DJF   | winter temperature (mean December, January, February)     |

|            |  |
|------------|--|
| GCM        | general circulation model, global climate model  |
| J-D        | annual temperature (mean January to December)  |
| JJA        | summer temperature (mean June, July, August)   |
| L/H        | atmospheric circulation feature reflecting variations between high and low pressure near the British Isles |
| LIA        | Little Ice Age   |
| MAM        | spring temperature (mean March, April, May)  |
| NAO        | North Atlantic Oscillation   |
| SLP        | sea level pressure   |
| SON        | autumn temperature (mean September, October, November)   |
| w. MAMJJAS | growing season temperature (weighted mean March to September)  |

### **Statistical terms and mathematical operands**

|           |  |
|-----------|--|
| EC        | expansion coefficient                                      |
| EOF       | empirical orthogonal function                              |
| PC        | principal component  |
| SNHT      | Standard Normal Homogeneity Test                           |
| $H_0$     | null hypothesis  |
| $H_A$     | alternative hypothesis                                     |
| $N$       | sample size  |
| $N_{eff}$ | effective sample size                                      |
| $Q$       | difference between candidate and reference value (in SNHT) |
| $r$       | correlation coefficient                                    |
| $T$       | test value (in SNHT)                                       |
| $Z$       | standardised $Q$ -values (in SNHT)                         |
| $z$       | Fisher-transformed correlation coefficient                 |

### **Institutes, programmes and datasets**

|           |  |
|-----------|--|
| ADVICE    | Annual-to-Decadal Variability in Climate over Europe (European Union project)  |
| ALOCLIM   | Austrian Long-Term Climate (ZAMG)  |
| ALP-IMP   | Multi-centennial climate variability in the Alps based on instrumental data, model simulations and proxy data (European Union project) |
| CRU       | Climatic Research Unit (University of East Anglia, United Kingdom)   |
| DNMI      | Norwegian Meteorological Institute (Norway)  |
| ECHAM     | European Centre Hamburg Model (MPI-M)  |
| ECHO-g    | <i>a global AOCGM consisting of ECHAM and HOPE-g</i> (MPI-M, ECMWF)  |
| ECMWF     | European Centre for Medium-Range Weather Forecasts (United Kingdom)  |
| GHCN      | Global Historical Climatology Network (National Climate Data Center, United States of America)   |
| GISS      | Goddard Institute for Space Studies (National Aeronautics and Space Administration, United States of America)                          |
| HadCRUT2v | <i>grid-box dataset of combined land and marine temperature anomalies (variance adjusted version)</i> (CRU)                            |

|         |  |
|---------|--|
| HISTALP | Historical Instrumental Climatological Surface Time Series of the greater Alpine region (ZAMG) |
| HOCLIS  | Homogenisation of Climate Series ( <i>software</i> )   |
| HOPE    | Hamburg Ocean Primitive Equation Model (MPI-M)   |
| IPCC    | Intergovernmental Panel on Climate Change (United Nations Organization)                        |
| IUP     | Institute of Environmental Physics (University of Heidelberg, Germany)                         |
| MPI-M   | Max Planck Institute for Meteorology (Germany)   |
| OASIS   | Ocean Atmosphere Sea Ice Soil ( <i>software</i> )  |
| RIHMI   | All-Russian Research Institute of Hydrometeorological Information (Russian Federation)         |
| SMHI    | Swedish Meteorological and Hydrological Institute (Sweden)                                     |
| WMO     | World Meteorological Organization (United Nations Organization)                                |
| ZAMG    | Central Institute of Meteorology and Geodynamics (Austria)                                     |



## References

- Alexandersson H (1986):** A homogeneity test applied to precipitation data. *Int J Climatol* 6, 661–675
- Alexandersson H, Moberg A (1997):** Homogenization of Swedish temperature data – Part I: Homogeneity test for linear trends. *Int J Climatol* 6, 661–675
- Auer I, Böhm R, Schöner W, Hagen M (1999):** ALOCLIM – Austrian-Central European long-term climate – Creation of a multiple homogenized long-term climate data-set. *Proceedings of the Second Seminar for Homogenisation of Surface Climatological Data*. November 9–13<sup>th</sup>, 1998, Budapest. WCDMP 41, WMO-TD 962. WMO: Budapest, 47–71.
- Auer I, Böhm R, Schöner W (2001a):** Austrian long-term climate 1767–2000 – Multiple instrumental climate time series from Central Europe. *Österreichische Beiträge zu Meteorologie und Geophysik* 25. Central Institute for Meteorology and Geodynamics, Vienna
- Auer I, Böhm R, Schöner W (2001b):** Long climatic series from Austria. In: Jones PD, Ogilvie AEJ, Davies TD, Briffa KR (eds.): *History and climate – Memories of the future?* Kluwer Academic/Plenum Publishers, New York
- Auer I, Böhm R, Jurkovic A, Lipa W, Orlik A, Potzmann R, Schöner W, Ungersböck M, Matulla C, Briffa KR, Jones PD, Efthymiadis D, Brunetti M, Nanni T, Maugeri M, Mercalli L, Mestre O, Moisselin JM, Begert M, Müller-Westermeier G, Kveton V, Bochnicek O, Stastny P, Lapin M, Szalai S, Szentimrey T, Cegnar T, Dolinar M, Gajic-Capka M, Zaninovic K, Majstorovic Z, Nieplova E (2006):** HISTALP – Historical instrumental climatological surface time series of the greater Alpine region 1760–2003. *Int J Climatol* (in press), doi: 10.1002/joc.1377
- Begert M, Schlegel T, Kirchhofer W (2005):** Homogeneous temperature and precipitation series of Switzerland from 1864 to 2000. *Int J Climatol* 25, 65–80
- Beniston M, Jungo P (2002):** Shifts in the distributions of pressure, temperature and moisture and changes in the typical weather patterns in the Alpine region in response to the behavior of the North Atlantic Oscillation. *Theor Appl Climatol* 71, 29–42
- Bergström H, Moberg A (2002):** Daily air temperature and pressure series for Uppsala (1722–1998). *Climatic Change* 53, 213–252
- Böhm R, Auer I, Schöner W, Hagen M (1998):** Long Alpine barometric time series in different altitude as a measure for 19<sup>th</sup>/20<sup>th</sup> century warming. AMS Boston, 72–76
- Böhm R, Auer I, Brunetti M, Maugeri M, Nanni T, Schöner W (2001):** Regional temperature variability in the European Alps 1760–1998 from homogenized instrumental time series. *Int J Climatol* 21, 1779–1801
- Böhm R (2003):** Mannheim revisited. Outline proposal for first call of ESF-Eurocore EuroCLIMATE
- Böhm R (2005):** The early instrumental paradoxon. Presentation at the ALP-IMP-third general annual meeting. April 6–8<sup>th</sup>, 2005, Bologna
- Bolius D, Laube A, Jenk T, Schwikowski M, Gäggeler HW, Sigl M (2006):** Neues aus dem Eis der Alpengletscher zur Klimageschichte des letzten Milleniums. 9. österreichischer Klimatag. March 16–17<sup>th</sup>, 2006, Vienna
- Brunetti N, Maugeri M, Monti F, Nanni T (2006):** Temperature and precipitation variability in Italy in the last two centuries from homogenised instrumental time series. *Int J Climatol* 26, 345–381
- Büntgen U, Esper J, Frank DC, Nicolussi K, Schmidhalter M (2005):** A 1052-year tree-ring proxy for Alpine summer temperatures. *Climate Dynamics* 25, 141–153
- Burga CA (2006):** *Klimatologie*. In: *Historisches Lexikon der Schweiz*. Version 15.06.2006. URL: <http://hls-dhs-dss.ch/textes/d/D8262.php>
- Cappelen J, Laursen EV, Jørgensen PV, Kern-Hansen C (2005):** DMI monthly climate data collection 1768–2004, Denmark, the Faroe Islands and Greenland. DMI Technical Report 05-05. Danish Meteorological Institute, Copenhagen

- Casty C, Wanner H, Luterbacher J, Esper J, Böhm R (2005):** Temperature and precipitation variability in the European Alps since 1500. *Int J Climatol* 25, 1855–1880
- Caussinus H, Mestre O (1996):** New mathematical tools and methodologies for relative homogeneity testing. Proceedings of the 1<sup>st</sup> seminar for homogenization of surface Climatological data. October 6–12<sup>th</sup>, 1996, Budapest
- Chen D, Hellström C (1999):** The influence of the North Atlantic Oscillation on the regional temperature variability in Sweden – Spatial and temporal variations. *Tellus* 51A, 505–516
- Crowley TJ (2000):** Causes of climate change over the past 1000 years. *Science* 289, 270–277
- CRU (2006):** The December press release 2005. Version 30.05.2006. URL: <http://www.cru.uea.ac.uk/cru/press/2005-12-WMO.pdf>
- Cubasch U, Voss R (2000):** The influence of total solar irradiance on climate. *Space Science Reviews* 94, 185–198
- Danis PA, von Grafenstein U, Masson-Delmotte V (2003):** Sensitivity of deep lake temperatures to past and future climatic changes – A modelling study for Lac d'Annecy (France) and Ammersee (Germany). *J Geophys Res* 108, D19, 4609
- Efthymiadis D, Jones PD, Briffa KR, Böhm R, Maugeri M (2006):** Influence of large-scale atmospheric circulation on climate variability in the greater Alpine Region of Europe. *J Geophys Res* (submitted)
- Eklund A (1999):** Long observation series of ice freeze and break-up dates in Swedish lakes. Paper presented at the 12<sup>th</sup> Northern Research Basins Symposium and Workshop, Iceland
- Frank DC, Esper J (2005):** Temperature reconstructions and comparisons with instrumental data from a tree-ring network for the European Alps. *Int J Climatol* 25, 1437–1545
- Frank DC, Büntgen U, Böhm R, Maugeric M, Esper J (2006):** Warmer early instrumental measurements versus colder reconstructed temperatures – hemispheric to regional evidence. *Quaternary Science Reviews* (submitted)
- González-Rouco JF, Beltrami H, Zorita E, von Storch H (2006):** Simulation and inversion of borehole temperature profiles in surrogate climates – Spatial distribution and surface coupling. *Geophys Res Lett* 33, L01703, doi: 10.1029/2005GL024693
- Gouirand I, Moberg A, Zorita E (2006):** Climate variability in Scandinavia for the past millennium simulated by an atmosphere-ocean general circulation model. *Tellus* (in press), doi: 10.1111/j.1600-0870.2006.00207.x
- Grudd H, Briffa KR, Gunnarson BE, Linderholm HW (2000):** Swedish tree rings provide new evidence in support of a major, widespread environmental disruption in 1628 BC. *Geophys Res Lett* 27(18), 2957–2960
- Grudd H, Briffa KR, Karlén W, Bartholin TS, Jones PD, Kromer B (2002):** A 7400-year tree-ring chronology in Northern Swedish Lapland – Natural climatic variability expressed on annual to millennial timescales. *Holocene* 12, 657–665
- Haerberli W, Holzhauser H (2003):** Alpine glacier mass changes during the past two millennia. *PAGES News* 11, 13–15
- Haerberli W, Noetzi J, Zemp M, Baumann S, Frauenfelder R, Hoelzle M (2005):** Glacier mass balance bulletin – Bulletin No. 8 (2002–2003). World Glacier Monitoring Service, Zürich
- Haerberli W, Hoelzle M, Paul F, Zemp M (2006):** Integrated monitoring of mountain glaciers as key indicators of global climate change – The European Alps. *IGS Symposium on Cryosphere Indicators of Global Climate Change*. August 20–25<sup>th</sup>, 2006, Cambridge
- Hansen JE, Ruedy R, Sato M, Imhoff M, Lawrence W, Easterling DR, Peterson TC, Karl TR (2001):** A closer look at United States and global surface temperature change. *J Geophys Res* 106, 23947–23963
- Heino R (1994):** Climate in Finland during the period of meteorological observations. Finnish Meteorological Institute contributions 12. Finnish Meteorological Institute, Helsinki

- Hurrell JW, Kushnir Y, Ottersen G, Visbeck M (2003):** An overview of the North Atlantic Oscillation. In: Hurrell JW, Kushnir Y, Ottersen G, Visbeck M (eds.): *The North Atlantic Oscillation – Climatic significance and environmental impact*. American Geophysical Union, Washington D.C.
- IPCC (2001):** Climate change 2001 – The scientific basis – Contribution of working group I to the third assessment report of the Intergovernmental Panel on Climate Change. Cambridge University Press, Cambridge, New York
- Jacobeit J, Jönsson P, Barring L, Beck C, Ekström M (2001):** Zonal indices for Europe 1780–1995 and running correlations with temperature. *Climatic Change* 48, 219–241
- Jones PD, Davies TD, Lister DH, Slonosky VC, Jónsson T, Barring L, Jönsson P, Maheras P, Kolyva-Machera F, Berriandos M, Martin-Vide J, Alcoforado MJ, Wanner H, Pfister C, Schuepbach E, Kaas E, Schmith T, Jacobeit J, Beck C (1999):** Monthly mean pressure reconstructions for Europe for the 1780–1995 period. *Int J Climatol* 19, 347–364
- Jones PD, Moberg A (2003):** Hemispheric and large-scale surface air temperature variations – An extensive revision and an update to 2001. *J Climate* 16, 206–223
- Lauscher F (1980):** Die Wärmeinsel des österreichischen Donauraumes zur Regierungszeit Kaiser Josephs II. *Annalen der Meteorologie* 16, 199–200
- Lean J, Beer J, Bradley R (1995):** Reconstruction of solar irradiance since 1610 – Implications for climate change. *Geophys Res Lett* 22, 3195–3198
- Luterbacher J, Xoplaki E, Dietrich D, Rickli R, Jacobeit J, Beck C, Gyalistras D, Schmutz C, Wanner H (2002):** Reconstruction of sea level pressure fields over the Eastern North Atlantic and Europe back to 1500. *Climate Dynamics* 18, 545–561
- Luterbacher J, Dietrich D, Xoplaki E, Grosjean M, Wanner H (2004):** European seasonal and annual temperature variability, trends and extremes since 1500. *Science* 303, 1499–1503
- Manley G (1974):** Central England temperatures – Monthly means 1659 to 1973. *Quart J R Met Soc* 100, 389–405
- Matulla C, Auer I, Böhm R, Ungersböck M, Schöner W, Wagner S, Zorita E (2005):** Outstanding past decadal-scale climate events in the greater Alpine region analysed by 250 years data and model runs. GKSS 2005/4. GKSS-Forschungszentrum Geesthacht GmbH, Geesthacht
- Maurer J, Billwiller R, Heß C (1909):** Das Klima der Schweiz – Auf Grundlage der 37jährigen Beobachtungsperiode 1864–1900. Erster Band. Kommissionsverlag von Huber & Co, Frauenfeld
- Min SK, Legutke S, Hense A, Kwon WT (2005a):** Internal variability in a 1000-yr control simulation with the coupled climate model ECHO-G – I. Near-surface temperature, precipitation and mean sea level pressure. *Tellus* 57A, 605–621
- Min SK, Legutke S, Hense A, Kwon WT (2005b):** Internal variability in a 1000-yr control simulation with the coupled climate model ECHO-G – II. El Niño Southern Oscillation and North Atlantic Oscillation. *Tellus* 57A, 622–640
- Moberg A, Alexandersson H (1997):** Homogenization of Swedish temperature data – Part II: Homogenized gridded air temperature compared with a sub-set of global gridded air temperature since 1861. *Int J Climatol* 17, 35–54
- Moberg A, Bergström H (1997):** Homogenization of Swedish temperature data – Part III: The long temperature records from Stockholm and Uppsala. *Int J Climatol* 17, 667–699
- Moberg A (1998):** Meteorological observations in Sweden made before A.D. 1860. *Paleoclimate Res* 23, 99–119
- Moberg A, Bergström H, Ruiz Krigsman J, Svanered O (2002):** Daily air temperature and pressure series for Stockholm (1756–1998). *Climatic Change* 53, 171–212
- Moberg A, Alexandersson H, Bergström H, Jones PD (2003):** Were Southern Swedish summer temperatures before 1860 as warm as measured? *Int J Climatol* 23, 1495–1521

- Moberg A**, Tuomenvirta H, Nordli PØ (2005a): Recent Climatic Trends. In: Seppälä H (ed.): The physical geography of Fennoscandia. Oxford University Press, Oxford
- Moberg A**, Sonechkin DM, Holmgren K, Datsenko NM, Wibjörn K (2005b): Highly variable Northern Hemisphere temperatures reconstructed from low- and high-resolution proxy data. *Nature* 433, 613–617
- Moberg A**, Kjellström E, Gouirand I, Rummukainen M, Schoning K, de Jong R, Linderholm H, Zorita E, Wohlfarth B (2007): Climate in Sweden during the past millennium – Evidence from proxy data, instrumental data and model simulations (in press)
- Nesje A**, **Dahl SO** (2000): Glaciers and environmental change. Arnold Publishers, London
- Nordli PØ** (2001a): Reconstruction of nineteenth century summer temperatures in Norway by proxy data from farmers' diaries. *Climatic Change* 48, 201–218
- Nordli PØ** (2001b): Farm diaries provide record of temperatures in Eastern Norway 1749–2000. *Cicerone* 2001/4, 19–21
- Nordli PØ**, Lie Ø, Nesje A, Dahl SO (2003): Spring-summer temperature reconstruction in Western Norway 1734–2003 – A data-synthesis approach. *Int J Climatol* 23, 1821–1841
- Oerlemans J** (2005): Extracting a climate signal from 169 glacier records. *Science* 10.1126/science.1107046
- Portis DH**, Walsh JE, El Hamly M, Lamb PJ (2001): Seasonality of the North Atlantic Oscillation. *J Climate* 14, 2069–2078
- Raab B**, **Vedin H** (eds.) (1995): National atlas of Sweden – Climate, lakes and rivers. Almqvist & Wiksell International, Stockholm
- Roeckner E**, Arpe K, Bengtsson L, Christoph M, Claussen M, Dümenil L, Esch M, Giorgetta M, Schlese U, and Schulzweida U (1996): The atmospheric general circulation model ECHAM4 – Model description and simulation of present-day climate. Report No. 218. Max Planck Institute for Meteorology, Hamburg
- Roeckner E** (2003): Allgemeine Zirkulationsmodelle, Atmosphäre. *promet* 29, No. 1–4, 6–14
- Roeckner E** (2004): Wirkung der erhöhten Treibhausgaskonzentration. *promet* 30, No. 3, 99–105
- Schnur R**, **Hegerl G** (2003): Geben die gekoppelten Ozean-Atmosphärenmodelle die natürliche Klimavariabilität wieder? *promet* 29, No. 1–4, 63–71
- Schöner W**, Auer I, Böhm R, Keck L, Wagenbach D (2002): Spatial representativity of air-temperature information from instrumental and ice-core-based isotope records in the European Alps. *Annals of Glaciology* 35, 157–161
- Schöner W**, **Böhm R** (2007): A statistical model for reconstruction of LIA ice mass for glaciers in the European Alps. *Annals of Glaciology* 46 (in press)
- Slonosky VC**, Jones PD, Davies TD (1999): Homogenisation techniques for European monthly mean surface pressure series. *J Climate* 12, 2658–2672
- Slonosky VC**, Jones PD, Davies TD (2001): Atmospheric circulation and surface temperature in Europe from the 18<sup>th</sup> century to 1995. *Int J Climatol* 21, 63–75
- Slupetzky H**, **Slupetzky N** (1995): Betref des Wachstums der Kletscher und Kälterwerdung des Klimas – Die Kreisamts-Präsidialakte Nr. 84–89 von 1820 im Salzburger Landesarchiv. Salzburger geographische Materialien 23. Institut für Geographie, Salzburg
- Smith LI** (2002): A tutorial on prinipal component analysis. (Tutorial) Version 31.05.2006. URL: [http://www.cs.otago.ac.nz/cosc453/student\\_tutorials/principal\\_components.pdf](http://www.cs.otago.ac.nz/cosc453/student_tutorials/principal_components.pdf)
- Smith TM**, **Reynolds RW** (2005): A global merged land and sea surface temperature reconstruction based on historical observations (1880–1997). *J Climate* 18, 2021–2036
- Stephenson DB**, **Benestad RE** (2000): Environmental statistics for climate researchers. (Tutorial) Version 14.05.2006. URL: <http://web.gfi.uib.no/~ngbnk/kurs/course.pdf>

- Stephenson** DB, Wanner H, Brönnimann S, Luterbacher J (2003): The history of scientific research on the North Atlantic Oscillation. In: Hurrell JW, Kushnir Y, Ottersen G, Visbeck M (eds.): The North Atlantic Oscillation – Climatic significance and environmental impact. American Geophysical Union, Washington D.C.
- Stott** PA, Tett SFB, Jones GS, Allen MR, Mitchell JFB, Jenkins GJ (2000): External control of twentieth century temperature by natural and anthropogenic forcings. *Science* 290, 2133–2137
- Tuomenvirta** H, Drebs A, Førland EJ, Tveito OE, Alexandersson H, Vaarby Laursen E, Jónsson T (2001): Nordklim data set 1.0 – Descriptions and illustrations. DNMI Report 08/01. Danish Meteorological Institute, Copenhagen
- Valcke** S, Terray L, Piacentini A (2000): The OASIS coupler user guide, version 2.4. Technical Report TR/CMGC/00-10. CERFACS, Toulouse
- van Oldenborgh** GJ, Burgers G (2006): The Climate Explorer. Version 05.06.2006. URL: <http://climexp.knmi.nl>
- Vollweiler** N, Scholz D, Mühlinghaus C, Mangini A, Spötl C (2006): A precisely dated climate record for the last 9 kyr from three high Alpine stalagmites, Spannagel Cave, Austria. *Geophys Res Lett* 33, L20703, doi:10.1029/2006GL027662
- von Storch** H, Zwiers FW (1999): Statistical analysis in climate research. Cambridge University Press, Cambridge
- Wagenbach** D, Keck L, Schock M, Preunkert S, Stenni B, Hoffmann G (2001): Isotope thermometry. In: Wagenbach D (ed.): Environmental and climatic records from high elevation Alpine glaciers (ALPCLIM) – Final Report
- Wallén** CC (ed.) (1970): Climates of Northern and Western Europe. World Survey of Climatology 5. Elsevier Publishing Company, Amsterdam
- Wanner** H, Gyalistras D, Luterbacher J, Rickli R, Salvisber E, Schmutz C (2000): Klimawandel im Schweizer Alpenraum. Hochschulverlag AG an der ETH Zürich, Zürich
- Wolff** JO, Maier-Reimer E, Legutke S (1997): The Hamburg Ocean Primitive Equation Model. Technical Report No. 13. German Climate Computer Center, Hamburg
- Zorita** E, von Storch H, González-Rouco JF, Cubasch U, Luterbacher J, Legutke S, Fischer-Bruns I, Schlese U (2004): Climate evolution in the last five centuries simulated by an atmosphere-ocean model – Global temperatures, the North Atlantic Oscillation and the Late Maunder Minimum. *Meteorologische Zeitschrift* 13, 271–289

## Curriculum vitae

Johann Hiebl

Seidenberg 1

A-3361 Aschbach-Markt

[johann.hiebl@gmx.at](mailto:johann.hiebl@gmx.at)

Hernalser Hauptstraße 20–22/7A

A-1170 Vienna

Birth date and place 27.07.1982 in Amstetten, Lower Austria

Nationality Republic of Austria

Parents Johann and Brigitta Maria Hiebl, agriculturists

1992–2000 attendance of the *Public Monastery Gymnasium of Benedictines* in Seitenstetten  
May 2000 school leaving examinations (GPA 1.8)

2001–(2007) studies of *Theoretical and Applied Geography* at the *Institute of Geography and Regional Studies*, University of Vienna, focus on *Landscape Ecology and Natural Space Analysis*

February 2004 completion of the first stage of study (GPA 2.0)

January–June 2005 term abroad at the *Department of Physical Geography and Quaternary Geology*, Stockholm University, Sweden

September 2005 practical training at the *Department of Climatology, Central Institute of Meteorology and Geodynamics* in Vienna,

March–June 2006 stay abroad in the course of the diploma thesis at the *Department of Physical Geography and Quaternary Geology*, Stockholm University

November 2006 completion of the second stage of study (GPA 1.4)

Interests climatology, the Alps, Scandinavia, local history

Languages English, Latin, French (school knowledge), Swedish (advanced)

## Erklärung

Ich versichere,

- dass ich die Diplomarbeit selbstständig verfasst, andere als die angegebenen Quellen und Hilfsmittel nicht benutzt und mich auch sonst keiner unerlaubten Hilfe bedient habe.
- dass ich dieses Diplomarbeitsthema bisher weder im In- noch im Ausland (einer Beurteilerin/ einem Beurteiler zur Begutachtung) in irgendeiner Form als Prüfungsarbeit vorgelegt habe.
- dass diese Arbeit mit der vom Begutachter beurteilten Arbeit übereinstimmt.

Aschbach-Markt, am 29. Dezember 2006

---

Unterschrift